ACID SENSING ION CHANNELS: COINCIDENT DETECTION OF ISCHEMIA BY A CHANNEL-CHANNEL INTERACTION

By

William T Birdsong

A DISSERTATION

Presented to the Neuroscience Graduate Program

and Oregon Health & Science University, School of Medicine

in partial fulfillment of the requirements of the degree of

Doctor of Philosophy

May 2008

Oregon Health & Science University

CERTIFICATE OF APPROVAL

This is to certify that the Ph.D. dissertation of

William Birdsong

has been approved.

[redacted]
Mentor/Advisor

[redacted]
Mentor/Advisor

[redacted]
Member

[redacted]
Member

[redacted]
Member

[redacted]
Member

Table of Contents

List of Figures:

List of Tables:

List of Abbreviations:

ASIC- Acid-sensing ion channel

P2X- ATP gated purinergic ion channel

ENaC- Epithelial sodium channel

DEG- degenerin

TRPV-1- vanilloid receptor

nACh- nicotinic acetylcholine receptor

ACh- Acetylcholine

GABA- Gamma-aminobutyric acid

ATP- Adenosine 5'-triphosphate

AMP-PNP- β,γ-Imidoadenosine 5′-triphosphate

ATPγS- Adenosine 5'-(3-thiotriphosphate)

ADPβS- Adenosine 5′-[β-thio]diphosphate

GTP- Guanosine 5′-triphosphate

GTPγS- Guanosine 5′-(3-thiotriphosphate)

GDPβS- Guanosine 5′-[β-thio]diphosphate

TNP-ATP-Trinitrophenyl adenosine 5'-triphosphate

BzATP- 2'-& 3'-O-(4-benzoylbenzoyl)-ATP

DRG- Dorsal root ganglion/ ganglia

AA- Arachidonic acid

LPC- Lysophosphatidyl choline

C12M- Dodecyl maltoside

FSEC- Fluorescent size exclusion chromatography

FPLC- Fast protein liquid chromatography

FRET- Fluorescent resonant energy transfer

TIRF- Total internal reflection fluorescence

TM- transmembrane

Acknowledgements:

Many people have contributed to this work and to my graduate training without whom the work presented here would not have been possible. Firstly, Ed, whose training, advice and guidance helped direct this project and made my graduate experience fulfilling and enjoyable deserves most of the credit for this work. John Adelman graciously adopted me and my project continuing what Ed began, providing guidance to help me complete this work. Many collaborators contributed to the success of this project. Leonardo Fierro began this work which was continued by Ligia Naves and Valeria Spelta. Josephine Marsh-Haffner did most of the cloning. Chris Bond provided assistance with cloning and molecular biology. Immunolocalization studies were performed by Robert Elde and Frank Williams. Immunoprecipitations were performed in the laboratories of John Adelman, John Scott and Mark Voigt. FRET studies were performed with the help and guidance of Michelle Knowles and Wolf Almers. FSEC was performed with help from Eric Gonzales and Eric Gouaux.

Former lab members Ken, Heather, Eric, Greg, Valeria, Junichi, Ulrich and Shelly helped make my graduate school experience enjoyable and satisfying. I would like to thank my family and especially Robin whose continued support made graduate school possible.

Abstract:

Acid-sensing ion channels (ASICs) are sodium selective channels gated by extracellular protons that may play a role in ischemia sensing. Ischemia occurs when a tissue receives insufficient oxygen to meet its metabolic demand which can result in metabolic changes, pain and tissue damage. A subtype of ASIC, ASIC3, has the ideal properties of an ischemia sensor; it is strongly expressed in ischemia sensing sensory neurons and is sensitive to the small pH changes that occur during ischemia. Acid alone, however, is insufficient to cause ischemic pain or excite ischemia sensitive sensory nerve afferents, creating an acid paradox.

Work presented in this dissertation sought to resolve this paradox and will describe the discovery of synergistic activity of acid and ATP. ATP was found to act on ASIC3 making it more sensitive to protons. Unexpectedly, this sensitization occurred through the interaction of two ion channels, ASIC3 and P2X. Activation of P2X by ATP modulated ASIC3 activity in a manner that had several unique features. 1) Modulation was slow to occur, taking tens of seconds to reach a peak, and slow to reverse- lasting for many minutes after washout of ATP. 2) Modulation increased the sensitivity of ASIC3 to protons, unlike previously described channel-channel interactions which caused mutual inhibition.

Using pharmacological, electrophysiological and optical methods it was determined that P2X5 was likely the endogenous P2X receptor that interacted with ASIC3 in sensory neurons, although co-expression of P2X2, P2X4 or P2X5 with ASIC3 reconstituted ATP dependent modulation of ASIC3 in several mammalian cell lines. P2X was found to both physically and functionally couple to ASIC3 and no

evidence suggested a role for common second messenger systems in ASIC modulation indicating the presence of a direct channel-channel interaction between ASIC and P2X.

Through its interaction with P2X5, ASIC3 is able to sense the coincident appearance of ATP and acid which are both released from working ischemic muscle so that ASIC3/ P2X5 is suited to distinguish between painful ischemic acidosis and other forms of acidosis. In addition to triggering pain this ion channel complex may be physiologically important for activation of sympathetic pressor reflexes which increase heart rate and blood pressure in response to vigorous exercise or cardiac ischemia to maintain cardiovascular homeostasis.

Chapter 1: Introduction

The nervous system is constantly integrating inputs from the outside world and the body and using the information to react to and interact with the environment and maintain the health of the body. Sensory neurons are the first line of detection which receive and relay information as diverse as touch, temperature, pain, muscle condition, hunger, heart rate, and blood pressure. A subset of sensory neurons called metaboreceptors sense metabolic changes that result in reflexes by the nervous system to control or respond to those changes in a variety of ways. It is thought that ion channels that are gated by metabolites and are located on sensory nerve endings may serve as the monitors of homeostasis and be the first step in reflex loops that aim to protect the body from damage. This dissertation focuses on two families of ion channels, the acid sensing ion channels (ASICs) and the ATP gated purinergic ion channels (P2X), and their potential role in forming a metabolic sensory complex by a functional interaction between them. This chapter will describe the context in which we think peripheral ASICs and P2Xs function and background into the properties of these channel families.

Physiology and pathology of muscle ischemia

Monitoring the metabolic state of the cardiovascular and muscular systems is vital for maintaining physiological conditions and responding to pathological states. The autonomic nervous system constantly monitors the metabolic conditions of the body to regulate heart rate, vascular tone and breathing to maintain homeostasis. When conditions in muscle stray from a normal and healthy range, a pathological state manifested by pain

and tissue damage can occur. One such state is muscle ischemia. When a working muscle receives insufficient oxygen to meet its metabolic demand ischemia occurs. Ischemia results anytime there is insufficient blood flow to a muscle including during a heart attack, peripheral artery disease and sickle cell anemia and can result in severe and sometimes chronic pain.

The heart is a particularly useful system for studying ischemic pain because the only conscious sensation that arises from the heart is ischemic pain. The heart is insensitive to touch or even burning. Chronic cardiac ischemic pain, angina, occurs when the heart has insufficient oxygen to meet its metabolic demand. Angina affects over three million Americans, often as a result of coronary artery disease, and can be debilitating. In addition to pain, chronic cardiac ischemia may trigger a paradoxical sympathetic reflex, increasing heart rate and blood pressure, thus leading to hypertrophy and heart failure (Malliani, Schwartz et al. 1969). Understanding the sensory mechanism underlying ischemic pain is a critical step along the path towards developing a treatment for angina. Angina and other ischemic muscle pain is thought to be caused by metabolites that are released from working muscle which would be dispersed rapidly during normal perfusion but instead build up when circulation is hampered.

In addition to pathological states, metabolites released from muscle are involved in maintenance of homeostasis. One well studied homeostatic mechanism is the exercise pressor reflex (Kaufman and Hayes 2002). The exercise pressor reflex is a nervous system dependent reflex loop that results in increased heart rate and blood pressure in

response to static muscle contraction. This reflex can also be accompanied by localized vasorelaxation allowing greater blood delivery to the working muscles while reducing blood flow to less active muscles and other organs, ensuring adequate cardiac and cerebral perfusion. It is clear that both mechanical and metabolic stimuli in muscle are crucial for transducing information during exercise to trigger the pressor response. One of the first descriptions of the exercise pressor reflex reasoned that metabolites released from muscle triggered the reflex since circulatory occlusion to the working muscle maintained the increase in blood pressure in the absence of muscle contraction until circulation was restored (Alam and Smirk 1937; Coote, Hilton et al. 1971). Like ischemia sensing, however, the identity of the metabolites and sensors involved in the pathway remains contentious.

The search for Factor P

Over 75 years ago Thomas Lewis first hypothesized that a metabolite released from working muscle was involved in transduction of ischemic pain (Lewis 1932). The hypothesis was based upon observations from tourniquet experiments. When blood flow is occluded to an extremity, no pain is felt. Pain is felt only when the extremity is exercised while blood flow is occluded, implying working muscle is essential for the mediation of ischemic pain (Lewis and Pickering 1931). This led to the suggestion that an unknown factor termed "Factor P" was a signaling molecule for transduction of ischemic pain. Factor P was hypothesized to be released from working muscle and act on sensory nerve endings innervating the muscle. Over the years numerous identities of Factor P have been suggested including bradykinin, substance P, adenosine, oxygen radicals, ATP,

lactate and protons (Meller and Gebhart 1992; Sutherland, Cook et al. 2000). The McCleskey lab has focused our recent efforts toward investigating the role of lactic acid in ischemia sensation since it is well documented that lactic acid is produced and released from muscle during anaerobic metabolism. In addition to its abundance during ischemia, there is functional evidence to argue that lactic acid may play a role in ischemia sensation (Pan, Longhurst et al. 1999). Acid has been well documented to be pain causing (algesic) when injected into muscle and the pH of ischemic cardiac tissue has been measured to drop from pH 7.4 to around pH 6.7 over the course of a 30 minute ischemic event (Cobbe and Poole-Wilson 1980), while pH in tourniquet pain experiments have been found to drop to around pH 7.0 (Issberner, Reeh et al. 1996), although precisely measuring localized changes in the interstitial pH is difficult.

One particularly useful physiological study of the role of protons in cardiac ischemia in the cat revealed that protons appear to be necessary but not sufficient to trigger excitiation of ischemia-sensitive small diameter afferents which are the likely triggers for ischemic pain (Pan, Longhurst et al. 1999). In this study it was observed that ischemia increased the firing rate of the likely nociceptors and this was mirrored by a decrease in tissue pH. If the cat was administered carbon dioxide (hypercapnia) rather than ischemia, a similar pH change occurred but there was no increase in the firing rate. This indicated that protons were not the trigger for ischemia sensing. However, if ischemia was induced and the pH of the receptive field of the afferent nerve terminal was buffered with a strong pH buffer, the firing rate was greatly diminished. This, in contrast to the previous result, implied a critical role for protons in ischemia sensing. These findings also agree with

clinical observations in humans relating to angina. Many patients have metabolic disorders or kidney failure that can cause the pH of the body to drop to levels similar to what is seen during ischemia, however, ischemic pain is not a symptom of these disorders. Thus, again protons alone appear insufficient for triggering ischemic pain. We therefore sought to investigate the role of ion channels as potential ischemia sensors and look for a synergistic effect of multiple metabolites.

Acid Sensing Ion Channel 3 (ASIC3) is sensitive to physiological pH changes and enriched on cardiac sensory neurons.

Candidate ischemia sensors must be suited to sense physiologically relevant changes in homeostasis. An ischemia sensor requires proper location on sensory nerve endings and sensitivity to the appropriate chemical stimuli. Various potential chemical stimuli are released during ischemia, notably H+ are released dropping the extracellular pH from a normal value of about 7.4 to the range of 7.0-6.8 (Cobbe and Poole-Wilson 1980; Sinoway, Prophet et al. 1989; Bangsbo, Johansen et al. 1993; Pan, Longhurst et al. 1999). Isolated cardiac sensory neurons are responsive to pH changes as small as drops from pH7.4 to 7.0 with large inward currents (Benson, Eckert et al. 1999). Such decreases in pH are common during ischemia. The Acid Sensing Ion Channels (ASICs) are obvious candidates for sensing such pH changes.

ASICs were first described nearly 30 years ago by Krishtal and Pidoplichko who observed several unique pH activated sodium selective currents in sensory neurons and subsequently elucidated their basic features but their identity remained a mystery

(Krishtal and Pidoplichko 1980; Krishtal and Pidoplichko 1981; Krishtal and Pidoplichko 1981). With advances in cloning, the molecular identity of the ASICs were discovered 17 years after their initial description (Waldmann, Bassilana et al. 1997; Waldmann, Champigny et al. 1997; Waldmann, Champigny et al. 1999). The ASIC's were revealed to be unique channels that are members of the Epithelial Sodium Channel/ Degenerin (ENaC/Deg) family of 2 transmembrane domain containing sodium channels and the chicken ASIC1 has been recently crystallized revealing an unexpected trimeric architecture with each subunit forming and hand-like tertiary structure (Figure 1-1A, B) (Jasti, Furukawa et al. 2007). There are now 4 known ASIC genes and two splice variants (ASIC1a, 1b, 2a, 2b, 3, and 4). ASIC1a, 1b, 2a, and 3 open in response to decreases in extracellular pH in a calcium dependent manner, while ASIC2b likely forms functional heteromers only with other subunits and an agonist for ASIC4 has yet to be identified. All ASICs are about as sodium selective as the voltage gated sodium channels and, like ENaCs and DEGs, all are blocked by amiloride with relatively low affinity. ASICs have varying calcium permeability and ASIC3 is relatively calcium impermeable. Calcium and protons appear to compete for a calcium binding site whereby proton binding catalyzes the release of calcium allowing the channel to open (Figure 1-1 D) (Immke and McCleskey 2003). Putative pH sensors were identified in the recent crystal structure (Figure 1-1 A, C) and suggested a potential gating mechanism with proton binding to acidic residues in the thumb/ finger interface promoting conformational changes that are transduced through the thumb to the transmembrane regions perhaps gating the channel (Jasti, Furukawa et al. 2007).

The sodium selective proton gated inward currents observed in cardiac sensory neurons and ASIC3 expressing COS-7 cells share nine nearly identical physical properties, which are clearly different from other ASIC family members (Sutherland, Benson et al. 2001). The most profound difference is the extreme proton sensitivity in the physiological pH range that occurs during ischemia (from pH 7.2-6.8). It was therefore proposed that ASIC3 is a cardiac ischemic sensor due to its localization and physical characteristics.

ASIC3 rapidly opens and desensitizes in response to prolonged pH changes. In contrast, ischemic pain is a sustained sensation lasting as long as sufficient stimulus is around. If ASIC3 is to be an ischemia sensor it must be able to respond to acid in a sustained fashion. Recent work has reported that ASIC3 can produce a sustained current in response to modest pH changes (7.2-6.8) overlapping the changes that occur during moderate exercise and ischemia (Yagi, Wenk et al. 2006).

There are several examples of modulation of ASICs in the literature (Xu and Xiong 2007). Most research has focused on ASIC1 modulation. We know that calcium plays a crucial role in gating and recovery from desensitization, so it is unsurprising that most divalent and trivalent cations inhibit the current flow through ASICs. Lactate which is a product of ischemic metabolism increases the acid evoked currents carried by ASIC3 by chelating extracellular calcium. This makes ASIC3 more sensitive to lactic acidosis than other forms of acidosis. Pathways that are possibly activated in ischemia that are shown to interact with ASICs include redox modulation (selectively modulating ASIC1), arachidonic acid (enhancing ASIC3), protein kinases PKA, PKC and CaMKII (only PKC

has been demonstrated to phosphorylate ASIC3), lactate, and scaffolding proteins including CIPP, PSD95, and Lin7b for ASIC3 (Catarsi, Babinski et al. 2001; Immke and McCleskey 2001; Allen and Attwell 2002; Anzai, Deval et al. 2002; Hruska-Hageman, Wemmie et al. 2002; Chu, Wemmie et al. 2004; Gao, Wu et al. 2004; Hruska-Hageman, Benson et al. 2004; Price, Thompson et al. 2004; Wu, Duan et al. 2004; Andrey, Tsintsadze et al. 2005; Chu, Close et al. 2006; Chu, Close et al. 2006; Wang, Chu et al. 2006; Cadiou, Studer et al. 2007; Cho and Askwith 2007; Smith, Cadiou et al. 2007; Wang, Yu et al. 2007; Sherwood and Askwith 2008).

Sensing ATP

ATP is maintained at millimolar concentrations in every cell and is critically important for the maintenance of most life. In contrast, ATP is normally at zero concentration outside cells because it is rapidly hydrolyzed to ADP, AMP and adenosine by various ecto-nucleotidases (Robson, Sévigny et al. 2006). It is, therefore, not surprising that ATP and its metabolites have been utilized for many kinds of cell-cell signaling ranging from fast synaptic transmission to paracrine trophic signaling in neuronal and non-neuronal cells and systems. Working skeletal and cardiac muscle release ATP, which rises to concentrations above micromolar levels in the interstitium when muscle becomes ischemic (Forrester and Williams 1977; Clemens and Forrester 1981; Hellsten, Maclean et al. 1998). There are several families of receptors capable of sensing ATP and its metabolic products and which one, if any, are involved in sensing the ATP that is released by muscle is not entirely clear (Abbracchio, Burnstock et al. 2006; Khakh and North 2006; Burnstock 2007). In addition to the P2X family of ATP gated ion channels,

P2Y and adenosine receptors have been well studied and described. P2Y receptors are G-protein coupled receptors (GPCR) that can be activated by ATP or ADP in addition to other nucleotides depending on the subtype of P2Y. Adenosine receptors (sometimes called P1) are also GPCRs which are activated by adenosine, serving as sensors for hydrolysis of ATP. The action of P2Y and Adenosine receptors is broad and their ability to sense the products of ATP hydrolysis is likely an important part of their function, since appearance of extracelluar ATP is transient, while ATP metabolites are more persistent.

The P2X receptors are ATP gated ion channels that are gated by micromolar concentrations of extracellular ATP. Like ASICs functional P2X channels are believed to form by a trimeric assembly of 2 transmembrane containing subunits with a short N- and highly variable C-terminal domain and a large extracellular loop (Figure 1-3) (Collo, North et al. 1996; Nicke, Baumert et al. 1998; Egan, Samways et al. 2006; Gever, Cockayne et al. 2006; Roberts, Vial et al. 2006). There are seven P2X subunits (P2X1-7) each having somewhat unique agonist and antagonist sensitivities. All P2X subunits are non-selective cation channels with varying amounts of calcium permeability rivaling that of the NMDA receptor. Human P2X5 has been reported to have significant chloride permeability as well (Bo, Jiang et al. 2003). There is significant heterogeneity between P2X subtypes in terms of activation and desensitization characteristics and ATP affinity. P2X1 and 3 both desensitize rapidly and completely and take minutes to recover from desensitization correlating with a relatively high ATP affinity. P2X2, 5, and 7 desensitize more slowly and recover relatively quickly. P2X4 is intermediate between slowly and quickly desensitizing subtypes and P2X6 does not form functional homomeric channels

forming only heteromeric channels with other subtypes. In addition to the seven subtypes, functional heteromeric channels have been reported for P2X1/5, P2X2/3, P2X2/6, P2X4/6, and recently P2X4/7 allowing for a wide variety of functions (Table 1-1) (Egan, Samways et al. 2006). Of the seven P2X receptors, mRNA for all but P2X7 are present in sensory neurons (Collo, North et al. 1996; Kobayashi, Fukuoka et al. 2005) but P2X3 and P2X2/3 are the major current carriers in sensory neurons (Lewis, Neidhart et al. 1995; Cook, Vulchanova et al. 1997; Vulchanova, Riedl et al. 1997). P2X5 is the least understood of the P2X subunits due to its small currents– about 100 fold smaller than other family members (for rat)– and more limited distribution when compared to other P2X subunits (Collo, North et al. 1996; Garcia-Guzman, Soto et al. 1996).

The P2X family was traditionally thought to mediate rapid cell-cell communication and P2X channels are indeed found both pre and post synaptically in the CNS, especially P2X2, 4 and 6. Their exact function is unknown, however the significant calcium permeability at all membrane potentials and ability to depolarize nerve terminals suggests that they may play some role in facilitating neurotransmitter release (Boehm 1999) and perhaps mediate some processes which involve post-synaptic calcium influx (Bardoni, Goldstein et al. 1997). In addition to fast synaptic function, slow trophic functions have been described for P2X receptors as well. P2X5 has been implicated in the regulation of skeletal muscle differentiation of satellite cells (Ryten, Dunn et al. 2002). The mechanism of regulation is thought to involve phosphorylation of the MAPK family of kinases, specifically p38 MAPK. It is not clear whether extracellular calcium is involved as an activator of these signaling events. Additionally, P2X5 has been reported to be present on

differentiating squamous epithelia and P2X7 has been implicated in ATP induced apoptosis (Groschel-Stewart, Bardini et al. 1999). This suggests that signal transduction may be an important role of the P2X channels. P2X2, 3, 4, and 7 are all currently being investigated by several pharmaceutical companies for their potential roles in various aspects of pain sensation. As a result, subtype selective agonists and antagonists are just now being discovered, which along with gene knockout technology should shed more light on what role specific P2X receptors play physiologically and pathologically.

P2X family member P2X2 inhibits several ion channels via physical interactions. The data within this thesis will show that ATP modulates ASIC channels by binding to a P2X receptor. The link between the P2X and ASIC ion channels is the critical mystery. There is precedent for P2X receptors to interact with other ion channels and with themselves. The best-studied example is the reciprocal inhibition of P2X2 and the $\alpha 3\beta 4$ subunits of the nicotinic acetylcholine channel (Nakazawa 1994; Khakh, Zhou et al. 2000). Application of either ATP or ACh produced a large inward current in Xenopus oocytes expressing P2X2 and $\alpha 3\beta 4$ channels (Figure 1-2). Co-application of ATP and ACh produced a much smaller than expected current appearing to occlude most of the Ach mediated current. This effect was transient and only occurs during co-application of both agonists as washout of either agonist relieves the cross-inhibition. Although a direct interaction was suspected, no attempts at co-immunoprecipitation of the two channels had been successful. Recently, the channels have been shown to closely associate using fluorescence resonance energy transfer (FRET) with cyan fluorescent protein labeled and yellow fluorescent protein labeled P2X2 and $\alpha 3\beta 4$ (Khakh, Fisher et al. 2005).

P2X2 has also been demonstrated to associate with ρ1/GABA and 5HT-3 in a similar cross-inhibitory manner that is thought to be a direct physical inhibition (Boue-Grabot, Barajas-Lopez et al. 2003; Boue-Grabot, Emerit et al. 2004; Boue-Grabot, Toulme et al. 2004). In addition to the inhibitory effects of P2X receptors on other channel subtypes, there is single channel evidence that suggest cooperativity between individual P2X2 channels. Channels from inside out patches containing multiple P2X2 channels display non-independent gating whereby one channel is more likely to open in response to agonist when another channel is already open (Ding and Sachs 2002). That is, gating of one channel affects gating of other channels that would not be expected if the channels gated independently. This would have the effect of increasing the sensitivity of the channels to ATP and is yet another piece of evidence that P2X receptors interact with other channels in their environment.

In response to prolonged applications of ATP, P2X2, 4, 5 and 7 have been reported to undergo slow conformational changes which result in a change in the permeability of the channels to the large cations NMDG+ and fluorescent dye YO-PRO1 (Khakh, Bao et al. 1999; Virginio, MacKenzie et al. 1999; Virginio, MacKenzie et al. 1999). It has been suggested that these changes in permeability represent an alternate open states of the channel and this is generally well accepted. It has been observed with P2X7, however, that dye uptake and NMDG+ permeability are distinct pathways and that perhaps the permeability to YO-PRO1 is secondary to activation of a second messenger rather than occurring as direct flux through the open P2X channel itself (Jiang, Rassendren et al.

2005). In either case, it indicates the susceptibility of slowly desensitizing P2X receptors to be influenced by long applications of ATP in a manner that may alter channel function and result in transitions to different states.

Some ion channels may moonlight as signal transducers by a G-protein coupled mechanism.

There have been several reports of ion channels that are linked to G-proteins by an unknown mechanism. Kainate, in dorsal root ganglia cells from mice expressing the ionotropic glutamate receptor subunit GluR5, inhibits K+ induced calcium increases (Rozas, Paternain et al. 2003). This inhibition is not seen in GluR5 knockout mice and is sensitive to Pertussis toxin and inhibitors of protein kinase C, implying a G-protein mediated inhibition of voltage gated calcium channels. The idea of ionotropic receptors linked to G-proteins is a provocative idea but it should be noted that this conclusion relies solely on the knockout of GluR5, which may cause unknown changes in these mice.

Another report consistent with several previous findings, implicates AMPA receptors in coupling to G-proteins (Takago, Nakamura et al. 2005). AMPA and the AMPA/Kainate agonist domoate applied to the calyx of held were demonstrated to inhibit presynaptic calcium currents in a G-protein dependent manner and this inhibition can be blocked by the AMPA receptor antagonists GYKI52466 and CNQX. These reports demonstrate the possibility of ion channels serving to activate G-proteins through an unknown mechanism, which may hold true for P2X5 modulation of ASIC3.

Significance:

The results in this thesis may provide a solution to the paradox that while acid appears necessary to trigger ischemic pain, it is not sufficient to do so. Coincident detection of acid and ATP is achieved by the physical coupling of two ion channels in a long lasting manner that is unlike previously described channel-channel interactions. The implications of this work may go beyond ischemic pain and apply more broadly to metabo-sensing in muscle physiology and exercise pressor responses and may mediate some aspects of tissue damage due to ischemia including stroke and chronic cardiac ischemia.

Goals of this work:

The work in this thesis aimed to offer a solution to the paradox that acid seemed necessary but not sufficient to cause ischemic pain. Upon the discovery of modulation of ASICs by extracellular ATP, the identity of the ATP receptor (a P2X channel) was sought. Next, this work aimed to identify the mechanism of interaction between ASIC3 and P2X and to describe changes in ASIC3 as a result of its interaction with P2X.

Figure 1-1: Trimeric architecture of Acid-sensing ion channels

A Structure of chicken ASIC1 demonstrating trimeric architecture with large extracellular domain. Arrow indicates putative pH sensor. B Structure of ASIC1 viewed from above demonstrating 3-fold symmetry. C Cartoon detailing potential mechanism of transduction of pH binding to channel gating. Binding of protons titrates acidic residues in the finger, thumb interface. This binding is transduced through the thumb region through the wrist and gates the channel by moving tramsmembrane domains. D Model of ASIC3 gating demonstrating competition between calcium and proton for a calcium binding site. Calcium and protons appear to compete for the same binding site and increasing proton concentration catalyzes unbinding of calcium. (A, B, C adapted from: (Jasti, Furukawa et al. 2007) with permission, D adapted from : (Immke and McCleskey 2003) with permission)

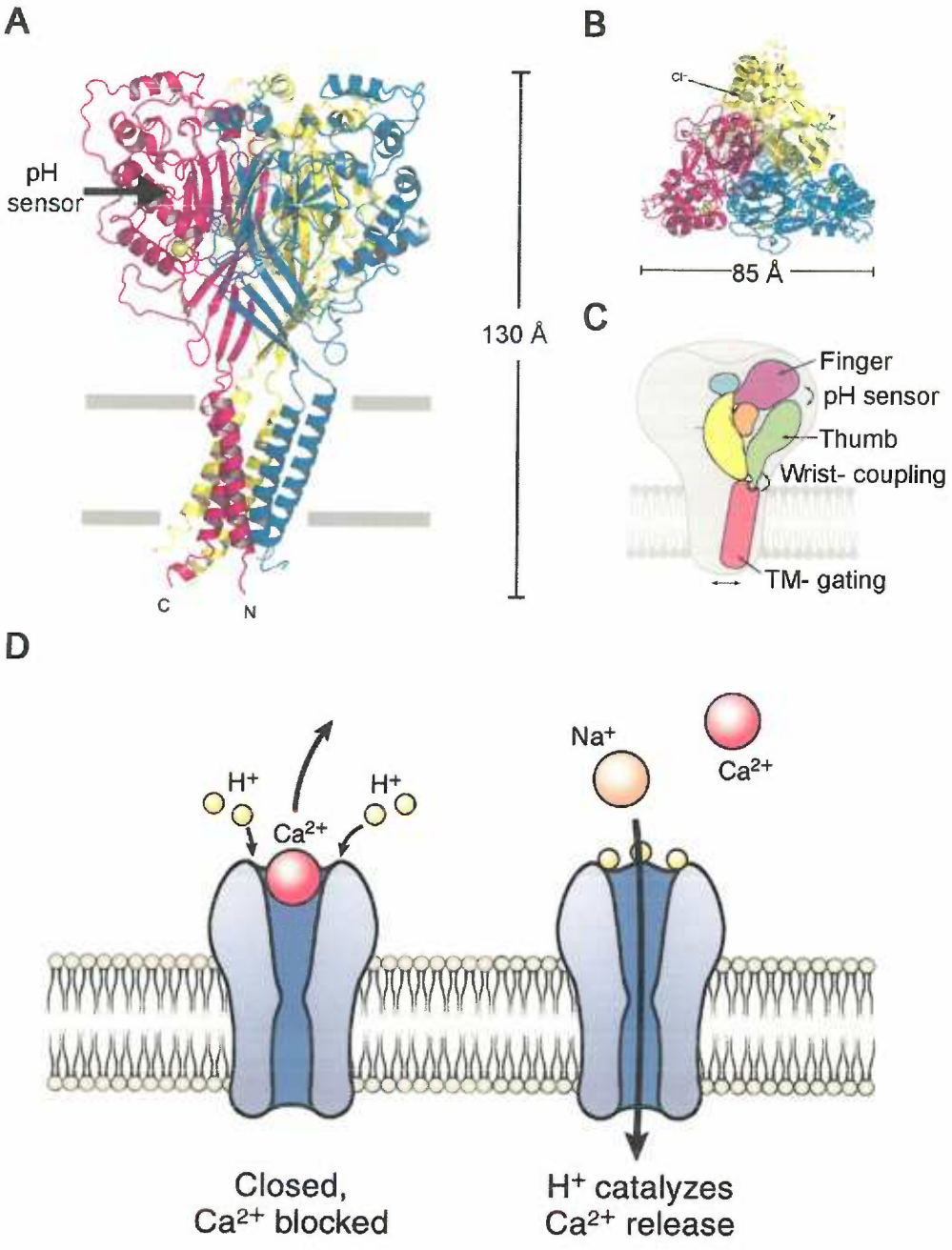
A
pH
sensor
C
N
130 Å
B
Cl-
85 Å
C
Finger
pH sensor
Thumb
Wrist- coupling
TM- gating
D
H+
H+
Ca2+
Na+
Ca2+
Closed,
Ca2+ blocked
H+ catalyzes
Ca2+ release

Figure 1-2: Cross-inhibition between P2X2 and nACh channels.

Application of ATP or acetylcholine (ACh) individually evoked large currents in oocytes expressing both P2X2 and $\alpha 3\beta 4$ nicotinic channels. When ATP or ACh is applied in the presence of the other agonist currents are smaller than expected from the sum of the two current components individually. This indicated that cross-inhibition was occurring between the two channels and is believed to be mediated by a direct channel-channel interaction. Note the temporal characteristics of this inhibition. Once the second agonist was removed the current immediately returned to the expected amplitude. From:(Khakh, Zhou et al. 2000) with permission.

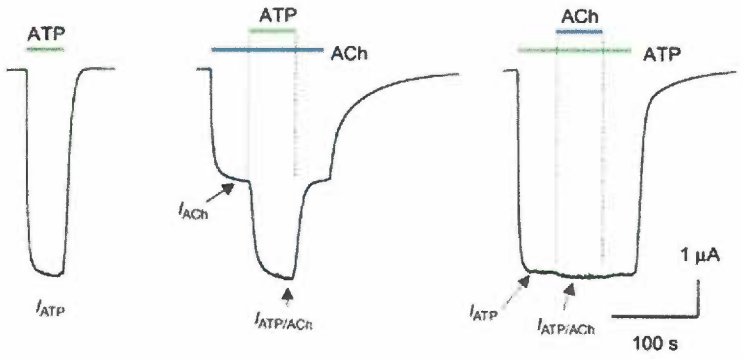
ATP
I_{ATP}
ATP
ACh
I_{ACh}
$I_{ATP/ACh}$
ACh
ATP
I_{ATP}
$I_{ATP/ACh}$
1 µA
100 s

	P2X1	P2X2	P2X3	P2X4	P2X5	P2X6	P2X7
P2X1	+	+	+	-	+*	+	-
P2X2		+	+*	-	+	+*	-
P2X3			+	-	+	-	-
P2X4				+	+	+*	-*
P2X5					+	+	-
P2X6						+	-
P2X7							+

Table 1-1: Potential heteromeric interactions among various P2X subtypes

Different combinations of P2X subtypes were assayed for co-immunoprecipitation of recombinant rat P2X receptors expressed in HEK 293 cells + and - indicates positive and negative co-immunoprecitpitation respectively [Table summarizes data from (Torres, Egan et al. 1999)]. Functional interactions with unique kinetic or pharmacological properties are noted with *. Note an interaction between P2X4 and P2X7 that was not revealed under these experimental but have been reported under other conditions (Guo, Masin et al. 2007). Also note that P2X5 potentially interacts with all other subunits exclusive of P2X7.

Figure 1-3: Sequence alignment of P2X subtypes

Multiple protein sequence alignment of the three subtypes of P2X receptors that modulate ASIC3: Red letters denote putative transmembrane spanning regions. Residues in white with black background denote location of truncation which did not affect modulation of ASIC3. * denotes conserved; : partially conserved; . partially homologous residues.

Note that most of the protein lies in the large extracellular loop with relatively small N- and C-terminal tails. Aligned using Clustal multiple sequence alignment.

```
                                                    TM1
P2X4      -MAGCCSVLGSFLFEYDTPRIVLIRSRKVGLMNRAVQLLILAYVIGWVFVWEKGYQETDS-VVSSVTTKAKGVAVTNTSQLGFRIWDV
P2X5      MGQAAWKGFVLSLFDYKTAKFVVAKSKKVGLLYRVLQLIILLYLLIWVFLIKKSYQDIDTSLQSAVVTKVKGVAYTNTTMLGERLWDV
P2X2      MVRRLARGCWSAFWDYETPKVIVVRNRRLGFVHRMVQLLILLYFVWYVFIVQKSYQDSETGPESSIITKVKGITMS-----EDKVWDV
                     :::*.*.:.:: :.::::*:: * :**:** *.: :**: :*.**: ::  *:: **.**:: :      ::***

P2X4      ADYVIPAQEENSLFIMTNMIVTVNQTQSTCPEIPDKTS-ICNSDADCTPGSVDTHSSGVATGRCVPFNESVK-TCEVAAWCPVENDVG
P2X5      ADFVIPSQGENVFFVVTNLIVTPNQRQGICAEREGIPDGECSEDDDCHAGESVVAGHGLKTGRCLRVGNSTRGTCEIFAWCPVETKS-
P2X2      EEYVKPPEGGSVVSIITRIEVTPSQTLGTCPESMRVHSSTCHSDDDCIAGQLDMQGNGIRTGHCVPYYHGDSKTCEVSAWCPVEDGT-
           ::* *.: . . ::*.: ** .*  . *.*     .  * .* ** .*.    . *: **:*:  ..   ***: ******

P2X4      VPTPAFLKAAENFTLLVKNNIWYPKFNFSKRNILPNITTSYLKSCIYNAQTDPFCPIFRLGTIVEDAGHSFQEMAVEGGIMGIQIKWD
P2X5      MPTDPLLKDAESFTISIKNFIRFPKFNFSKANVLETDNKHFLKTCHFSS-TNLYCPIFRLGSIVRWAGADFQDIALKGGVIGIYIEWD
P2X2      SDNHFLGKMAPNFTILIKNSIHYPKFKFSKGNIAS-QKSDYLKHCTFDQDSDPYCPIFRLGFIVEKAGENFTELAHKGGVIGVIINWN
              . :* * .**: :** * :***:*** *:   .. :** * :.  :: :******* **. ** .* ::* :**::*: *:*:
                                                                                          TM2
P2X4      CNLDRAASLCLPRYSFRRLDTRDLEHNVSPGYNFRFAKYYRDLAGKEQRTLTKAYGIRFDIIVFGKAGKFDIIPTMINVGSGLALLGV
P2X5      CDLDKAASKCNPHYYFNRLDN-KHTHSISSGYNFRFARYYRDPNGVEFRDLMKAYGIRFDVIVNGKAGKFSIIPTVINIGSGLALMGA
P2X2      CDLDLSESECNPKYSFRRLDP--KYDPASSGYNFRFAKYYKINGTTTTRTLIKAYGIRIDVIVHGQAGKFSLIPTIINLATALTSIGV
          *:** : * * *:* *.***     .  *.*******:**:      * * ******:*:** *:****.:***:**:.:.*: :*.

P2X4      ATVLCDVIVLYCMKKKYYYRDKKYKYVEDYEQGLS---------------GEMNQ-----------------------------------
P2X5      GAFFCDLVLIYLIRKSEFYRDKKFEKVRGQKEDAN---------------VEVEANEMEQERPEDEPLERVRQDEQSQELAQSGRKQNS
P2X2      GSFLCDWILLTFMNKNKLYSHKKFDKVRTPKHPSSRWPVTLALVLGQIPPPPSHYSQDQPPSPPSGEGPTLGEGAELPLAVQSPRPCSI
          .:.:** ::: :.*.  * .**:. *.  :.  .                        .

P2X4      ---------------------------------------
P2X5      NCQVLLEPARFGLRENAIVNVKQSQILHPVKT--------
P2X2      SALTEQVVDTLGQHMGQRPPVPEPSQQDSTSTDPKGLAQL
```

Chapter 2: Methods

Cell Culture

Chinese hamster (*Cricetulus griseus*) ovary (CHO) cells were cultured on 10cm plates in F12 medium (GIBCO) containing 10% heat inactivated fetal bovine serum (FBS) with or without 1% penicillin/streptomycin at 37 degrees C. Cells were grown to about 60% confluency and split at a 1:8 to 1:15 dilution every two to three days. Cells were resuspended by removal of media and application of 2.5mL warm Trypsin/EDTA mixture (0.5g/l trypsin, 0.2g/l EDTA, Fisher #BW17-161E) and incubation at 37 degrees for approximately 5 minutes. Trypsin was quenched by addition of 7.5mL F12 medium + 10% FBS. One-half to 1.2mL of the cell suspension was then added to a new 10cm plate containing 10mL of pre-warmed medium. The remaining cells were transfected for experiments. Cells were used generally from passages 4 through 15.

Freezing and thawing cells:

CHO cells were grown to approximately 70% confluency and stocks were frozen down. Cells were resuspended as described above. Suspended cells were transferred to a 15mL conical vial and centrifuged for 2-3 minutes at approximately 800 rpm to pellet cells in a Sorvall RT6000B swinging bucket centrifuge. The trypsin solution was aspirated and cells were resuspended in 1mL freezing medium containing 92% F-12 + FBS and 8% DMSO. The cell solution was then transferred to freezer eppendorf tubes and placed in an insulated cell freezer (Nalgene Cryo 1°C) in isopropanol and stored at -80°C to slow-freeze the cells to prevent ice crystal formation. Once frozen

cells are removed from cell freezer and stored at -80°C until needed. Cells are thawed rapidly in a 37°C water bath and immediately added to 10mL pre-warmed media in a 10cm tissue culture dish. Cells are allowed to adhere to the dish for 3-5 hours and then the media is aspirated to remove DMSO and new warm F-12 media media is added.

Transfection:

CHO cells were transiently transfected using electroporation. After suspending cells with trypsin and quenching with F-12 medium, cells were transferred to a 15mL conical vial and spun for 2 minutes at 800rpm to pellet cells. Supernatant was removed and cells were resuspended in 400-700uL of cold HBS electroportaion buffer.

HBS Electroporation buffer in 500mL:

NaCl	4.09g
Hepes	2.975g
Na_2CO_3	0.1g
pH	7.4 with NaOH

0.4 to 10ug of plasmid DNA containing ASIC, pCMV-DsRed-Express (Clontech) and P2X were added to a 0.4cm electroporation cuvette (Invitrogen) to this was added 100uL of resuspended CHO cells. Cuvette was placed in a BioRad Gene Pulser electroporator with capacitance extender. Cells were electroporated with voltage set

at 0.360V and capacitance set at 0.075mF for approximately 1 second. Cells were immediately transferred to room temperature F-12 medium in 35mm culture dishes containing 7 glass cover slips and incubated at 37 degrees Celsius in 5% CO2. Cells were used between 18 and 48 hours later.

Alternate transfection protocol:

Electroportation buffer was changed to 100 uL of serum free OPTI-MEM medium and voltage and capacitance were increased to 0.380V and 0.075mF (high viability) or 0.100mF (high efficiency) respectively. Otherwise, electroporation protocol was identical.

Lipid transfection:

For lipid transfections CHO or HEK cells were plated on 35mm tissue culture dishes or six well plates one day prior to transfection so that they were 80% confluent on the day of transfection. Medium was replaced with 1mL of OPTI-MEM about 1 hour prior to transfection. For each dish 1.5uL of Lipofectamine 2000 (Invitrogen) was added to 100uL of OPTI-MEM and incubated for about 5 minutes. This was added to 100uL of OPTI-MEM containing 1-2ug of plasmid DNA and incubated for 20 minutes at room temperature. The mixture was added to cells for three to five hours and then lipofection was quenched by adding the appropriate serum containing growth medium- F12 for CHO and DMEM for HEK. Cells were used 24 to 48 hours later.

Plasmids:

P2X1-7 were obtained from M. Voigt. ASICs were kindly provided by M Lazdunski. Both were driven by CMV containing promoters in JPA or PCI vectors. pCMV DsRed-express was purchased from clontech. JPA5-CFP and YFP and JPA5-NgCAM CFP and YFP were provided by G. Banker. YC3.1 and mCherry C1 were provided by W. Almers. GFP-ASIC3 was provided by Eric Gouaux. Chicken NgCAM is a neuronal cell adhesion molecule of 1280 amino acids in length containing a single transmembrane domain with a large extracellular N-terminus and relatively intracellular C-terminus {Buchstaller, 1996 #549}.

Cloning:

To fluorescently tag ASIC and P2X constructs, two EcoRI restriction sites were PCR amplified onto the N and C termini of each parent construct. The PCR amplified product was then ligated into JPA5-CFP or JPA5-YFP cloning vector (provided by G. Banker) into an EcoRI site.

Truncation mutations of P2X2 and P2X5 were constructed by by insertion of a stop codon using site directed mutagenesis to replace P2X2-H375Z CAT→TAG and P2X5 E381Z GAG→TAG.

Chimeric P2X DNA constructs were synthesized using a serial PCR approach with overlapping primers containing sequences homologous to P2X5 and P2X3 to create

various combinations of P2X5 and P2X3 containing C-terminal domain/ TM1, extracellular domain, and TM2/ N-Terminal domain.

Electrophysiology

Data were collected using an Axopatch 1B patch clamp amplifier from Axon Instruments with a CV-4 headstage with 0.1/100U gain, digitized using Axon Instruments Digidata 1322 converter and recorded on to a hard drive using Clampex 8.2 software. Data were generally collected at 10kHz and filtered at 2kHz using the Lowpass Bessel filter of the 1B amplifier. Rapid solution exchange was accomplished using computer driven solenoid valves with gravity flow. 10 solenoid valves were controlled by an Isolatch Valve Driver purchased form General Valve Corporation. One solution was switched off and another switched on simultaneously resulting in rapid solution switching.

Cells were visualized on a Nikon inverted microscope with a 10X Phase objective and 10X eyepieces. The DsRed was visualized by epiflourescence using a mercury arc lamp (Osram HBO103W/2) and a rhodamine filter set (Nikon DM580, excitation below 546 nm, emission above 590 nm). DsRed is maximally excited at 556 nm, and emits maximally at 586 nm.

Pipettes were pulled from Sutter borosilicate glass O.D.: 1.5mm, I.D.: 0.86mm and 10cm in length (BF150-86-10) containing filament and fire polished on the ends. A Sutter Instruments P-87 puller was used to pull pipettes which were polished on a

Narishige MF-83 microforge to a final tip resitiance of between 1.5 and 4 MΩresistance.

Fluorescent Imaging

Fluorescent imaging was carried out on an Olympus IX71 inverted microscope using a mercury arc lamp for fluorescent excitation and excitation filters described below (excitation: 436nm for CFP and 514nm for YFP from Chroma Technology Corporation). Images were acquired on a Princeton Instruments NTE/CCD camera that was cooled to -45°C controlled using Metamorph 6.2r6 software.

Fluorescent Resonant Energy Transfer (FRET) experiments were carried out by the donor dequenching method. Cyan fluorescent protein (CFP) conjugated protein was co-transfected with yellow fluorescent protein (YFP) conjugated protein. If the two proteins are in close proximity to one another (10-100nm), excitation of CFP (donor) will result in the fluorescence of YFP (acceptor) and loss of fluorescence for CFP. Therefore, destroying YFP by photobleaching will result in an increase in CFP fluorescence proportional to the closeness of the two fluorophores and the efficiency of resonant energy transfer. CFP fluorescence was measured by exciting transfected cells with a mercury arc lamp with light filtered through a 436/20 nm band pass filter and reflected off of a 450 nm long pass dichroic mirror. Fluorescent emission was detected by using a Dual View beam splitter with a 520 nm dichroic mirror to split CFP and YFP fluorescence and passed though a 485/25nm band pass filter for CFP and 535/25nm band pass filter for YFP/FRET/ and some CFP. This produced two

images, one of CFP only fluorescence centered around 485nm and one image containing YFP fluorescence from direct excitation, YFP from FRET excitation, and some long wavelength CFP fluorescence centered around 535nm. A second image was then acquired using a 514/10nm band pass filter to directly excite YFP. The resulting image was almost entirely YFP fluorescence. YFP was then photobleached for 4 times for 30 seconds. Two images (436 and 514 excitation) were taken after each photobleaching period. Fluorescence intensities were determined by outlining each cell and calculating the average intensity of the cell subtracted from the average background intensity using Metamorph software. Relative CFP fluorescence was then calculated and plotted as a function of YFP fluorescence remaining. The fraction of CFP that was quenched due to energy transfer to YFP was then calculated.

TIRF imaging

Total internal reflection fluorescence imaging was carried out on a Zeiss axiovert 135 TV inverted microscope to image expressed recombinant CFP and YFP conjugated membrane proteins. Helium/Cadmium (Kimmon IK series) and Argon/Krypton (Coherent, Innova 70C) lasers were used to excite the fluorophores using the laser lines of 442nm and 514nm to excite CFP and YFP respectively. To achieve total internal reflection, a high numerical aperture objective 60X NA= 1.49 was used (Olympus, APO N 60X 1.49). Total internal reflection of light produces a shallow evanescent field that extends into the sample being imaged up to approximately 200nm (Axelrod 1981; Steyer and Almers 2001). The angle of incident light was then

optimized to provide the shallowest evanescent field while maintaining brightness by moving the laser path with a focusing lens and mirror (Newport).

Photobleaching of the CFP fluorophore was a major problem when imaging in TIRF. A relatively small number of fluorophores are present, making detection more difficult requiring longer exposure times and more intense light. To find cells expressing higher amounts of protein, thus requiring less illumination and to identify transfected cells without bleaching CFP or YFP, soluble mCherry was co-expressed. The absorption and emission properties of mCherry are such that it is spectrally separated from CFP and YFP so that it will not interfere with imaging of those fluorophores, although FRET between YFP and mCherry is possible. A custom polychroic mirror which reflected the laser lines at 442, 514, and 568nm was used (442/514/658 ex, Chroma Scientific). Soluble mCherry was excited with the 568nm line to find and focus on transfected cells. Red transfected cells were identified by eye which allowed identification of the relatively bright and highly expressing cells, similar to the conditions used for electrophysiological experiments in which DsRed was co-expressed and those cells brightly expressing DsRed were recorded from. DsRed has relatively broad absorption and emission spectra potentially providing comtaminating fluorescence in the YFP and possibly CFP channel. Dim red fluorescence generally correlated with very small or non-existent currents, indicating very few or no functional channels on the cell surface, so these were avoided when imaging.

Images were collected using a quad view beam splitter (Optical Insights) with appropriate bandpass filters which spectrally split the image into four images, one CFP image (482/35, Semrock), two YFP images (530/40, Chroma) of opposite polarity, and one red image (650/75). Standard bandpass filters in the quad view were replaced as noted to maximize efficiency while preventing bleed though. A 514nm notch filter was required in the detection pathway to filter out excitatory 514nm light bleed-through which was not fully reflected by the polychroic mirror. Images were acquired using a cooled EMCCD camera (Cascade Quantum: 512C). One image of CFP (442nm ex/ 482/35em) and YFP (514 nm ex, 530/40 em) was taken before and after 30 photodestruction of YFP and then two additional images of CFP (442 ex) were taken to determine the rate of photobleaching of CFP due to image acquisition. Images were acquired in the following order: 442, 514, bleach 514, 514, 442, 442, 442 (excitation wavelength). To correct for photobleaching of CFP between the 1^{st} and 2^{nd} CFP (442nm) images due to image acquisition, the difference in intensity between the 2^{nd} and 4^{th} CFP images was measured and the intensity decrease per image was estimated. This was then added to the average intensity of the 2^{nd} CFP image to correct for bleaching. Any photobleaching casued by 514nm illumination was not accounted for.

Since separate lasers were necessary to excite CFP and YFP, care was taken to maintain consistent laser power and maintain co-linearity between the lasers. The power of both 514nm and 442nm lines was measured and set to 105nW for each experiment and the TRIF alignment was kept constant.

To increase cell density and image quality a few modifications in transfection protocol were made for TIRF imaging. Round #1.5 coverslips (Hoecht) were coated with Poly-L Lysine solution (Sigma) for about 1 hr and washed 3X with sterile water in a 35mm tissue culture dish. A 100µL drop of F12 + FBS was applied to each coverslip. After electroporation, transfected cells in serum free Optimem (100µL) were added to the F12 droplet and placed in the incubator for 45min – 1hr to allow cells to adhere to the coverslip. The dish was then carefully flooded with 2mL F12 + FBS and cells were incubated for 24-30 hrs. Since photobleaching in TIRF only bleaches a fraction of the total cell area, cells were fixed in 4% formaldehyde (diluted from 16% formaldehyde solution, Ted Pella) in calcium and magnesium containing PBS (GIBCO) for 20 minutes. Cells were washed 3X in PBS + Ca/Mg and stored at 4°C for 1-3 days in imaging media, or PBS + Ca/Mg. Fixation prevented diffusion of fluorophores into the TIRF field, which was apparent with soluble YC3.1 which did not show recovery of YFP fluorescence after photobleaching.

Muscle afferent sensory neuron preparation: McCleskey Lab protocol

DiI injection

A 5% stock solution of DiI was made by dissolving 5mg in 100µL DMSO. Stock was diluted in standard extracellular solution to 5%. Adult rats were anesthetized with halothane and injected with rat cocktail (0.1 mL/100 g body weight). Area around the thigh was disinfected with betadine. The skin was lifted with forceps and scissors were used to cut skin until the muscle was visible. 25-50 µL of DiI was injected into

each thigh muscle and incision was sutured. Rats were allowed to recover and returned to cage for 4 weeks prior to DRG dissociation to allow retrograde transport of DiI to the DRG cell bodies.

Detailed description of sensory neuron dissociation from lab protocol

There are five sections:

1) Media;
2) Surface coating materials;
3) Preparation and dissection;
4) Enzyme treatments and trituration;
5) Plating.

1) MEDIA

CMFHepes-Hanks for tissue dissociation.

Hanks Balanced salts without calcium or magnesium. 5 mM Hepes.

200 ml of 1X HBSS w/o Ca/Mg. 1 Hepes aliquot (1 ml). Filter.

Hepes-L15 media for storing cells in air.

- Full media: L15; 5 mM Na-Hepes; 5 mM glucose; 10% FCS; 50 U/ml Pen/Strep;
- 200 ml w/o NGF: 177 ml L15; 1 Hepes aliquot (1 ml); 180 mg D-glucose; 2 serum aliquots (20 ml); 2 P/S aliquots (2 ml 5000 U/ml)

- 20 ml w/ NGF (2.5 S) for 50 ng/ml: add one 1 µg aliquot (100 µl @ 10 µg/ml) to 20 ml complete media.

F12 media for storing cells in 5% CO_2.

- Full media: F12; 10% FCS; 50 U/ml Pen/Strep.
- 100 ml w/o NGF: 89 ml F12; 10 ml FCS; 1 ml P/S (5000 U/ml).
- 20 ml w/ NGF (50 µg/ml): add one 1 µg aliquot (100 µl) to 20 ml complete media.

Stock solutions and Aliquots (store in sterile tubes)

- FCS fetal calf serum, heat-inactivated. Hyclone is preferred source.

Make 10 ml aliquots in centrifuge tubes; heat-inactivate in 57°C water bath for 30 minutes; freeze at -20 °C; mark storage box with source, lot number, expiration date, aliquot date, and name.

- Pen/Strep: 1 ml aliquots of 5000U/ml pen/strep solution (TC supply). Freeze.
- NGF: 1 µg aliquots. Sigma 2.5 S NGF (N-6009). Add 1 ml F12 to the 10 µg vial of NGF. Divide into 10 100 µl aliquots. Freeze.
- 1 M Hepes. 1 ml aliquots of 1 M Hepes buffer solution (TC supply). Label and refrigerate.
- Glucose: 5 mM: 90 mg/100ml; 180 mg/200ml.

Sources of media etc.

All media are in the Tissue Culture supply refrigerator/freezers except: L15 media (Life Technologies/GIBCO 11415-064); NGF (Sigma 2.5 S NGF N-6009); glucose. Sterile microfuge tubes and pipette tips from Autoclavia. Sterile centrifuge tubes from Research Stores.

2) COATING SURFACES: poly-d-lysine / laminin

General: Coat sterile cover slips/ Petri dishes with poly-d-lysine solution and leave it overnight in refrigerator; meticulously rinse the surfaces, coat with laminin, always working at cold temps, and place in refrigerator for 5-24 hours; aspirate the laminin just before plating cells.

Important notes: 1) Laminin in solution must never get above a few degrees C or it will form a gel;

2) PDL and laminin should be stored in plastic, not glass;

3) don't treat PDL or laminin plates with UV lights, sterilize prior to application.

I. Poly-D-Lysine

1) Coating solution: 20 µg/ml (add 10 ml d.i. water to 100 µl aliquot).
2) Application: Cover surface with solution and store overnight, refrigerated. Classic number is 5 µg poly lysine per cm^2 of glass.

3) Removal: Aspirate the lysine and then rinse the cover glass 3-5 times with sterile water to remove the toxic bromide. Plates may be stored dry and coated for several weeks.

II. Laminin

1) Coating solution: 20 μg/ml.

Always use cold solution for reconstitution, always thaw laminin in the refrigerator and store excess stock laminin at –70 °C (for up to 6 mos). For coating entire plate surface, use 1 ml aliquots of 200 μg/ml and add 9 ml cold CMF Hanks to dilute. Each plate requires 1.5-2 ml. To coat only a small area, use 100 μl aliquots of 200 μg/ml and add 0.9 ml cold Hanks to dilute.

2) Application: Use dry, PDL-coated dishes. Set dishes on ice. Add desired amount diluted laminin to a cover slip, spread around the area being coated. Store refrigerated for at least 5 hours and preferably, overnight. Do NOT let it dry out (store with source of humidity).

3) Plating cells: Just before plating, remove dishes from refrigerator, aspirate laminin until plate is completely dry, and apply the cells.

Note: if cells are to be placed at a discrete location on a cover slip, cells should be applied with a pipetman after drying the cover slip very thoroughly.

III. Stock solutions

- Poly-D-lysine: 2 mg/ml (stock)

(Becton Dickinson, catalog no 40210)

Add sterile water to vial to make 2 mg/ml, aliquot in 100 µl quantities, store in PLASTIC, not glass, frozen at –20°C. 100 µl aliquots make 10 ml coating solutions (1:100 dilution=20 µg/ml).

- Laminin: 200 µg/ml (stock)

(Sigma, catalog no L-2020, 1 mg). Add 5 ml ice-cold CMF-Hanks solution to the 1 mg of laminin (200 µg/ml). Aliquot in desired quantities, store in plastic, freeze at –20°C for shorttimes or –70°C for long times. Always keep the laminin solution cold; avoid thawing once frozen. 100 µl aliquots make 1 ml (working dilution=20 µg/ml).

3) TISSUE RECOVERY

Preparation:

- Coated culture dishes (see above): one dish (35 mm glass bottom) for each adult ganglia.
- CMF (Ca/Mg-free) Hanks for all enzyme solutions.
- Complete media (F12 and L15 with additives).
- Dissection tools.

Dissection:

- Prep:

Chemical Hood: halothane, guillotine, animal bag, dissection dish.

Dissection Hood: Two 35 mm dishes with CMF Hank's; 10 ml syringe full of Hank's; dissection tools and 70% EtOH. Tools: Two big scissors, one big forcep, two fine forceps, small sharp spring scissors.

- In chemical hood, anesthetise animal with halothane and behead with guillotine. Hold the body firmly within a plastic bag until it stops twitching.
- Use large scissors and forceps to cut away fur and skin from the upper body. Cut through the shoulder muscles and remove arms. Then cut away the entire lower body immediately below the rib cage. Isolate the spinal cord and remove as much muscle tissue as possible.
- Use the 10 ml syringe to rinse the tissue with Hanks, removing any visible blood and hair.
- Use scissors to carefully cut away the anterior portion of the spinal cord. Cut as close to the ribs as possible, while leaving the spinal cord intact. Cutting too deep may sever the ganglia and cause them to be lost, while cutting too high will make them very difficult to remove around the ribs.
- Rinse the cord again with Hanks and transfer to the dissecting microscope for ganglia removal. The ganglia should be easily visible as white bulbs that exit the spinal cord and lay between the cord and the surrounding muscle tissue. Use the forceps and spring scissors to pluck out individual ganglia and transfer them to a dish of L15. For labeled cardiac cells, use

C8-T3; C8 is the one directly above the first rib. For labeled thigh muscle afferents, use L3-L6

- Clean up each ganglion by removing as much axonal tissue and dura mater as possible. Transfer to a fresh dish of L15.
- Cut the ganglia in half so that they will easily fit in a pasteur pipette.

4) ENZYME TREATMENT

- Enzyme preparation 1 (Papain)

item	final conc.	amt. to use
CMF Hanks		3 ml
L-cysteine	0.03%	1 mg (few crystals)
Na2HCO3 (saturated)	to pH 7.4	about 4 µl
Papain (Worthington Biochemical cat#3126)	20 U/ml	60 units (60 µl or 3 mg)

- **Enzyme preparation 2 (collagenase and dispase)**

Item	**final conc.**	**amt. to use**
CMF Hanks		3 ml

10 mM $CaCl_2$	25 µM	7.5 µl
Dispase II	0.4%	12 mg
(Roche Applied Science cat# 765859)		
Collagenase Type2	0.3%	9 mg
(Worthington Biochemical cat#4176)		
	pH 7.4	

A) Combine in centrifuge tube, then pass through a 0.2 µm filter syringe into a clean tube. Set aside.

B) Spin cells out of first enzyme solution at 2K RPM (level 4.5) for 3-5 min.

C) Discard supernatant, add enzyme solution 2.

D) Vortex; incubate 10-30 min gently mixing every ten minutes.

E) Prepare polished Pasteur pipettes including one with a narrowed tip for trituration.

F) When enzyme treatment is complete, fluid should appear grainy.

G) Spin cells, remove supernatant and add 3 ml F12 media to inhibit enzymes.

H) Gently agitate, spin, remove supernatant and resuspend in 1-2 ml F12 + NGF.

I) Triturate with fire polished pipette for 10-20 sec, passing the solution up and down through the pipette 6-7 times. It is NOT necessary to completely break up all pieces; doing so will result in less healthy cells.

5) PLATING

- After trituration put a 50 µl on a dish and look it in a microscope to determine cell density. Adjust volume as desired.

- Pre-plating: Transfer the solution to a Petri dish and incubate at 37° C for 30 minutes. Agitate the dish slightly to dislodge DRGs that may have stuck down. Transfer the cell suspension into a tube.
- Aspirate laminin from the surfaces.
- With the polished pipette, plate approximately 150 µl of the cell suspension into the center of each plate or enough volume to cover each cover slip.
- Incubate in the 37° incubator for 2-3 hours until most of the cells have stuck down.
- Feed with complete L-15 + NGF and store in room temperature humidified chamber for 2-3 days OR feed with F12 + NGF and store in the incubator.

Data Analysis:

Electrophysiolgy data were analyzed using Clampfit 8.0 software from Axon Instruments, compiled in Excel and plotted using Origin 7.

Reagents

Standard Extracellular Solution:

Compound	Formula weight	[mM]	10X In 500mL
NaCl	58.44	140	40.908
KCl	74.55	5	1.864
HEPES	238.3	10	11.192
MES	195.2	10	9.76
CaCl2	1M stock	Variable	
MgCl2	1M stock	variable	

10X stock was diluted to 1X in deionized water and calcium and magnesium were then added, generally to 1mM CaCl2 for pH tests and 2mM CaCl2 and 1MgCl2 for bath solutions and ATP solutions. Ph was adjusted to desired pH with 3M N-methyl glucamine (NMG) to avoid altering sodium concentrations.

Standard Internal Solution: Potassium Methane Sulfonate/ 10mM EGTA:

Compound	Formula weight	[mM]	1X in 25mL
KOH	1.0N stock	140	3.5mL
KCl	74.55/ 1M stock	10	250□L 1M stock
NaCl	58.44/ 1M stock	4	100□L 1M stock
MOPS	209.3	10	.0523g
EGTA	380.4	10	.0951

Use 1:10 dilution of Methane Sulfonic Acid to bring pH down to pH 7.0. Osmolarity should be about 305mOsm.

Calcium Activation Curve:

Standard Extracellular Solution was used with HEDTA or EDTA/ calcium added as indicated. NMG was then added to adjust pH to pH 8.0 after addition of calcium and calcium chelator. 100mM stock of HEDTA 3.72g/100mL and EDTA 2.78g/100mL were diluted 10X into solutions.

[Ca2+]free	HEDTA	EDTA	[Ca2+] total	1M CaCl2 in 25mL
1mM	-	-	1mM	25µL
100µM	-	-	100µM	2.5µL
10µM	10mM	-	9.40mM	235µL
3µM	10mM	-	8.23mM	205µL
1µM	10mM	-	6.06mM	151.5µL
100nM	10mM	-	1.33mM	33.25µL
10nM	-	10mM	6.31mM	157.75µL

Minimal Calcium activation curve solutions:

Standard extracellular solution was modified with 10mM EDTA and 2mM CaCl2 and pH adjusted to various pH values. The concentration of free calcium was calculated using the EGTAetc program as described in ( ). The calculated free calcium and pH are stated below (approximately 10nM free Ca^{2+}).

pH	[EDTA] mM	[Ca^{2+}] total mM	pCa [Ca^{2+}]free
8.0	10	2	8.83
7.8	10	2	8.63
7.5	10	2	8.31
7.3	10	2	8.10
7.0	10	2	7.76

6.0	10	2	6.36

Reagent concentrations used

Fluorescent size exclusion chromatography (FSEC)

CFP tagged ASIC3, P2X4 or P2X5 were expressed in HEK or CHO cells either alone or in tandem with either P2X4 or P2X5 in the case of ASIC3 CFP or with ASIC3 for the P2X4 CFP or P2X5 CFP channels. GFP-his ASIC3 (from Eric Gonzales) was co-expressed with P2X4 or P2X5. Cells were plated onto 35mm tissue culture dishes and transfected with lipofectamine 2000 and incubated for two days post transfection. Cells were suspended by incubation in phosphate buffered saline in the absence of calcium and magnesium and pelleted by a brief centrifugation. Cell pellet was resuspended in 150uL solublization buffer.

Solublization Buffer:	In 10mL
150mM NaCl	8.76mg
20mM C12M (dodecyl maltoside)	102.2mg
2mM CaCl2	40uL 500mM stock
20mM TRIS pH to 8.0	22.44mg
Protease inhibitors	1X concentration from stock

Membranes were solublized by rotating at 4 degrees for 1 hour. Non-soluble material was pelleted by centrifugation for 40 min at 40,000 rpm in a benchtop ultracentrifuge. Lysate was then carefully removed and put into the SEC autosampler. One hundred

μL samples were automatically injected into the column and run in a Running buffer identical to the solublizaiton buffer with only 1mM C12M.

Lysate was separated with fast protein liquid chromatography (FPLC) carried out using the following equipment from Shimadzu:

DGU-20A5 Degasser

LC-20AD liquid chromatograph

CBM-20A communications module

RF-10Axl fluorescence detector

SPD-20A Uv-Vis detector

SIL-20AC autosampler

The column was a Superose 6 10/300 GL size exclusion column from GE Biosciences run at 0.5mL/minute. GFP Fluorescence of the eluate was monitored by excitation at 450 nm and emission measured at 500 nm in-line with the column.

Analysis:

Electrophysiological analysis was done using Clampfit 9.2 software from Axon Instruments. Data were filtered if necessary, and baselines were zeroed. To measure current amplitude the peak current was determined by the Clampfit program as the average of 20 data points around the peak to eliminate noise contributions to peak amplitude measurements. All data was organized using Excel (Microsoft Office 2003) where data were averaged. Statistical analysis was performed using Origin 7 SR2 software from Origin Lab Corporation. All data were plotted using Origin 7. Dose response curve data were fit in Origin using the Hill Equation shown below.

Proton activation:

$$I_{pH}/Imax=Imax * \frac{pH^n}{pH_{50}^n + pH^n}$$

Calcium activation:

$$I_{[Calcium]}/Imax=Imax * \frac{[Ca^{2+}]^n}{[Ca^{2+}]_{50}^n + [Ca^{2+}]^n}$$

The Hill equation provides constants for half-maximal activation, Hill slope which measures cooperativity, and maximal current amplitude for each data set which are compared between different conditions.

Time constants of desensitization were determined by fitting the desensitizing phase of pH evoked current traces with a single exponential using Clampfit. The single exponential fit yielded a time constant τ which describes the rate of desensitization.

Single exponential decay: $A(t) = C + A_0 e^{-t/\tau}$

Time constants were then collected and organized using Excel, and graphing and statistics was done using Origin.

FRET was quantified using Metamorph software (MetaImaging). Regions of interest were selected and the average fluorescence intensity was determined. This was subtracted from the background fluorescence by subtracting the average intensity of a nearby area where there were no cells present. The relative fluorescence intensity of CFP was plotted as a function of relative YFP fluorescence and fit linearly. A linear fit was extrapolated to the point where no YFP remained and yielded a fractional increase in CFP fluorescence due to YFP photobleaching. This value was then used to find the efficiency of FRET which is a measure of the fraction of CFP fluorescence that is lost due to resonant energy transfer with YFP such that:

Efficiency= CFP increase/ CFP total

The efficiency of FRET is dependent upon the distance between fluorophores, the degree of spectral overlap between the two fluorophores and their relative orientations. No effort was made to estimate the distance between fluorophores since the stoichiometry was complex and calculations rely on assumptions of random fluorophore orientation which may not be applicable with membrane proteins which are spatially constrained. Thus efficiency was used only to quantitatively gauge whether or not FRET occurred.

For TIRF experiments bleaching of CFP during image acquisition was a problem. To roughly account for CFP photobleaching, the following protocol was employed. 1) One image was acquired using 442nm illumination (all images were the average of 5X 50ms exposures) before YFP photobleaching (514nm). 2) One image of YFP (514nm) was acquired before and after a 30 second bleaching period of YFP which

destroyed roughly 80% of the YFP. 3) Three images of CFP (442nm) were collected following photodestruction of YFP. 4) CFP photobleaching was estimated by measuring the decrease in CFP intensity of the three images acquired after YFP photobleaching and an average decrease in CFP intensity was estimated per image. 5) This estimated intensity loss was then added to the CFP intensity measured immediately following YFP photodestruction and the adjusted intensity of CFP after photobleaching was compared to the intensity of CFP before YFP photodestruction and a linear extrapolation to 100% YFP destruction was used to estimate the FRET efficiency.

Efficient FRET measurements using the acceptor photobleaching method require an equal or excess amount of YFP relative to CFP. To estimate stoichiometry of YFP: CFP expression levels, the positive FRET control yellow CaMeleon 3.1 was used. This contains YFP and CFP fused to opposite ends of calmodulin and a calmodulin binding domain and exhibits significant basal FRET. Since YFP and CFP are fused to the same protein, this construct has a 1: 1 ratio of YFP: CFP fluorophores assuming that both fluorophores are properly folded and fluorescent. The intensity of YFP before photodestruction and CFP after YFP photodestruction was measured and averaged and this intensity ratio was used as a standard of a 1:1 YFP: CFP ratio. Relative expression levels of YFP and CFP under other conditions were then estimated using this value. For TIRF experiments, this was done with each experiment to account for any slight intensity differences in laser power or TIRF illumination field since TIRF field thickness is dependent upon wavelength and the

two laser lines originated from different lasers and had independent power adjustments.

Estimates of stoichiometry of P2X2 and ASIC3 required for modulation were calculated using previously published single channel data. A modified version of Ohm's law was used:

$$I=n*P_o*\gamma*V$$

Rearranged so that:

$$n=I/(P_o*\gamma*V)$$

n is the total number of functional channels, I is current amplitude, P_o is the open probability γ is the single channel conductance and V is the potential $V_{holding}$-E_{rev}. A single channel conductance of 25pS—reported conductance 21 – 30 pS (Evans 1996; Ding and Sachs 1999), -70mV driving force, and open probability of 0.6 for P2X2, yields an estimate of about 950 P2X2 channels per nA ATP evoked current. Assuming a maximum open probability of 0.9, 15pS conductance, -120mV driving force and that IpH 6.9 is about 15% of maximal current yields an estimate of about 5000 ASIC3 channels/nA (pH6.9) (Sutherland, Benson et al. 2001; Immke and McCleskey 2003). These estimates of channels per nA of current were used to assess the number of functional P2X2 and ASIC3 channels in each cell for comparison with the degree of modulation.

Table 2-1: List of reagents used

Reagent	Stock (μM)	Final Concentration (μM)
2 methylthio-ATP		50
ADP		50
AMP-PNP	5000	50 external/5000 internal
Arachidonic Acid		20
ATP	50000	50
ATPγS		100
BzATP		100
C12M		20000/1000
Caffeine		10mM
CHS		200
CTP-AMP		100
Cyclopiazonic acid		10
Cyclosporin A	20000 in DMSO	40
Cytochalasin A	5000 in DMSO	5
DiI		5% in DMSO
DTSSP		2000
DTT		3000
Forskolin		10
GTP beta S		3000
GTP gamma S	1000	300
Ivermectin B1a	10000	1
Lactate		15000
Lysophosphatidyl choline		2.5
Methyl beta cyclodextrin		5000
NEM		10
Okadaic acid	500	0.5
Phenylarsine oxide		200
PIP2 long chain		10
PMA		1
PPADS	4000	4
SB203580		10
SNAP	100000 DMSO	100/1500
Sodium Nitroprusside	10000	10
Staurosporine		
Suramin	50000	100/150
TNP-ATP		0.3/ 50
U73122		10
UTP		50
αβ methylene ATP		50

Chapter 3: Results

ATP modulation of ASIC3 through a channel-channel interaction between ASIC3 and P2X5

Introduction:

The pain of a heart attack and the pain of a 40 second sprint both occur when oxygen-deprived, working cardiac or skeletal muscle releases a chemical signal that is detected by nearby nociceptive (pain-sensing) nerve terminals(Lewis 1932). Acid sensing ion channels (ASIC) (Krishtal 2003; Wemmie, Price et al. 2006), particularly ASIC3 (Waldmann, Bassilana et al. 1997), are thought to be sensors for the lactic acidosis created by anaerobic muscle metabolism because of their high density on ischemia-sensing neurons(Benson, Eckert et al. 1999; Molliver, Immke et al. 2005), their extreme acid sensitivity(Waldmann, Bassilana et al. 1997; Sutherland, Benson et al. 2001; Yagi, Wenk et al. 2006), and their ability to detect lactic acid at lower concentration than other acids(Immke and McCleskey 2001). However, lactic acid is only one of many possible mediators of ischemic pain(Longhurst, Tjen et al. 2001). Its role is particularly controversial (Meller and Gebhart 1992; Kaufman 2003) because the drop in extracellular pH during muscle ischemia is small (from pH 7.4 to ca. 6.8(Cobbe and Poole-Wilson 1980; Momomura, Ingwall et al. 1985)) and can occur systemically with kidney or lung pathologies that do not cause muscle and cardiac pain. Acid was found to be necessary but not sufficient to excite ischemia sensitive cardiac afferents in decerebrate cats suggesting other mediators in addition to acid are involved in ischemia sensing (Pan, Longhurst et al. 1999). This acid paradox might be resolved if another compound released from ischemic muscle

works synergistically with acid. Here it is shown that extracellular ATP, which reaches high levels when muscle works in low oxygen (Forrester 1972; Clemens and Forrester 1981; Mo and Ballard 2001; Li, King et al. 2003), dramatically increased ASIC currents that were evoked at physiological pH (7.1-6.8) in rat sensory neurons. At or above 1 micromolar, ATP acted by increasing ASIC sensitivity to pH; the effect took tens of seconds to develop and ASIC current remained elevated many minutes after removal of ATP. Surprisingly, the binding site was an ATP-gated ion channel, a P2X receptor, although flux through the P2X channel was irrelevant for modulation. ASIC modulation was reconstituted in mammalian cell lines using P2X2, P2X4 and P2X5 receptors, but not P2X1 or P2X3. Comparison of the responses in native rat neurons and in cell lines implicated P2X5, an electrically quiet ion channel that has not previously been ascribed a function in sensory neurons. The mechanism of modulation does not involve common second messenger pathways, rather it likely involves a physical interaction between ASIC and P2X. Thus ASIC3 can function as a coincident detector of ischemia by sensing acid, lactate and ATP through its interaction with a P2X channel. Furthermore, the long lasting effect of ATP modulation provides a temporal integration of coincidence outlasting the transient appearance of ATP which is rapidly degraded by ectonucleotidases.

Results:

ATP modulated ASIC3-like currents in sensory neurons.

Seeking to resolve the paradox of acid being necessary but not sufficient to excite ischemia sensitive nociceptors and moderate pH changes not being sufficient to cause

ischemic pain, other metabolites that might be released from muscle to act on nearby sensory nerve endings were considered. Currents evoked in response to moderate pH tests (pH 6.8) in sensory neuron cultured from dorsal root ganglion (DRG) of adult rats were studied using whole cell voltage clamp techniques. ASIC3 is the only rat ASIC that responds when pH changes to the vicinity of 7.0(Sutherland, Benson et al. 2001; Yagi, Wenk et al. 2006), so such currents are termed "ASIC3-like". ATP, applied transiently in the extracellular medium, increased ASIC3-like currents in most, but not all, sensory neurons that expressed the current (Fig. 3-1a). Sensory neurons that innervated skeletal muscle (skeletal muscle afferents) were fluorescently labeled by injecting DiI into the thigh muscle of anesthetized rats. The dye was allowed to be transported to the cell bodies in the DRG for about two weeks at which time the DRG were dissected, cultured and fluorescently labeled DRG were examined (Fig. 3-1a inset). ATP modulated 64% of the muscle afferents that had ASIC3-like currents (Fig. 3-1b. Mean increase 2.3 fold +/- 0.15 s.e.m.). Though many muscle afferents are small ($\leq$30 μm), the larger cells ($\geq$35 μm) were more likely to respond to ATP, suggesting that ATP acted on myelinated afferents. The ATP dependence of modulation appeared to be an all or none process. No effect was seen with 0.1 μM ATP, whereas 1 μM gave essentially maximal enhancement (Fig. 3-1c), though lower concentrations of ATP took longer for modulation to reach a peak.

Modulation was slow, persistent and desensitizing.

ATP acts with a time course (Fig. 3-1d) that had three key features: 1) modulation by ATP (50 μM) took 30-80 seconds to reach maximum; 2) currents remained elevated

above baseline for minutes after removal of ATP; 3) the slow return to baseline was actually a desensitization that proceeded whether ATP was present (not shown) or absent. Thus, ATP action was slow, persistent, and desensitizing. We could evoke the full ATP response only once on each cell in our experimental conditions. ATP failed to increase ASIC currents if they were evoked at or near the peak of their activation curve (~ pH 6, Fig. 3-1e). Thus, ATP altered the acid sensitivity of ASICs, not their density or conductance. The pH where modulation was evident (7.1 to 6.8) coincides with the range reached in extracellular spaces during heart attack and severe muscle exercise (Cobbe and Poole-Wilson 1980; Momomura, Ingwall et al. 1985).

The binding site for ATP is a P2X channel

The identity of the binding site for ATP was investigated. Some cells that expressed ASIC3-like current were not modulated by ATP, so the binding site could not be the ASIC channel itself. The slow and persistent time course suggested P2Y receptors, which are ATP-activated, G-protein coupled receptors. This was ruled out because modulation failed to occur with either ADP or UTP (Fig. 3-2), compounds that activate the various P2Y receptors as well as or better than ATP(Abbracchio, Burnstock et al. 2006). Considering P2X receptors—ATP-activated ion channels—αβmethylene-ATP, which activates the two channels (P2X3 homomers and P2X3/2 heteromers) that carry ATP-evoked currents in rat sensory neurons(Lewis, Neidhart et al. 1995; Khakh and North 2006) failed to modulate ASIC current. Thus, neither ASICs, nor P2Y receptors, nor the dominant P2X receptors on sensory neurons were the binding sites for the ATP that modulates ASIC3-like current.

Two traditional (and somewhat non-selective) P2 antagonists, suramin and PPADS, both blocked the action of ATP, as did high concentrations of trinitrophenol-ATP but not the low concentrations that selectively affect P2X3-containing channels (Fig. 3-2). Two agonists, ATPγS and 2methylthio-ATP, successfully modulated ASIC current whereas benzoyl-ATP did not. This pharmacological profile of agonists and antagonists fit P2X2 and P2X5, but none of the other five homomeric rat P2X receptors (Gever, Cockayne et al. 2006).

Various combinations of recombinant ASIC and P2X were expressed in several mammalian cell lines (Fig. 3-3). ASIC3 transfected alone showed no modulation by ATP, but there was robust modulation if P2X2, P2X4, or P2X5 were co-transfected with ASIC3. P2X1 and P2X3, as well as P2X2 when it forms heteromers with P2X3, failed to modulate. ASIC1 channels could also be modulated through P2X receptors.

Evidently, activation of certain ATP-gated ion channels alters sensitivity of a different molecule, an acid sensing ion channel. There are several other examples of P2X receptors directly altering another type of ion channel: nicotinic acetylcholine receptors (Khakh, Zhou et al. 2000), 5HT3 channels(Boue-Grabot, Barajas-Lopez et al. 2003), and GABA channels (Boue-Grabot, Emerit et al. 2004). The effect here is different in two ways. First, the P2X receptor enhanced ASICs, whereas it inhibited the other channels. Second, the other channel-channel interactions all occurred immediately upon application of ATP and reversed immediately upon removal. Here,

modulation built slowly and remained long after removal of ATP. Most significantly, enhancement of ASICs by ATP occurred only once in a given cell in our experimental conditons. In sensory neurons and HEK293 cells, the enhancement desensitized (eg. Fig. 3-1d) and ATP sensitivity was lost. In COS and CHO cells, the enhancement persisted without desensitizing for as long as we were able to record (ca. 1 hour, see figure 4-2) and it could not be increased further by ATP.

ATP hydrolysis was irrelevant to ASIC modulation because modulation occured with the non-hydrolyzable agonist AMP-PNP (tested on P2X4 channels) and in the absence of external Mg^{2+} (Fig. 3-4). Flux through the P2X channel appeared irrelevant because modulation occurred equally well whether membrane voltage forced the current inward or outward (Fig. 3-4a) through the P2X channel. Modulation in sensory neurons was Ca^{2+}-independent, occurring even with Ca^{2+} chelators both outside and inside the cell and with intracellular Ca^{2+} stores depleted (Fig. 3-4b). This property—Ca^{2+} independence—was reproduced in cell lines transfected with P2X4 and P2X5 receptors, but not P2X2. Modulation by P2X2 failed if there is no extracellular Ca^{2+}, though it occurred without intracellular Ca^{2+}.

P2X5 resembled the endogenous P2X modulator of ASIC3-like currents in sensory neurons.

P2X currents in sensory neurons exhibited a variety of waveforms, but nothing about the waveform predicted whether ASIC modulation would occur (Fig. 3c). The large, transient currents carried by P2X3 channels were irrelevant to ASIC modulation, and

modulation could occur even when ATP-evoked current was barely discernable (lower cell, Fig. 3c). This contrasts with reconstituted P2X2/ASIC3: no modulation occurred if P2X2 current was below 1 nA, and modulation increased linearly with increasing current out to 20 nA (squares, Fig. 3e). Substantial modulation occurred in sensory neurons even though they had only modest persistent P2X current (triangle, Fig. 3e). Transfected P2X5 channels mimicked this property (circle, Fig. 3e) because, even with high expression density, they pass little current(Collo, North et al. 1996) (Fig. 3d). We conclude that the relevant P2X receptor in rat sensory neurons is electrically quiet—it generates little or no current. P2X5 meets this criterion. In another context, P2X5 receptors, acting independently of their ability to pass current, are proposed to mediate ATP-induced differentiation of skeletal muscle stem cells via activation of a kinase cascade(Ryten, Dunn et al. 2002).

Table 3-1 lists the nine pharmacological or kinetic properties that were identified on native neurons and tested on six different P2X channels expressed in cell lines. P2X5 satisfies each property, whereas P2X2 and P2X4 each fail in two respects: they each generate large currents; modulation by P2X2 requires external Ca^{2+}; P2X4 activation is not blocked by suramin or PPADS. Thus, P2X5 is the likely mediator of ASIC modulation in rat sensory neurons. However, P2X5 protein has not been demonstrated in sensory neurons, although its mRNA has(Collo, North et al. 1996; Kobayashi, Fukuoka et al. 2005). To address this, P2X5 antisera were raised and characterized. The distribution of P2X5 among sensory neurons was compared to ASIC3 and to P2X2. Most neurons that stained brightly for P2X5 also stained

brightly for ASIC3 (Figure 3-5, left). There was far less overlap between P2X2 and ASIC3 (Figure 3-5, right). Blind counts of all labeled cells (both bright and dim) in sections from 3 rats found that 25% of sensory neurons were P2X5-positive and just over 50% of these also stained for ASIC3. This is twice what would occur by chance, as 26% of all neurons were ASIC3-positive. Although P2X2 antisera labeled a similar fraction (27%) of neurons as P2X5, only 10% of them were ASIC3-positive. P2X2-positive neurons were small (30 micrometer average equivalent diameter), whereas P2X5-positive and ASIC3-positive neurons were clearly larger (36 and 42 micrometer average, respectively; double-labeled cells averaged 40 micrometer). P2X5 protein was indeed expressed in sensory neurons and, unlike P2X2, was expressed together with ASIC3 in a substantial fraction of cells.

While P2X5 was likely the endogenous P2X modulator of ASIC3-like currents in DRG, it is possible that other P2X modulate ASIC3 occasionally. One labeled skeletal muscle DRG that expressed ASIC3-like currents was modulated by ATP and carried a P2X current that resembled P2X4 (Figure 3-6). The presence of P2X4-like currents does not exclude the possibility that this neuron also expressed P2X5, however. Aside from this one observation, data were consistent with P2X5 being the primary P2X modulator of ASIC3.

Common second messengers do not mediate modulation of ASIC3

The slow and persistent modulation of ASIC3 by P2X suggested a second messenger may be involved in modulation, so the involvement of any common signaling

pathways was investigated. P2X5 dependent modulation of ASIC3 was examined, since it was the P2X receptor likely to modulate ASIC in sensory neurons. The most common signaling mechanisms generally associated with ion channels involve calcium influx and activation or kinases or G-proteins through numerous intracellular pathways. No requirement for calcium influx, or even intracellular calcium dynamics was found. By lightly buffering intracellular calcium with EGTA (0.1mM) and incubating cells in caffeine, intracellular calcium levels should increase. This had no effect on modulation, neither mimicking nor inhibiting it (Figure 3-7c). Conversely, clamping calcium concentrations at a low level by removing all extracellular calcium, chelating calcium intracellularly with BAPTA (10mM), and depleting intracellular stores of calcium with cyclopiazonic acid (CPA, 10μM) (Figure 3-7a, b) resulted in no change in P2X5's ability to modulate ASIC3. Thus it appears that calcium influx played no role in modulation by P2X5, though, as demonstrated previously there was a requirement for extracellular calcium in the case of P2X2 modulation of ASIC3.

The role of kinases, phosphatases or G-proteins in modulation was investigated. Standard intracellular solution was supplemented with a solution containing the non-hydrolyzable ATP analogues AMP-PNP (5mM) or ATPγS (5mM) and no influence on modulation was found, suggesting no role for ATP hydrolysis and therefore kinases (Figure 3-8). Likewise, phosphatases appeared to play no role as okadaic acid (500nM) and cyclosporine A (40μM), two general protein phosphatase inhibitors did not affect modulation. Constitutively activating or inhibiting G-proteins with the non-hydrolyzable GTP and GDP analogues, GTPγS or GDPβS to constitutively activate

or inhibit G-proteins respectively, had no effect. Hydrolysis of extracellular ATP was not necessary since the non-hydrolyzable ATP analogue AMP-PNP and ATP in the absence of magnesium both activated P2X4 and modulated ASIC3 (Figure 3-9 a, b).

The most common signaling pathways therefore appeared not involved in modulation of ASIC3 which suggested that perhaps, as with P2X2 and numerous other channels, there was a direct physical interaction between P2X5 and ASIC3. Tables 3-2 and 3-3 summarize the results of various pharmacological manipulations of signaling pathways found to not be involved in modulation in cell lines of sensory neurons respectively.

Nitric Oxide donors were recently reported to modulate ASICs (Cadiou, Studer et al. 2007). The nitric oxide donor S nitroso-acetyl penecillamine (SNAP) was found to have no effect on ASIC3 when 100μM SNAP was used under standard buffer conditions with SNAP present only in the bath and not in the pH 6.9 test solution. Increasing SNAP concentration to 1.5mM resulted in modulation of ASIC3 that was consistent with a pH artifact (Figure 3-10a). SNAP added only to the bath solution decreased pH evoked current amplitude. SNAP added to only the pH 6.9 test solution increased the amplitude of the pH evoked currents and SNAP in both the bath and test solutions had intermediate effects. In contrast, bath application of SNAP inhibited ATP (50μM) evoked currents carried by P2X4 which reversed slowly over the course of several minutes indicative of a real covalent modification. This effect on ASIC3 is easily explained if SNAP decreased the pH of the bath solution (desensitization), the

test solution (potentiation) or both bath and test solutions (intermediate). The pH of the bath solution was measured and found to have decreased from 7.42 to 7.19 (Table 3-3). SNAP solutions were then made in buffer conditions similar to the conditions used in the report of SNAP induced modulation of ASICs and the effect of 100μM SNAP on the pH of various test solutions was measured over time (Table 3-4). As expected SNAP decreased the pH of the solutions over time, presumably as nitric oxide is evolved. SNAP appears to have no real effect on ASIC3 and thus nitric oxide is not likely responsible for modulation of ASIC by P2X.

With common signaling pathways ruled out as a mediator of P2X modulation of ASIC, several approaches were undertaken to examine whether a physical interaction was involved in mediating the modulation of ASIC3. Firstly, several collaborators attempted to co-immunoprecipitate ASIC3 and P2X5 or P2X2. Two groups found that ASICs had a tendency to aggregate and thus P2X2 as well as any negative control proteins would immunoprecipitate with ASIC3. A third group found no evidence for an interaction between ASIC3 and P2X5 under conditions that did not result in non-specific aggregation of ASIC3 and P2X5. Importantly, while P2X2 and the nicotinic receptor are thought to couple directly through a physical interaction, they have not been successfully co-immunoprecipitated. Given the conflicting results, the lack of successful co-ips involving other P2X channel interactions and information from researchers familiar with immunoprecipitation of P2X receptors, it was determined that co-immunoprecipitation was unreliable and even a positive result would have to be approached with caution.

FRET occured between ASIC3 and P2X5

Fluorescent resonance energy transfer (FRET) is a sensitive assay to look for close association of proteins in intact cells without the need to solublize and extract the channels from their normal environment within a lipid bilayer, which could potentially destabilize weak interactions or cause aggregation of proteins unstable outside of their native environment. FRET occurs when excitation of one fluorophore (donor) results in excitation of a second fluorophore (acceptor) that has an excitation spectrum that overlaps the emission spectrum of the donor fluorophore. This results in fluorescent emission from the acceptor fluorophore (of longer wavelength) and a decrease in donor fluorescence. The efficiency of energy transfer between the two fluorophores is proportional to the degree of spectral overlap between the donor emission and acceptor excitation, the sixth power of the distance between the fluorophores, and their relative orientations. The steep distance dependence of FRET efficiency makes FRET useful for examining interactions that are between 10 and 100 angstroms, a molecular scale. P2X5-CFP and ASIC3-YFP were constructed and found to interact functionally (figure 3-11).

To determine whether FRET occurred between a P2X5-CFP and ASIC-YFP the donor dequenching method was used. This involved measuring the fluorescence intensity of CFP before and after photodestruction of YFP. If FRET is occurring, some of CFP's resonant energy will be transferred to YFP. When YFP is photodestroyed, it is expected that there would be an increase in CFP fluorescence.

Epifluorescence microscopy was used to measure the fluorescence intensity of the entire cell. Photobleaching of YFP occurred over several minutes and resulted in an increase in CFP fluorescence of approximately 20% (Figure 3-12a). CFP and YFP were imaged before and then following each of 4 30-second photobleaching periods (using appropriate filters as describe in methods). The increase in CFP fluorescence was proportional to the decrease in YFP, as would be expected if the CFP increase is a direct result of loss of YFP fluorescence. The increase in CFP fluorescence was substantial but less than that of Yellow CaMeleon 3.1 (YC3.1), a CFP and YFP fused to opposing ends of calmodulin and a calmodulin binding domain peptide which served as a positive control (Miyawaki, Griesbeck et al. 1999). In contrast with P2X5/ ASIC3 and YC3.1, P2X5-CFP expressed alone or P2X5-CFP co-expressed with the neuron-glia cell adhesion molecule (NgCAM) fused to YFP showed little to no increase in CFP fluorescence. NgCAM-YFP, an axonal cell adhesion molecule involved in neurite outgrowth, cell adhesion and growth cone guidance {Buchstaller, 1996 #549}, is a large membrane spanning glycoprotein with YFP fused to the intracellular C-terminal end which served as a negative control. Extrapolation of the linear fit of CFP increase relative to fraction of YFP photodestroyed (Figure 3-12b) to 1.0 (where 100% of YFP is photodestroyed) yielded an estimate of the total increase in CFP fluorescence possible. Comparing the increase in CFP fluorescence to the total CFP fluorescence provided a measurement of FRET efficiency (Figure 4-13d, P2X5 CFP alone efficiency was calculated as if ASIC3 YFP had been present based on the rate of photodestruction of ASIC3-YFP). FRET is proportional to the distance between fluorophores but it is difficult to determine the average distance between

fluorophores in this case— functional channels contain three subunits each with a fluorophore with unknown stoichiometry between channels— but it can be said with confidence that a substantial fraction of P2X5 CFP localized within 10-100 angstroms of ASIC3 CFP. To put the average distance between fluorophores into perspective, the widest distance between two subunits in the extracellular domains of the recently solved crystal structure of ASIC1 is 85 angstroms (Jasti, Furukawa et al. 2007) and the distance across the beta barrel structure of GFP protein is 40 angstroms (Ormö, Cubitt et al. 1996). Since FRET efficiency decreases with the sixth power of distance between the fluorophores, it is reasonable to assume that most CFP fluorophores were associated on a scale consistent with a direct channel-channel interaction. Thus the channels appeared physically coupled on a molecular scale.

Epifluorescence microscopy has the drawback that the entire cell is illuminated and therefore the fluorescence of channels on both the plasma membrane and intracellular membranes were imaged. There was clearly surface expression of both P2X5-CFP and ASIC3-YFP measured optically and electrically but there appeared to be a substantial amount of protein that was not localized to the plasma membrane. This contributed to a large amount of unfocused fluorescence and may generate false-positive interactions due to concentration of channels in intracellular compartments. Non-specific concentration of fluorophores was probably not the source of FRET between ASIC3 and P2X5, since P2X5-CFP and NgCAM-YFP did not demonstrate FRET yet were expressed at a similar density, nevertheless it is possible that FRET between ASIC3 and P2X5 occurred only in intracellular compartments. The best way

to ensure that imaged receptors that are on the plasma membrane is through total internal reflection fluorescence (TIRF) microscopy.

TIR microscopy utilizes laser light focused on the edge of a high numerical aperture objective which is reflected off the interface between the coverslip and sample. A small amount of incident light creates an evanescent field which decays exponentially as a function of distance from the coverslip so that only fluorophores within about 200nm of the coverslip-sample interface are excited (Axelrod 1981; Steyer and Almers 2001). This greatly reduced background fluorescence and allowed for the imaging of cell-surface localized channels. For TIRF experiments, P2X5-CFP and ASIC3-YFP were co-expressed with soluble mCherry. The red mCherry fluorophore was excited using 568nm light to identify and focus on cells that were robustly expressing recombinant fluorophores to prevent bleaching of the CFP and YFP before image acquisition. Cells were fixed with 4% formaldehyde to prevent diffusion of fluorophores into and out of the TIRF field. P2X5-CFP and ASIC3-YFP were imaged using TIRF microscopy and a photobleaching protocol similar to that described previously was used except that a single time-point of photobleaching was obtained. This was due to the fact that both YFP and CFP bleached rapidly in TIRF and prolonged bleaching of YFP had the potential to bleach CFP as well. Approximately 70% of the YFP was photodestroyed after a 30 second illumination with 514nm light. TIRF revealed that ASIC3 organized into clusters. When P2X5-YFP was co-expressed, it also concentrated in clusters that co-localized with ASIC3-CFP on a sub-cellular level (Figure 3-13). P2X5-CFP and NgCAM-YFP did not appear to co-

localize and P2X5-CFP did not appear qualitatively to form the same clusters in the absence of ASIC3, though this was not quantified or rigorously investigated.

FRET measurements using TIRF microscopy demonstrated that P2X5-CFP undergoes FRET with ASIC3-YFP (Figure 3-13b, e). Destruction of YFP increased CFP fluorescence in cells expressing P2X5-CFP/ ASIC3-YFP, ASIC3-CFP/ ASIC3-YFP or YC3.1 to a greater extent than P2X5-CFP alone or P2X5-CFP with NgCAM-YFP. Comparison of FRET efficiency using both epifluorescent and TIRF microscopy with various fluorophores are summarized in Figure 3-13d. FRET was slightly less efficient in TIRF with both YC3.1 and P2X5-CFP/ ASIC3-YFP but the reason for the difference is not clear. Cells used in TIRF experiments were fixed 1-3 days prior to imaging and co-expressed soluble mCherry. Imaging CFP in TIRF caused a bleaching with the acquisition of each image. This was accounted for by averaging the rate of CFP bleaching from 3 images taken after destruction of YFP to estimate CFP intensity loss due to imaging. It is possible that the estimate of CFP bleaching, fixation or mCherry co-expression resulted in lower FRET efficiency measurements. Nonetheless, P2X5-CFP and ASIC3-YFP expressed on the plasma membrane underwent FRET with moderate efficiency (9.5%) again supportive of the hypothesis that P2X5 modulated ASIC3 by a direct channel-channel interaction.

To look for further evidence of a stable interaction between proteins, fluorescent size exclusion chromatography (FSEC) was used. FSEC couples a fluorescence detector with fast protein liquid chromatography (FPLC). FPLC uses moderate pressure with a

size exclusion column to rapidly separate proteins based on size. This allowed the separation of monomeric and multimeric proteins and has been used on both P2X and ASIC channels (Kawate and Gouaux 2006). GFP-ASIC3 was expressed alone or co-expressed with P2X4. P2X4 was used because it expressed robustly and didn't decrease ASIC3 expression. Membrane proteins were extracted using dodecylmaltoside, isolated from insoluble material and loaded onto the FPLC column. A truncated GFP tagged chicken ASIC1 that was used in the recently reported ASIC crystal structure was used as a positive control. The chromatogram pictured displays fluorescence intensity as a function of time. Larger proteins or complexes will pass through the column and be eluted more quickly. Interestingly, when P2X4 was co-expressed with ASIC3, the GFP-ASIC3 was retained in the column longer (Figure 3-14). This suggested that GFP-ASIC3 was smaller in the presence of P2X4, perhaps monomeric instead of the functional trimeric channel. If P2X4 wire simply interacting with ASIC3, a larger protein complex would be expected be form which would have eluted at an earlier timepoint. P2X4 could have destabilized interactions between ASIC3 subunits resulting in fewer multimeric complexes. More experiments are necessary to determine if this is a real result and if it has functional significance. It was not investigated further since the results were not definitive.

Stoichiometry of modulation

It was possible to roughly estimate the average number of channels expressed and gauge the stoichiometry of P2X2 to ASIC3 from data which correlated the percent

increase in ASIC3 current and P2X2 current amplitude (Figure 3-4e) as described in the methods section. Using estimates of 950 P2X2 channels/ nA (ATP 50μM) and 5000 ASIC3 channels/ nA (pH 6.9) with data collected when co-expressing ASIC3 and P2X2 allowed for plotting P2X2:ASIC3 channel ratio versus the percent modulation. While this was an extremely rough estimate, actual channel ratios were probably within about 2-4 fold of the estimate. The degree of expression of ASIC3 and P2X2 varied widely but there was a correlation between greater proportional P2X2 expression and increasing modulation. Modulation was most efficacious when the ratio of P2X2:ASIC3 was greater than about 0.5 (Figure 3-15), as would be expected for a physical interaction, and contrasting with most signaling processes which display large amplification steps. Modulation increased with excess P2X2 suggesting that the interaction between ASIC3 and P2X2 may be relatively weak or have stoichiometry beyond a 1:1 ratio of P2X2:ASIC3. Since both ASIC and P2X are thought to form trimeric functional channels, a direct physical coupling could require anywhere from a 1: 3 to 3: 1 ratio of P2X: ASIC. While the estimates of channel number are rough, they are consistent with a direct physical interaction between P2X and ASIC being responsible for modulation of ASIC3 proton sensitivity.

Functional coupling of subpopulations of ASIC and P2X

FRET measurements demonstrated a physical coupling between ASIC and P2X. If the physical association between ASIC and P2X was necessary for modulation, functional coupling between discrete ASIC and P2X channels would be expected, while a diffusible second messenger would result in a general modulation of ASICs

when discrete P2X were activated. This may be investigated by asking if two separate populations of P2X modulate ASIC in an occlusive manner, that is, does activation of one population of P2X cause modulation which then prevents modulation by a second population. Occlusion is a common assay for second messengers, whereby activation of a pathway by one trigger prevents further activation by a second trigger. This is primarily due to the large amplification steps that normally occur with second messengers resulting in a maximal response when only a fraction of initiators are activated. While P2X5 has been reported to potentially interact with both P2X2 and P2X4, P2X2 and P2X4 were not found to associate as judged by co-immunopreciptation studies of recombinant channels (Table 1-1, (Torres, Egan et al. 1999)). P2X4 is unique among P2X subtypes in its insensitivity to suramin (Bo, Zhang et al. 1995). Indeed, P2X2 was inhibited by the non-selective P2 antagonist suramin while P2X4 was not (Figure 3-16). Co-expression of P2X2 and P2X4 resulted in both suramin sensitive and suramin insensitive currents, demonstrating the presence of two distinct populations of P2X receptors.

By adding ATP (5μM) first in the presence of suramin (150μM), all ASICs that are available to P2X4 could be modulated. Washout of suramin followed by a second application of ATP (50μM) should then all remaining P2X, largely P2X2 and those P2X4 that were not previously desensitized. When this protocol was carried out on cells expressing ASIC3 with P2X2 and P2X4 there was clear biphasic modulation (Figure 3-17). Each phase was nearly equal in amplitude to the modulation by P2X2 and P2X4 expressed individually indicating an inability of P2X4 to occlude P2X2

dependent modulation. A biphasic response was not seen when ASIC3 was co-expressed with either P2X2 or P2X4, only when both P2X were expressed this suggested that P2X2 and P2X4 interacted with unique subsets of ASIC3 as would be expected for a physical interaction. In addition to a lack of occlusion, indicating functional coupling between discreet P2X and ASIC channels, modulation was largely additive which indicated that activation of neither P2X2 nor P2X4 alone resulted in a saturating amount of ASIC3 modulation. This suggested a lack of amplification and perhaps a relatively low affinity interaction. This seems especially true of P2X2 dependent modulation which had a strong dependence on expression level (figure 3-4e, 3-15). Thus, P2X and ASIC appeared both physically and functionally on a molecular scale which allowed ASIC3 to sense the appearance of ATP by an increased proton sensitivity.

Discussion:

Muscle releases ATP during normal contraction(Li, King et al. 2003) and ATP accumulates to micromolar levels in the extracellular space when contraction occurs in low oxygen(Forrester 1972; Clemens and Forrester 1981; Mo and Ballard 2001). PPADS and amiloride, a blocker of certain P2X and P2Y receptors and ASICs respectively, inhibit exercise-induced sensory nerve activity and vascular reflexes when perfused into the muscle arteries of decerebrate cats(Li, Maile et al. 2004; Kindig, Hayes et al. 2006; Hayes, Kindig et al. 2007; Kindig, Hayes et al. 2007). Here it was shown that ATP, acting through an electrically quiet P2X receptor, increased ASIC sensitivity in rat sensory neurons. This doubled the size of ASIC currents that

were evoked by pH values typical of heart attack or skeletal muscle ischemic pain. By integrating two signals—acid and ATP—that appear together in the extracellular space during muscle ischemia, ASIC modulation should promote sensory selectivity for ischemic acidosis over systemic acidosis. This interaction may also contribute to the neuronal damage during stroke that is mediated by ASIC1(Xiong, Zhu et al. 2004). This interplay between P2X and ASIC channels differs from other examples of channel-channel interactions(Khakh, Zhou et al. 2000; Boue-Grabot, Barajas-Lopez et al. 2003; Boue-Grabot, Emerit et al. 2004) by its slow onset and by its persistence; these suggest that a fundamentally different mechanism is used.

Intriguingly, both P2X and P2Y receptors mediate a long lasting modulation of the ASIC related epithelial sodium channels (ENaCs) but the mechanism of modulation is unknown. P2X dependent inhibition of ENaC was not blocked by known second messenger modulators of ENaC activity, leaving open the possibility of a direct physical association. There is emerging evidence for heteromerization between ASICs and ENaCs suggesting that these two channel sub-families share enough homology to form functional heteromeric channels and providing another possible means of association between P2X and ENaC. ENaCs are not traditional ligand gated channels, rather they are constitutively active and modulators alter the open probability and trafficking to affect activity. If P2X interacts with ENaCs in a manner similar to its interaction with ASICs it may suggest that modulation occurs independent of proton binding since ENaCs are not acid gated.

Co-localization of ASIC3 and P2X5 immunoreactivity in DRG sensory neurons was observed consistent with pharmacological and electrophysiological observations suggesting that P2X5 was the endogenous P2X receptor responsible for modulation of ASIC3 like currents in sensory neurons. ASIC modulation provides a novel functional role for P2X5 which has been largely ignored due to the relatively small currents it passes. Perhaps a renewed interest in P2X5 will shed more light on its function.

While P2X5 was likely the predominant P2X receptor that modulated ASIC, it is possible that other P2X receptors, particularly P2X4, may also modulate some endogenous ASICs in a minority of cases. It is unknown if heteromeric P2X receptors are capable of modulating ASICs particularly P2X1/5, P2X2/6 and P2X4/6.

P2X appeared to modulate ASIC3 by a direct physical interaction. Calcium, kinases, phosphatases and G-proteins were not required for modulation of ASIC3. In contrast to a recent report, no effect of the nitric oxide donor SNAP was seen on ASIC3 (Cadiou, Studer et al. 2007). Any action of SNAP could be attributed to pH changes of the buffer solution caused by SNAP. ASIC and P2X appeared to be both physically and functionally coupled indicating that modulation was caused by a direct action of P2X on ASIC3. Apparently, prolonged application of ATP slowly altered or induced an interaction between P2X and ASIC.

While there appeared to be a direct interaction between ASIC and P2X, there was no evidence for ASIC and P2X forming a single cross-family channel. Kinetics of ASIC3 appeared to resemble wild-type with no differences noticeable to the eye. As will be demonstrated in the next chapter, the Hill slope of proton activation which is approximately 4 was not altered by the co-expression of P2X. If one of the ASIC subunits within the trimeric channel was replaced by P2X it would be expected to decrease the Hill slope by 1/3. Suramin, which inhibited modulation when applied in the presence of ATP did not inhibit previously modulated proton evoked responses, indicating that P2X did not become proton gated and suggesting that P2X was not present within the ASIC channel.

Experiments with fluorescently tagged P2X5 and ASIC3 revealed that FRET occurred with relatively high efficiency using both epifluorescent (17%) and TIRF (9.5%) microscopy. The efficiency was comparable to that of previously studies involving P2X2 and nACh (Khakh, Fisher et al. 2005) and ASICs (Meltzer, Kapoor et al. 2007). The efficiency of FRET was slightly lower for TIRF compared with epifluorescence but the reasons are unclear. It is possible that FRET measurements using epifluorescence were artificially high due to concentration of fluorophores in intracellular compartments that were not seen when using TIRF. TIRF was carried out on cells that had undergone fixation and storage for 1-2 days while epifluorescent measurements were made using live cells. It is also possible that the FRET signal gradually diminished as fluorophores became degraded as a result of or after fixation.

More experiments will be necessary to determine if FRET efficiency decreases over 1-3 days after fixation.

ASIC3 formed pronounced clusters on the membrane consistent with a previous electron microscopic study of epithelial sodium channels expressed in oocytes which were shown to form large clusters of channels (Eskandari, Snyder et al. 1999; Awayda, Shao et al. 2004). One report with single channel recordings of P2X2 reported non-independent gating between individual channels, channels open more often when other channels are open than would occur by random chance. This suggests that P2X receptors may posses the ability to cluster as well. Perhaps clustering is a property of both families of channels that may affect their activity and their interactions. Using TIRF microscopy, it is apparent that P2X5 was enriched in clusters containing ASIC3, but the clusters of P2X5 did not appear as pronounced. This may have been due to the lower fluorescence intensity of CFP decreasing the signal to noise or it may be an intrinsic property of P2X5. Previously published TIRF experiments with P2X2 observed no clustering on the membrane (Fisher, Girdler et al. 2004; Khakh, Fisher et al. 2005). TIRF experiments using brighter more stable fluorophores such as Venus and Cerulean or GFP/ mCherry would be helpful for future experiments examining membrane distribution of P2X and ASIC. It is possible to observe single molecules of GFP using TIRF. Time lapse imaging of ASIC3-GFP clusters using TIRF may be able to provide an estimate of the number of channels in each cluster and allow observation of dynamics not possible with CFP and YFP.

Selective activation of two distinct P2X populations resulted in biphasic modulation of ASIC3 suggesting that the two P2X populations interacted with different subsets of ASICs. Additionally, the expression of a large number of P2X2 channels did little to suppress modulation by P2X4 since the degree of suramin-insensitive modulation was similar in the presence or absence of P2X2. This lack of suppression of P2X4 modulation by P2X2 suggests that there was sufficient ASIC3 present to interact with both P2X4 and P2X2 virtually independently, perhaps indicating that the interaction between ASIC and P2X is fairly weak and excess P2X may be required for maximum modulation to occur.

A rough estimate of the stoichiometry of modulation revealed that molar excess P2X2 was likely required to achieve high levels of modulation, consistent with the suggestion of a somewhat weak physical interaction between the ASIC and P2X. The trimeric nature of ASIC and P2X make it possible that a ratio of P2X: ASIC of anywhere from 1:3 to 3:1 could be required to fully modulate ASIC.

Co-immunoprecipitation data were inconclusive suggesting either non-specific aggregation or no interaction between ASIC and P2X. A previous report found no evidence for heteromerization of P2X4 and P2X7 under conditions identical to those in which no interaction between ASIC3 and P2X5 was observed (Torres, Egan et al. 1999). Recent contradictory data indicated that P2X4 and P2X7 may be co-immunoprecipitated under different solubilization conditions (C12M solubilization) and display novel kinetic features (Guo, Masin et al. 2007). FSEC and EM of P2X4

solubilized with C12M demonstrated that P2X4 formed large multimeric aggregates (Toshi Kawate, Eric Gouaux personal communication). Thus, it is possible that ASIC and P2X may be co-immunoprecipitated under some conditions, but questions regarding specificity would still persist. Alternatively, it is possible that a dynamic equilibrium existed where P2X interacted with ASIC by rapidly associating and dissociating in which case stable ASIC/ P2X complexes could not be isolated and interactions would be expected to be of relatively lower affinity as has been suggested as a model of syntaxin clustering (Sieber, Willig et al. 2007).

Modulation of endogenous ASIC by P2X was calcium independent occurring in the absence of both intra and extracellular calcium. This was mimicked by the co-expression of ASIC3 with P2X4 and P2X5 but not with P2X2. P2X2 required extracellular calcium but not intracellular calcium or ion flux through the channel. This suggested that there may be an extracellular calcium binding site on P2X2 that promotes conformational changes necessary for modulation of ASIC3. This is consistent with recordings from excised outside-out patches of P2X2 expressing cells that reported calcium dependent desensitization of P2X2, suggesting that calcium dependent conformational changes occur in P2X2 (Ding and Sachs 2000).

Taken together it is interesting to hypothesize that P2X5 may modulate ASIC3 by a direct physical coupling that is slow to initiate and slow to reverse. The slow temporal characteristics are unlike any previously described channel-channel interactions and may reflect slow conformational changes in P2X receptors that alter or initiate an

interaction between ASIC and P2X. This interaction is likely not very high affinity since convincing co-immunoprecipitations could not be carried out convincingly and saturation of modulation was not readily achievable with expression of large amounts of P2X2 or P2X4. Experiments further addressing the nature of the interaction between ASIC and P2X will be described in the following chapter.

Figure 3-1: Extracellular ATP increased acid sensitivity of ASIC channels in rat sensory neurons.

a. Whole cell patch clamp currents evoked by changing the external pH from 7.4 to 6.8 on a sensory neuron that innervated skeletal muscle. The smaller current was evoked before applying extracellular ATP and the larger was 10 seconds after washout of ATP (50 μM for 25 sec). Inset: phase and fluorescence micrographs showing dissociated sensory neurons tagged through retrograde transport of DiI injected into thigh muscles. Scale bar: 20 mM. **b.** Distribution of muscle afferents by cell diameter (white bars). Note that larger cells are more likely to respond to ATP (black bars) and that some cells that have ASIC current (grey bars) are not modulated by ATP. **c.** Mean (+/- s.e.m.) percent increase (100% = 2-fold increase) in ASIC3-like current (pH 6.9) at different ATP concentrations, each applied for 1 minute ($n \geq 5$ for each concentration). **d.** A representative time course of ATP modulation. Each point is the peak amplitude of current evoked every 20 seconds (2 sec pulse from pH 7.4 to 6.9). Bars indicate application of ATP (50μM) outside the cell. Note that it took a minute for currents to reach their highest level, current remained high for several minutes after ATP was removed, and a subsequent ATP application had little effect. Continual ATP application generated similar desensitizing time courses (not shown). **e.** Mean percent increase in ASIC3-like current evoked at the indicated pH. 50 μM ATP was applied at pH 7.4 for 1 minute. ASICs were evoked by brief (2 sec) steps to the indicated pH before and 20 seconds after removal of ATP. Currents at the peak of the ASIC activation curve (ca. pH 6) were unchanged, indicating that ATP did not increase the total number of available ASIC molecules.

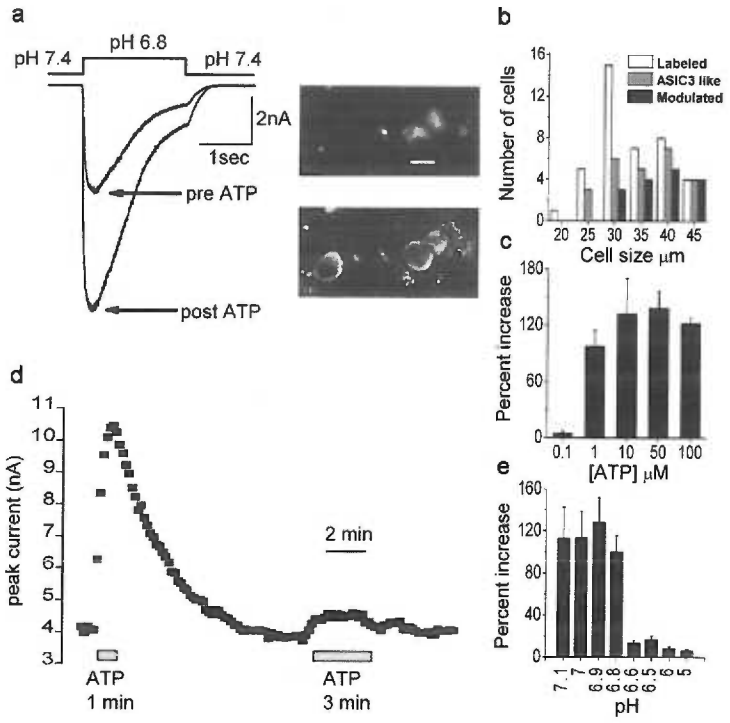
a
pH 7.4
pH 6.8
pH 7.4
2nA
1sec
pre ATP
post ATP
b
Number of cells
Labeled
ASIC3 like
Modulated
Cell size μm
c
Percent increase
[ATP] μM
d
peak current (nA)
2 min
ATP
1 min
ATP
3 min
e
Percent increase
pH

Figure 3-2: The ATP binding site is a P2X receptor.

Pharmacological profile in sensory neurons: Each pair of traces was from a single representative cell (n $\geq$5 cells for each). Purinergic agonists were applied at 50 μM for 1 minute except BzATP (100 μM). Antagonists (TNP-ATP, 100 μM suramin, 4 μM PPADS (not shown)) were applied together with ATP. Negative results were followed by ATP application to assure that the cell responded. Summary of conclusions drawn by pharmacology are shown in the table at the bottom of the figure. The pharmacological profile was only consistent with either P2X2 or P2X5 being involved in modulation. Scale bars: 1 sec; 0.5 nA.

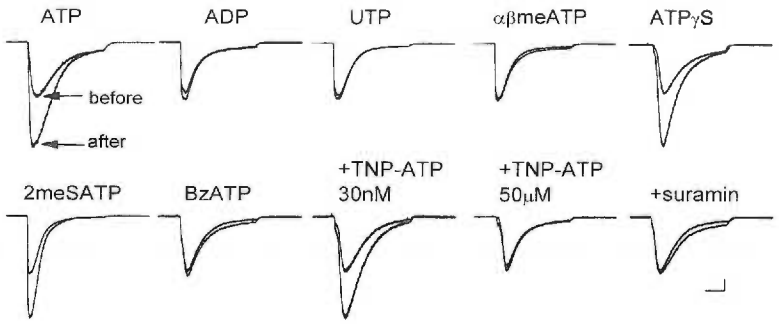

Receptors implicated:	Pharmacology:
Not P2Y	ADP and UTP failed to modulate
Not P2X1, 2, 2/3	αβmethylene ATP failed to modulate/ low TNP-ATP does not inhibit modulation
Not P2X4, 4/6, 7	Modulation inhibited by Suramin/ PPADS
P2X2 and P2X5 remaining	All pharmacology consistent with P2X2 or P2X5

Figure 3-3: Modulation can be reconstituted in cell lines.

a. Reconstitution of ATP modulation in cell lines. Each trio of traces is from a single COS or CHO cell transfected with the indicated cDNAs. The ASIC3 currents, evoked by 2 second steps to pH 6.9 before ATP application and after removal, flank a trace showing the first 3 seconds of a 30 second ATP application. αβ-methylene-ATP was used on the P2X2/P2X3 co-transfection to assure only activation of the heteromer and not homomeric P2X2. **b.** Mean percent ASIC current increase (n = 7-83 cells, each from dishes not previously exposed to ATP) in sensory neurons (DRG, dorsal root ganglia) or cell lines transfected with ASIC3 or ASIC1 together with the indicated P2X receptors. P2X2, P2X4, and P2X5 can mediate modulation of ASIC3; ASIC1 was also modulated. Scale bars: 1 sec; 0.5 nA.

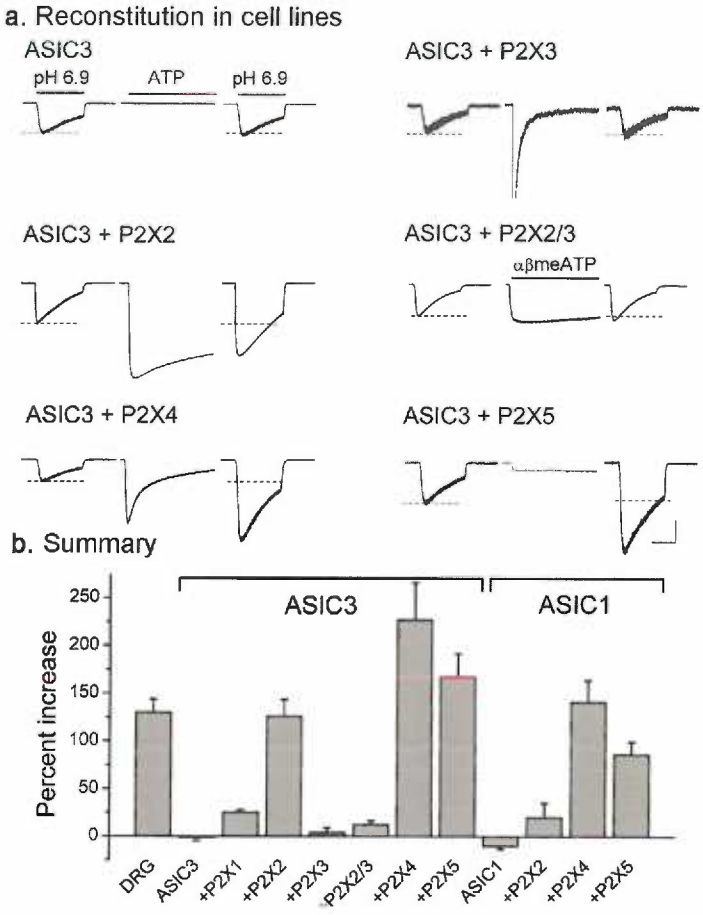
a. Reconstitution in cell lines
ASIC3
pH 6.9
ATP
pH 6.9
ASIC3 + P2X3
ASIC3 + P2X2
ASIC3 + P2X2/3
αβmeATP
ASIC3 + P2X4
ASIC3 + P2X5
b. Summary
ASIC3
ASIC1
Percent increase
250
200
150
100
50
0
DRG
ASIC3
+P2X1
+P2X2
+P2X3
P2X2/3
+P2X4
+P2X5
ASIC1
+P2X2
+P2X4
+P2X5

Figure 3-4: The P2X receptor is electrically quiet and Ca2+ independent.

a. ASIC modulation occured when a positive membrane potential (+40 mV) forces outward current during the ATP application. Thus, direction of ATP-driven flux is irrelevant. Similar results were seen with sensory neurons (n=6) and P2X5-transfected cells (not shown), neither of which exhibited the substantial outward currents of P2X2 (left) and P2X4 (right). **b.** ASIC currents before and after ATP when extracellular and intracellular Ca2+ are both chelated (10 mM EGTA inside and outside, no added Ca2+). Similar results found with 10 mM BAPTA inside. Modulation by P2X2 failed in the absence of extracellular Ca2+, but proceeded in sensory neurons and with P2X4 or P2X5 expression. **c.** Three different sensory neurons. The waveform of ATP-evoked current did not predict whether ASIC modulation occurred. **d.** Representative amplitudes of three kinds of P2X currents each transfected with 10 μg/ml of the indicated cDNA. P2X2 and P2X4 made substantial currents whereas P2X5 mades little current. **e.** Plot of percent increase of ASIC current vs. the amplitude of sustained ATP-evoked current in sensory neurons (triangle), and cell lines transfected with ASIC3 plus P2X2 (squares) or P2X5 (circle). High P2X2 currents correlated with successful modulation, whereas modulation occurred with little sustained P2X current in native neurons or P2X5 cells. Sustained current was measured as the amplitude 2 seconds after the start of the ATP application. Scale bars for a,b,c: 1 sec; 1 nA (except 0.5 nA for middle traces of **c**).

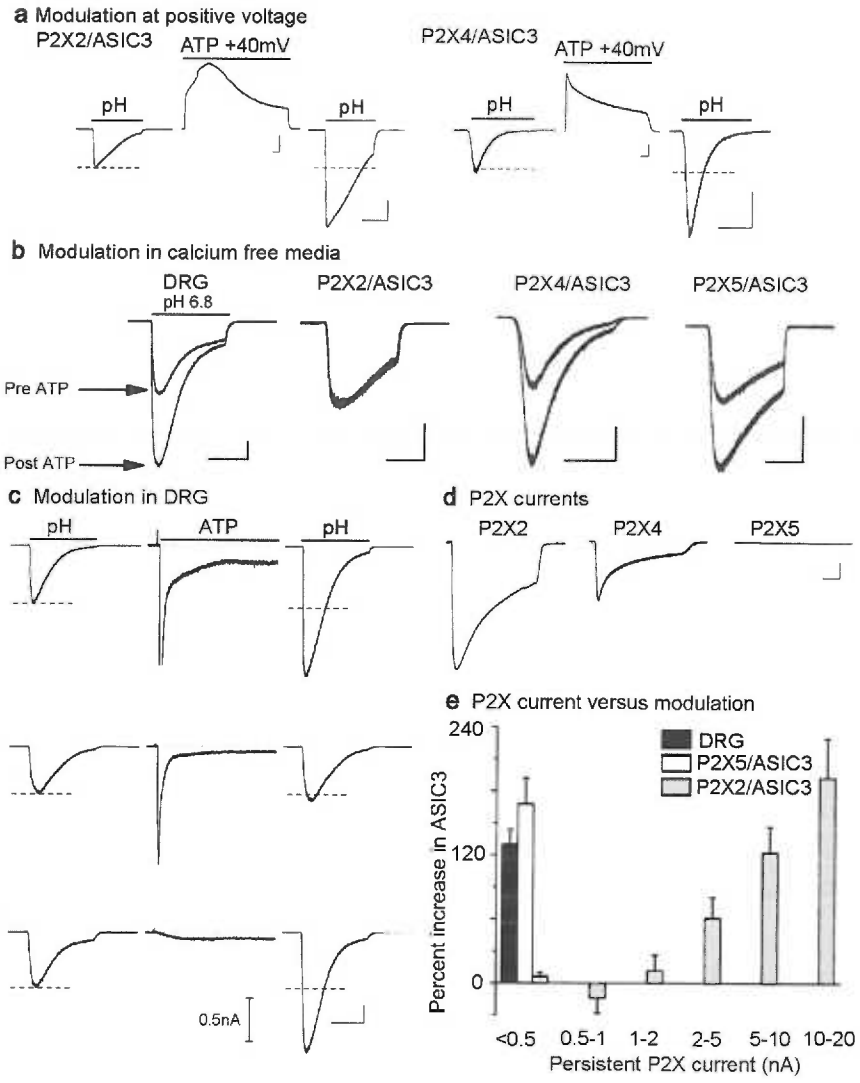
a Modulation at positive voltage
P2X2/ASIC3
ATP +40mV
pH
pH
P2X4/ASIC3
ATP +40mV
pH
pH
b Modulation in calcium free media
DRG
pH 6.8
P2X2/ASIC3
P2X4/ASIC3
P2X5/ASIC3
Pre ATP
Post ATP
c Modulation in DRG
pH
ATP
pH
0.5nA
d P2X currents
P2X2
P2X4
P2X5
e P2X current versus modulation
240
120
0
DRG
P2X5/ASIC3
P2X2/ASIC3
Percent increase in ASIC3
<0.5
0.5-1
1-2
2-5
5-10
10-20
Persistent P2X current (nA)

Figure 3-5: P2X5 immunoreactivity co-localizes with ASIC3.

Sensory neurons in two sections taken from a lumbar dorsal root ganglion are pictured. Left: section labeled and imaged for **a,** P2X5 and **b,** ASIC3 antisera. Right: section labeled and imaged for **d,** P2X2 and **e,** ASIC3. Bottom image (**c** and **f**) superimposes the two above with the P2X in red and ASIC in green; strongly double-labeled cells look yellow. P2X receptors were stained with cy3 secondary antibodies and ASIC3 with cy5. Counts of all labeled (bright and dim) cells were made blindly in well stained sections from 3 rats. P2X5-stained sections had 623 total cells with clear nuclei, 157 P2X5+, and 81 P2X5+/ASIC3+. P2X2 sections had 653 total cells, 170 P2X2+, and 18 P2X2+/ASIC3+. Total number of ASIC3+ cells in all sections: 328 of 1276. Note that most of the brightest cells for either P2X5 or ASIC3 are larger in diameter. This contrasts with P2X2, where most of the brightest cells are smaller in diameter.

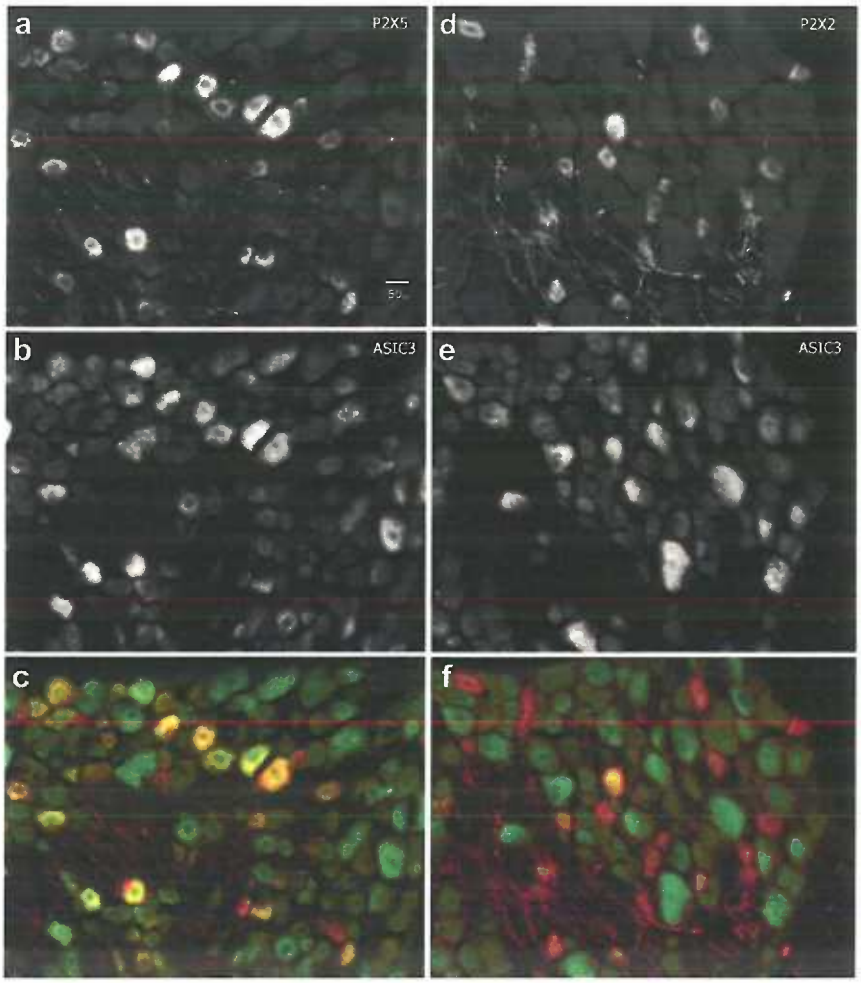
a
P2X5
d
P2X2
b
ASIC3
e
ASIC3
c
f

Figure 3-6: A P2X4-like current modulates ASIC3-like sensory neuron currents

Currents evoked by pH 6.9 flank an ATP evoked current in a skeletal muscle afferent DRG. ATP (50μM) application resulted in an increase in the current amplitude of the pH evoked current indicating that P2X4 may modulate ASIC in a minority of cases. The presence of a P2X4-like current does not rule out the presence of P2X5, however.

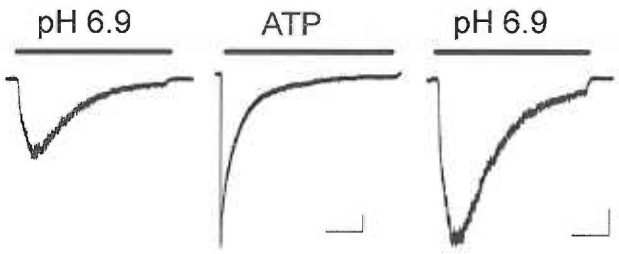
pH 6.9
ATP
pH 6.9

Figure 3-7: Intra- and extracellular calcium did not affect modulation of ASIC3.
a. Removal of extracellular calcium and buffering of intracellular calcium with BAPTA (10mM) did not affect modulation of ASIC3 pH sensitivity by extracellular ATP (30 seconds, 50uM). **b.** Depleting intracellular calcium stores by addition of 10uM cyclopiazonic acid (CPA) in the absence of extracellular calcium for 5 minutes did not prevent modulation either. **c.** Increasing intracellular calcium concentration by lightly buffering (0.1mM EGTA) and inducing release from intracellular stores with caffeine (10mM, 3 minutes) neither mimics nor inhibits modulation by ATP. Currents pictured were evoked by 2 second application of pH 6.9 (**a and b**) or 6.8 (**c**) before and after a 30 second application of ATP.

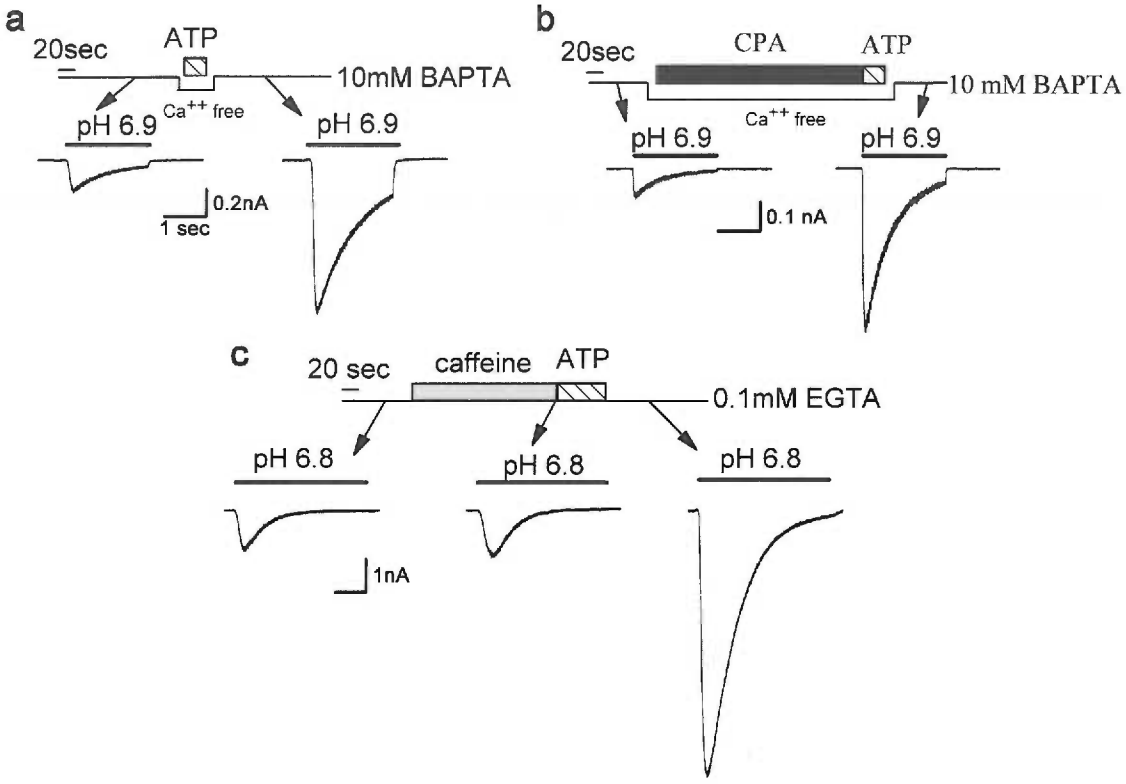
a
20sec
ATP
10mM BAPTA
pH 6.9
Ca++ free
pH 6.9
0.2nA
1 sec
b
20sec
CPA
ATP
10 mM BAPTA
Ca++ free
pH 6.9
pH 6.9
0.1 nA
c
20 sec
caffeine
ATP
0.1mM EGTA
pH 6.8
pH 6.8
pH 6.8
1nA

Figure 3-8: Modulation does not involve kinases, phosphatases, G-proteins or intracellular ATP/GTP.

a. Pairs of acid evoked currents before (smaller) and after (larger) modulation by ATP (50uM). Currents were evoked by pH 6.9 in cells co-expressing ASIC3 and P2X5. The standard internal solution was supplemented with AMP-PNP (5mM), okadaic acid (500nM) and cyclosporin A (40uM), GTPγS (300μM), or GDPβS (2mM) as indicated. None of these conditions prevented ATP dependent modulation. Scale bars 0.5 sec, 0.5 nA except for GDPβS 0.5 sec, 1nA. **b.** Bar graph summarizing data represented above using the stated variations from the standard internal solution. Currents evoked by pH 6.9 were recorded immediately after break-in, after 5 or 10 minutes of dialysis time (pre ATP) and after ATP application. Peak amplitude was measured and normalized to amplitude immediately preceding ATP application. **c.** Time course plotting peak current amplitude evoked by pH 6.9 from an individual cell under the same conditions as above. Amplitude was normalized to the trace immediately preceding application of ATP. Pipette solution was allowed to equilibrate with cytosol for 5 or 10 minutes prior to application of ATP while pH was dropped to 6.9 every 30 seconds to measure ASIC3 currents.

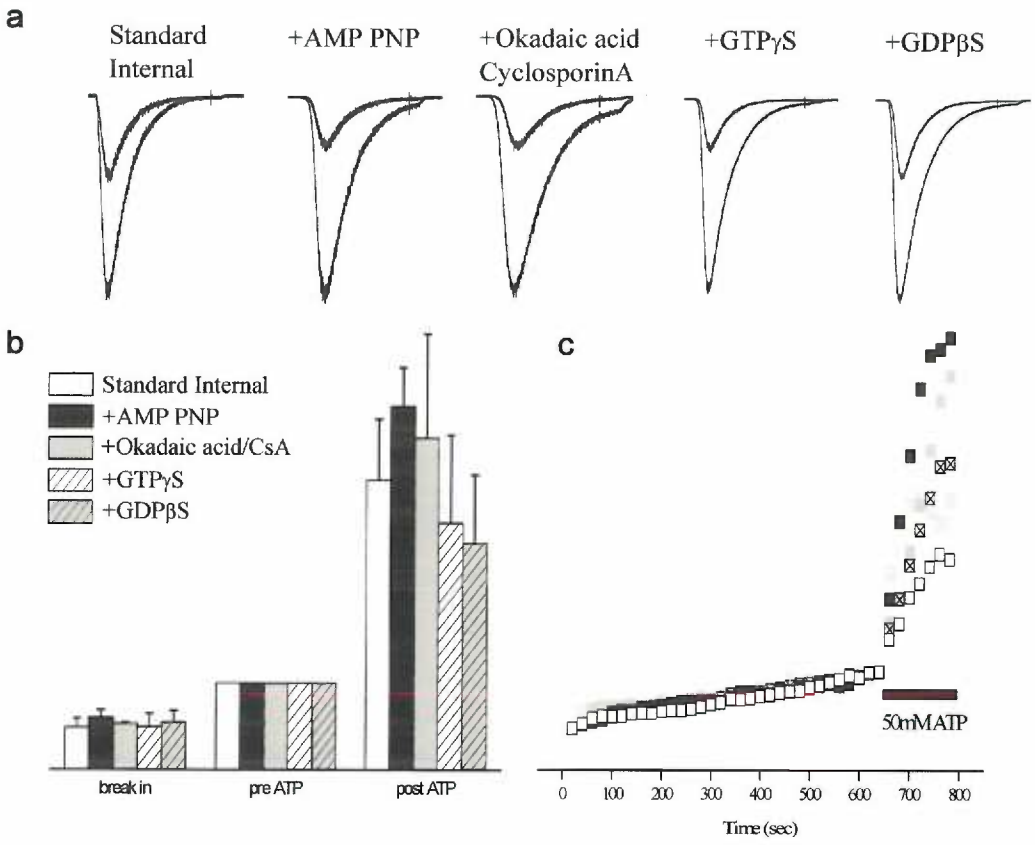
a
Standard Internal
+AMP PNP
+Okadaic acid CyclosporinA
+GTPγS
+GDPβS
b
Standard Internal
+AMP PNP
+Okadaic acid/CsA
+GTPγS
+GDPβS
break in
pre ATP
post ATP
c
50mMATP
0
100
200
300
400
500
600
700
800
Time (sec)

Figure 3-9; Extracellular ATP hydrolysis was not required for modulation of ASIC3. **a.** Application of the non-hydrolyzable ATP analogue AMP-PNP (gray hatched bar) resulted in modulation of currents evoked by pH 6.8 (black bars). AMP-PNP (50μM) was applied for 3 X 10 seconds with a two second pH 6.8 stimulus before and then following each AMP-PNP application in cells expressing ASIC3 and P2X4 demonstrates that extracellular ATP hydrolysis was not important for modulation. **b.** Extracellular magnesium, calcium, and inward current flux were not necessary for modulation of ASIC3 by P2X4. ATP (50μM) was applied (2x 10 sec, gray hatched bars) in the absence of magnesium and calcium with 10mM EDTA while the cell was held at +40mV. The amplitude of the pH 6.8 stimulus (black bars) was increased after ATP application.

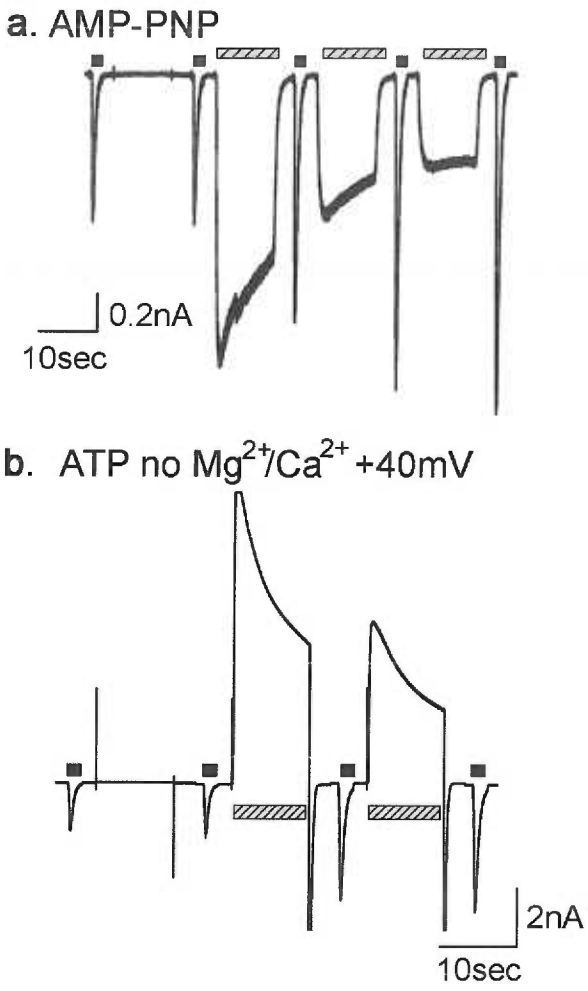
a. AMP-PNP
0.2nA
10sec
b. ATP no Mg^{2+}/Ca^{2+} +40mV
2nA
10sec

Table 3-2: Signaling molecules not involved in modulation in CHO cells

Method of modulation	Test: Effect
Extracellular atp hydrolysis	AMPPNP 50μM: modulation/ ATP no Mg++: modulation
Calcium	CPA 10μM/ 10mM BAPTA:no change 0.1mM EGTA/ Caffeine 10mM : no change
Kinases	5mM AMPPNP: no change SB203580 10μM/ Staurosporine 1μM: no change
Phosphatases	Cyclosporin A 40μM/ Okadaic acid 500nM: no change
G-proteins	GTPγS 300μM/ GDPβS 2mM: no change
Nitric Oxide	Sodium Nitroprusside 10μM/SNAP 100μM: no effect on ASIC3 L-NAME 500μM + carboxy-PTIO 300μM: no effect on modulation
PIP2	PIP2-long chain 10μM / PAO 200μM: no change ATP modulation requires P2X5 reported endogenous P2Y on CHO cells

Table 3-3: Signaling molecules not involved in modulation in sensory neurons

Method of Modulation	Test: Effect
G-proteins	GTPγS 300μM: no effect NEM 10μM: no effect
cAMP	Forskolin 10μM: no effect
PKA	CTP-AMP 100μM: no effect
PKC	PMA 1μM: no effect
Calcium	BAPTA internal 10mM: no effect
PLC, PLA_2	U73122 10μM: no effect

Figure 3-10: The nitric oxide donor SNAP does not appear to act directly on ASIC3 as reported

a. SNAP acted in a non-specific manner consistent with a pH change of the solution it was applied in. If SNAP (1.5mM) was only applied in the pH 6.9 test solution (pH test 3), it greatly "potentiated" the pH evoked current of ASIC3 in cells expressing ASIC3 and P2X4. If SNAP was present in both the control and test solution (pH test 4), the effect was somewhat attenuated, presumably due to lower pH test solution (larger currents) and lower pH control solution (more steady state desensitization). Desensitization of ASIC3 was caused if SNAP was only present in the control and not in the test solution (pH test 5). After the conclusion of this experiment pH of the buffer solution was measured. Bath – SNAP pH=7.42, Bath + SNAP pH=7.19. **b.** In contrast to the apparently non-specific action on ASIC3 current, SNAP appears to inhibit P2X4 function. In the same cell as in **a** SNAP was pre applied prior to the start of ATP (50μM) application. ATP was applied for 20 seconds at 35 second intervals. The first ATP application in the presence of SNAP produced little current. Subsequent applications of ATP revealed a gradual increase in current consistent with reversal of an inhibition by nitric oxide. This demonstrated that the SNAP used in **a** was active. Scale bars: a. 200pA, 0.5 sec, c. 2nA, d. 200pA, 5 sec.

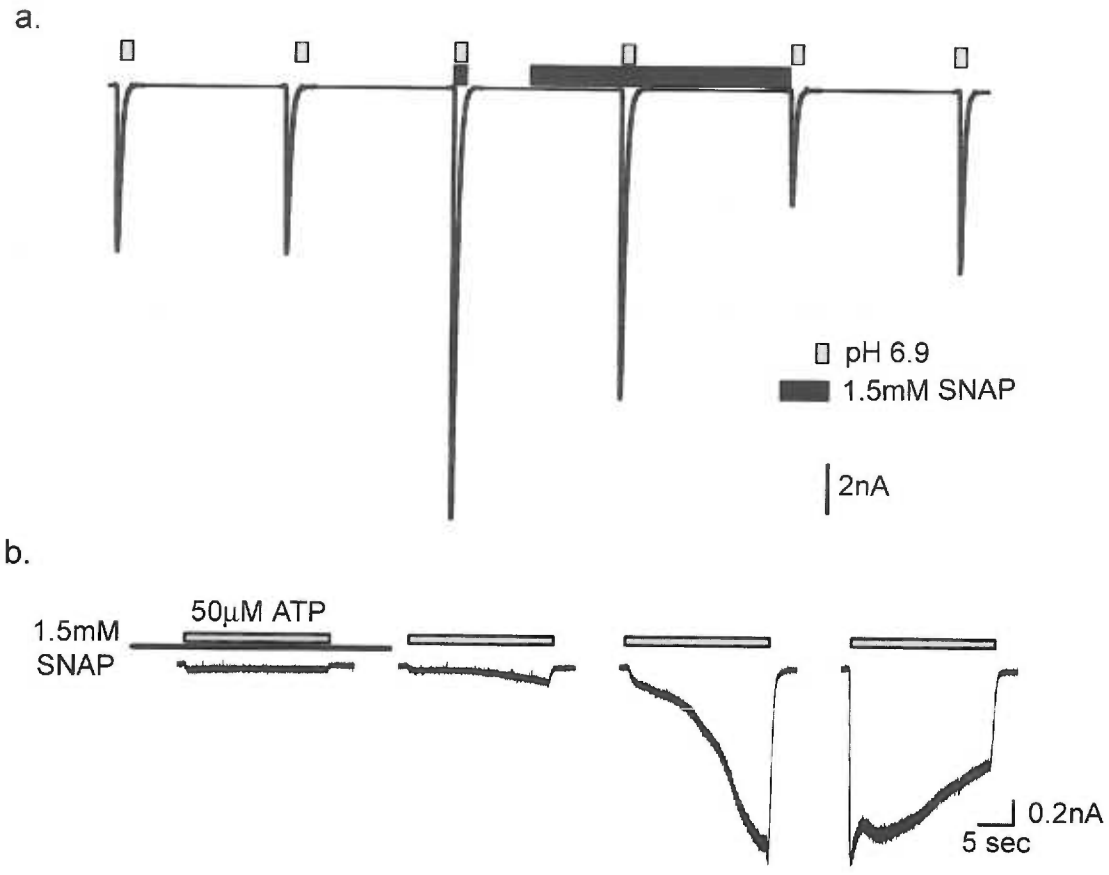
a.
pH 6.9
1.5mM SNAP
2nA
b.
1.5mM
SNAP
50μM ATP
0.2nA
5 sec

Time(hrs)	pH 7.4	pH 7.4 + SNAP 100μM	pH 6.9	pH 6.9 + SNAP 100μM	pH 6.3	pH 6.3 + SNAP 100μM	pH 7.4	pH 7.4 + SNAP 1.5mM
0	7.42	7.40	6.88	6.85	6.31	6.20		
1	7.40	7.38		6.81	6.29	6.12		
2	7.40	7.37		6.81	6.30	6.09	7.42	7.19
4	7.40	7.37		6.79	6.30	6.07		
6	7.39	7.35		6.77	6.29	6.06		
O/N	7.39	7.33		6.78	6.29	6.07	7.40	6.98

Table 3-4: SNAP caused a decrease in the pH of test solutions.

SNAP (100μM) was reported to modulate ASICs in a manner similar to the actions of ATP through P2X. Table 1 shows pH measurements of a buffer used to characterize the effect of SNAP (10mM HEPES is the pH buffer) in the previous report. The pH of various solutions both with and without SNAP was measured at the times indicated. SNAP caused a large and immediate drop in pH of the buffer solution at pH 6.3 and had measurable but less severe pH changes in the pH 6.9 and 7.4 solution. The reported effect of SNAP on ASIC activity is likely due to poor buffering of HEPES at pH 6.3 and 6.9. The last two columns are pH measurements from experiments done in figure 3-7 with 10mM HEPES, 10mM MES as the pH buffer. SNAP (1.5μM) decreased the pH of the solution from 7.42 to 6.19 after two hours. Overnight the pH of the SNAP solution dropped further to 6.98 while the control solution remained nearly constant.

Figure 3-11: P2X5-CFP modulated ASIC3-YFP.

ASIC3 YFP was modulated in an ATP dependent manner by P2X5-CFP. Test applications of pH 6.9 were delivered every twenty seconds. After the third pH test, ATP (50μM) was added to the bath solution until the end of the experiment. ATP was not present during the pH 6.9 tests. Scale: 20seconds, 1nA.

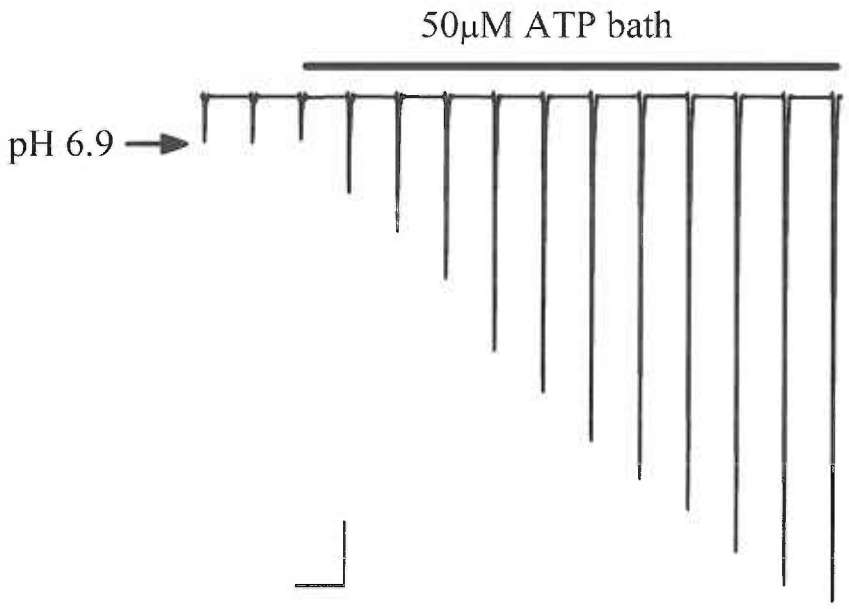
50μM ATP bath
pH 6.9

Figure 3-12: Fluorescent resonant energy transfer occurred between P2X5 CFP and ASIC3 YFP.

Photodestruction of ASIC3 YFP resulted in an increase of P2X5 CFP fluorescence. **a.** Relative CFP (blue circles, right axis) and YFP (black squares, left axis) intensities were plotted as a function of time of photobleaching of YFP in cells co-expressing P2X5 CFP and ASIC3 YFP. When only P2X5 CFP was expressed (open blue circles), there was no increase in CFP fluorescence. **b.** The increase in CFP flourescence was proportional to the fraction of YFP that was photodestroyed. P2X5 CFP appeared closely associated with ASIC3 YFP with a FRET efficiency of approximately 20%. FRET did not occur between P2X2 CFP and NgCAM YFP. Yellow CaMeleon 3.1 (YC3.1) served as a positive FRET control, exhibiting a high FRET efficiency.

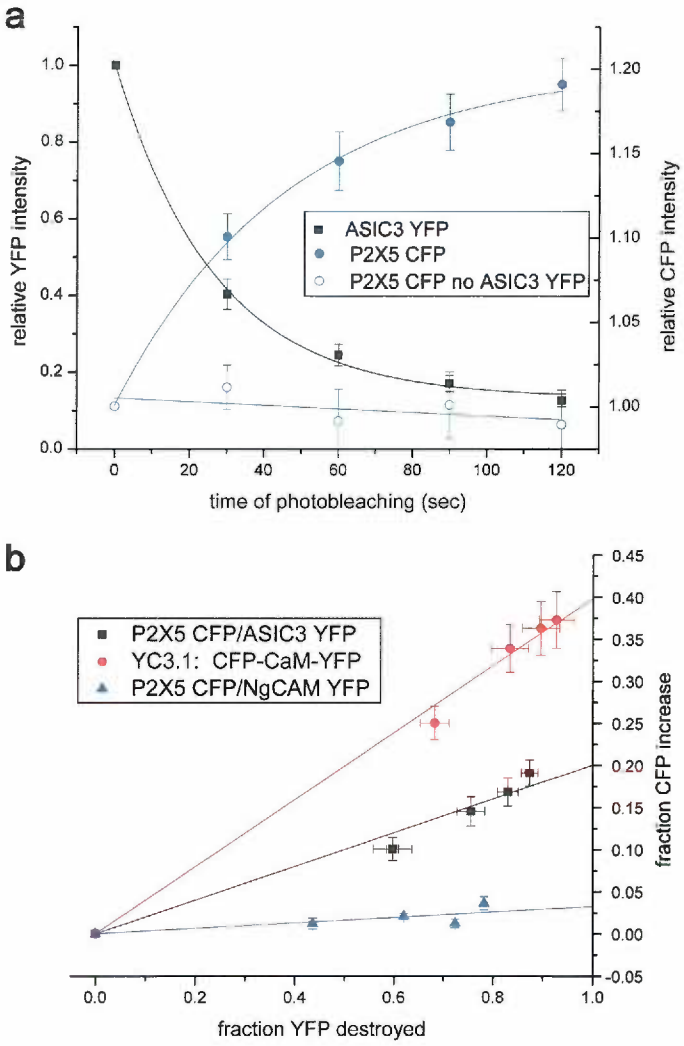
a
relative YFP intensity
relative CFP intensity
time of photobleaching (sec)
ASIC3 YFP
P2X5 CFP
P2X5 CFP no ASIC3 YFP
b
fraction CFP increase
fraction YFP destroyed
P2X5 CFP/ASIC3 YFP
YC3.1: CFP-CaM-YFP
P2X5 CFP/NgCAM YFP

Figure 3-13: FRET between P2X5-CFP and ASIC3-YFP measured using TIRF microscopy.

a. TIRF images of ASIC3-CFP and P2X5-YFP revealed clusters enriched in both ASIC3 and P2X5 in cells expressing ASIC3-CFP, P2X5-YFP and soluble mCherry. Light blue in merged images show where CFP and YFP co-localized. **b**. FRET was measured by donor dequenching. CFP fluorescent intensity was measured before (442nm ex, 483/25 em) and after a 30 second photodestruction of YFP (514nm ex) in cells expressing soluble mCherry with stated combinations of CFP and YFP fusion proteins. The change in CFP intensity was plotted as a fraction of YFP destroyed. P2X5-CFP/ ASIC3-YFP exhibited FRET with a similar intensity to ASIC3-CFP/ ASIC3-YFP and intermediate between the positive control (YC3.1) and negative control (P2X5-CFP/ NgCAM-YFP) n=8-21. **c**. Average brightness of YFP and CFP of regions of cells quantified in b were measured. YFP intensity was measured before photodestruction and CFP was measured after YFP photodestruction. Data indicated that average brightness was greater in cells expressing P2X5-CFP/ NgCAM-YFP than in those that expressed P2X5-CFP/ ASIC3-YFP suggesting that expression density is likely not the cause of the increased FRET seen between P2X5-CFP and ASIC3-YFP. **d**. Summary data of FRET efficiency measured as the relative increase in CFP fluorescence compared to total CFP fluorescence when imaged with Epifluorescence or TIRF microscopy. The increase and total CFP fluorescence were estimated by linearly extrapolating data in 3-12b (epi) and 3-13b (TIRF) to total photodestruction of YFP. **e**. Representative cell in pseudocolor (black is darkest, white brightest) expressing P2X5-CFP (upper images) and ASIC3-YFP (lower images) before and after a 30 second photobleaching of YFP. Destruction of YFP resulted in increased CFP fluorescence. Black and white images demonstrate co-localization of P2X5-CFP and ASIC3-YFP. **f**. Same as in **e** except that YC3.1 was expressed. A robust increase in CFP fluorescence was observed. Scale bar: 10μm.

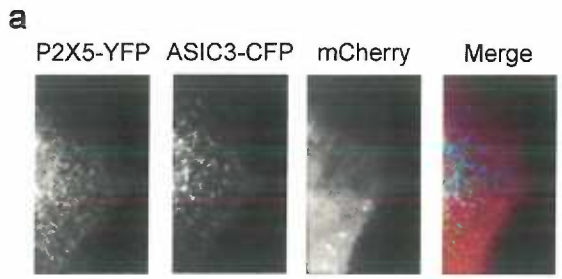

d

Constructs	FRET Efficiency %	
	Epi	TIRF
P2X5 CFP/ ASIC3 YFP	17	9.5
P2X5 CFP/ NgCAM YFP	3	4
YC3.1	29	25
P2X5 CFP	0	-0.5

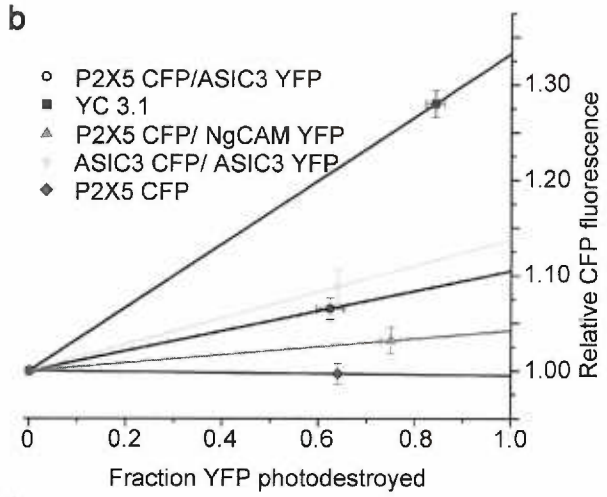

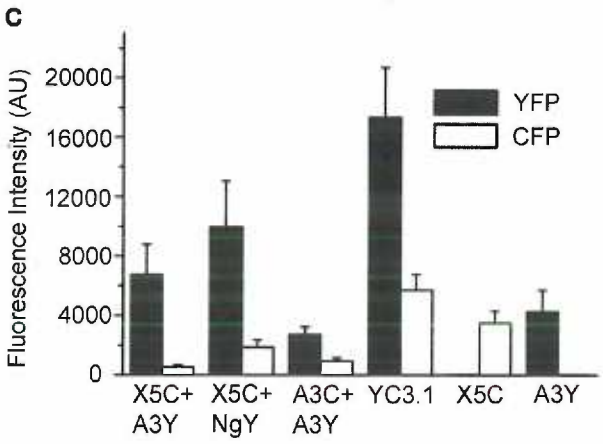

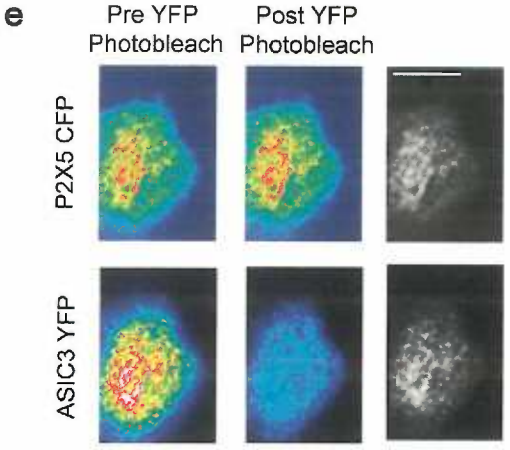

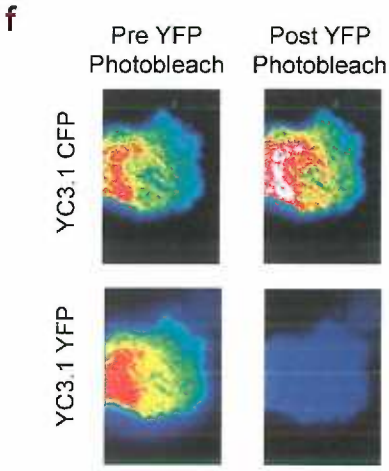

Figure 3-14: Fluorescent size exclusion chromatography shows change in relative size of ASIC3 multimers.

Fluorescent size exclusion chromatography was carried out on solubilized membrane material from cells expressing GFP-rASIC3, GFP-rASIC3 + P2X4 or GFP-cASIC1. Membranes were solubilized using C12M as described in methods section. Material was loaded onto a fast protein liquid chromatography column and fluorescence intensity of eluate was montored and plotted to detect the appearance of GFP. Protein complexes of larger size will elute more quickly. In the presence of P2X4, GFP ASIC3 eluted more slowly indicating a decrease in size of the complex. The GFP-ASIC3 has thrombin proteolysis site between GFP and ASIC3 so there is some free GFP that eluted at the indicated time point. The chicken ASIC1 construct that was recently crystallized was run as a control.

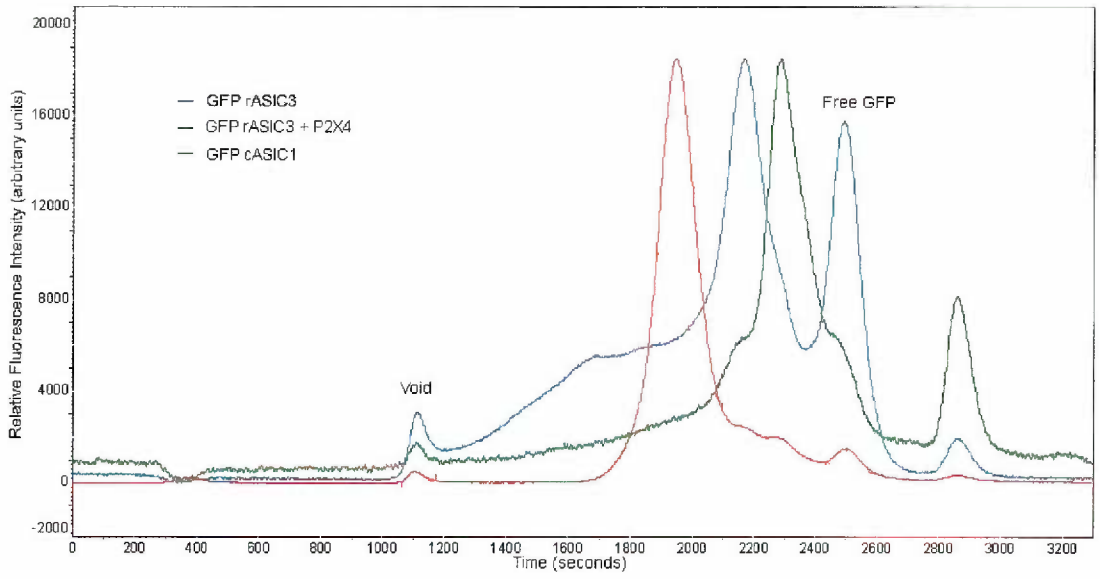
GFP rASIC3
GFP rASIC3 + P2X4
GFP cASIC1
Void
Free GFP
Relative Fluorescence Intensity (arbitrary units)
Time (seconds)
20000
16000
12000
8000
4000
0
-2000
0
200
400
600
800
1000
1200
1400
1600
1800
2000
2200
2400
2600
2800
3000
3200

Figure 3-15: Relationship between P2X2 and ASIC3 expression levels.

Current amplitudes evoked by ATP (50μM) and pH 6.8 were measured from data in figure 3-4e and the number of functional P2X2 and ASIC3 channels were estimated based on previously reported single channel conductances and open probabilities. The percent increase in ASIC3 current was then plotted as a function of the ratio of P2X2: ASIC3. The mean, median, and range of 25- 75% are summarized in the table below. Significant modulation required a P2X2: ASIC3 ratio of greater than about 0.5.

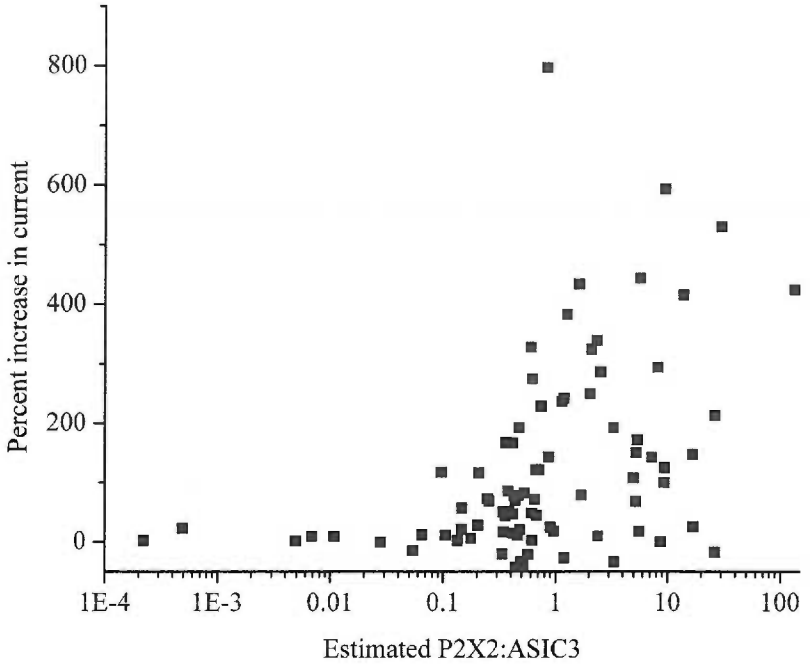

	Mean	Stdev.	s.e.m.	P25	P75	median
P2X2:ASIC3	4.7246	15.57273	1.69912	0.343	2.54	0.62
percentincrease	124.3298	159.9683	17.45397	11.1	171.8	70.8

Figure 3-16: Suramin inhibits P2X2 mediated currents but not P2X4 mediated currents.

ATP evoked currents were measured in cells expressing P2X2, P2X4 or P2X2 and P2X4 along with ASIC3. First, ATP (5μM) was applied for 20 seconds in the presence of suramin (150μM) to evoke suramin insensitive currents. After washout of suramin a 20 second application of ATP (50μM) was delivered to the same cell. P2X2 was inhibited by suramin while P2X4 was not. When P2X2 and P2X4 were co-expressed, there was a clear suramin sensitive and insensitive current component suggesting two different populations of P2X receptors. Vm= -30mV, scale: 5sec, 1nA.

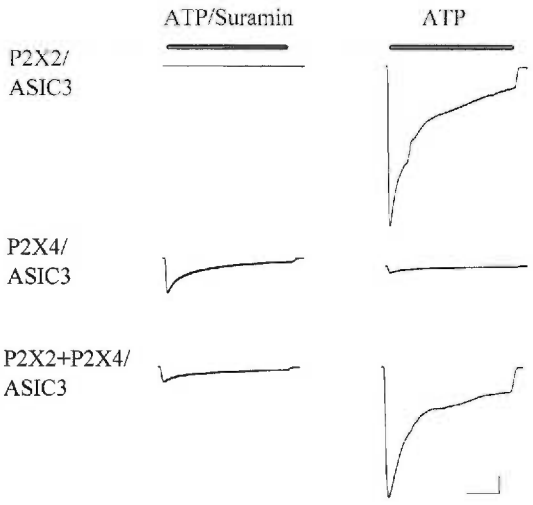
ATP/Suramin
ATP
P2X2/
ASIC3
P2X4/
ASIC3
P2X2+P2X4/
ASIC3

Figure 3-17: Modulation by P2X2 and P2X4 is non-occlusive and additive.

Modulation of ASIC3 occurred with ATP (5μM) in the presence of suramin (150μM) only in cells expressing P2X4. In cells expressing both P2X2 and P2X4 with ASIC3, modulation of ASIC3 by P2X4 (ATP + Suramin) did not occlude subsequent modulation by P2X2 (ATP). **a.** Currents evoked by pH 7.0 are shown before, after 20 seconds of ATP + Suramin, and then after a 20 second ATP (50μM) application in a representative cell co-expressing ASIC3 with P2X2, P2X4, or P2X2+ P2X4. Suramin blocked modulation by P2X2 but not by P2X4. Scale bar 1 sec, 0.5nA (P2X2, P2X4), 0.1nA P2X2 + P2X4. **b.** Summary data of percent increase in peak current (pH 7.0) caused by ATP + suramin and then subsequent application of ATP.

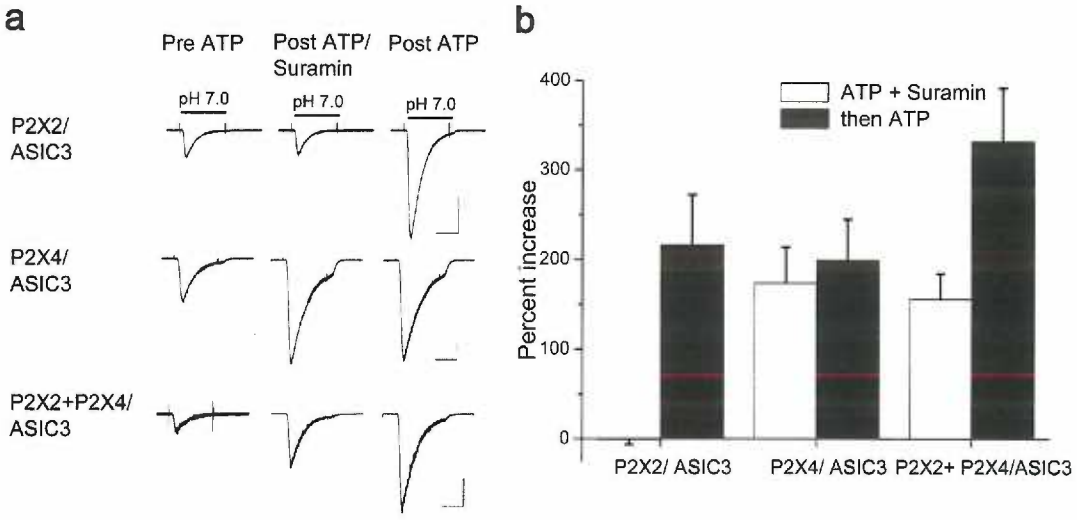
a
Pre ATP
Post ATP/ Suramin
Post ATP
pH 7.0
pH 7.0
pH 7.0
P2X2/ ASIC3
P2X4/ ASIC3
P2X2+P2X4/ ASIC3
b
ATP + Suramin
then ATP
Percent increase
400
300
200
100
0
P2X2/ ASIC3
P2X4/ ASIC3
P2X2+ P2X4/ASIC3

Chapter 4: Results

Purinergic P2X channels modulate the proton sensitivity of acid sensing ion channel 3 (ASIC3) in a subtype specific manner.

Introduction:

Ischemia occurs when a tissue receives insufficient oxygen to meet its metabolic demand and, in the case of muscle ischemia, results in pain. Metabolites released from contracting ischemic muscle are thought to accumulate in the interstitium and activate receptors on sensory nerve afferents innervating the muscle, triggering pain (Sutherland, Cook et al. 2000; Benson and Sutherland 2001). Coincident detection of acid and other metabolites could provide context specificity to acid sensing creating an "ischemia sensor" capable of distinguishing between ischemic and non-ischemic acidosis.

Modulation of ion channel function by other ion channels may serve an important function for regulating context specific channel activity. One situation in which this may be particularly important is in ischemia sensing. Acid has been proposed to be a mediator of ischemic pain but this suggestion has been controversial and pH changes appear to be necessary but not sufficient to excite ischemia sensitive sensory afferents (Pan, Longhurst et al. 1999). Small decreases in extracellular pH alone are not painful and have proven insufficient to excite cardiac sensory afferents. However, the drop in pH that accompanies ischemia is necessary for ischemia induced afferent excitation. This suggests that other signaling molecules in addition to acid are important for distinguishing ischemic acidosis from non-ischemic forms of acidosis to establish

context specificity. We have found that ATP may serve as this second signaling molecule.

One candidate acid sensor that is highly expressed on sensory neurons innervating cardiac and skeletal muscle is acid-sensing ion channel 3 (ASIC3) (Sutherland, Benson et al. 2001). In the previous chapter we demonstrated that ASICs expressed on skeletal muscle sensory neurons are modulated by extracellular ATP- another metabolite released by working muscle during ischemia. This modulation is long lasting and involves an ATP gated ion channel of the P2X family. P2X dependent modulation by ATP results in acid evoked currents that are much larger providing increased proton sensitivity to ASICs. Thus, ATP and acid can act in a synergistic manner through the interaction of two distinct classes of ion channels to make ASICs more sensitive to protons when extracellular ATP is or has been present. Modulation of ASIC's by ATP can be reconstituted in heterologous systems by the co-expression of recombinant ASIC3 with P2X2, 4, or 5 but the mechanism by which P2X receptors modulate ASICs has remained unclear. Work in the previous chapter demonstrated that there is an apparent physical and functional coupling of P2X and ASIC3 suggesting a direct protein-protein interaction but the changes that occur in ASIC3 remain uncharacterized.

This chapter focuses on characterizing the changes in various physical properties of ASIC3 in a search for the mechanism of modulation and insight into ASIC3 function and gating. P2X5 was shown to alter the proton sensitivity of ASIC which was

expected from results presented in the previous chapter. Unexpectedly, P2X5 appears to act by suppressing the proton sensing ability of ASIC3 and ATP relieves the suppression. P2X5 dependent modulation by ATP also slows the rate of desensitization but there were no effects on the apparent calcium affinity or the proton dependence of steady state desensitization. Examining the interactions of P2X2 and P2X4 revealed that while all P2X receptors modulate the apparent proton affinity and desensitization rate, each P2X subtype interacts with ASIC3 in a unique manner. The interaction between ASIC and P2X will be examined and the implications of this interaction will be discussed in this chapter.

Results:

ASIC3 was modulated by ATP in P2X5 dependent manner in CHO cells.

ASIC3 is a sodium selective ion channel of the ENaC/DEG family of channels that opens in response to rapid decreases in extracellular pH (increasing proton concentration). ASIC3 is modulated by the transient application of extracellular ATP. This modulation is mediated by an ATP gated ion channel of the P2X family, either P2X2, 4, or 5. While P2X2 and P2X4 can modulate ASIC3, we believe that P2X5 is the receptor responsible for modulation of ASIC3 in sensory neurons. This interaction was examined further in CHO cells co-expressing ASIC3 and P2X5.

As shown previously, ASIC3 expressed in CHO cells elicits an inward current in response to a 2 second drop in the pH from control pH of 7.4 to pH 6.9. Application of ATP (50μM, 30sec) elicited no current from cells expressing ASIC3 alone (not

shown) and a subsequent pH drop to pH 6.9 evoked a current similar to that evoked before ATP application (figure 4-1A). In contrast, when P2X5 was co-expressed with ASIC3, a small ATP evoked current was seen and the pH evoked current after a 30-second ATP application and washout was larger than the current evoked before ATP (figure 4-1B). This striking modulation was unusual in several regards. One unique aspect of modulation is its time course. As shown previously for ASIC3-like currents in sensory neurons, modulation was slow to initiate taking several minutes to reach a peak. Unlike modulation in sensory neurons, the increase in pH evoked currents in CHO cells was irreversible on the timescale of these experiments (figure 4-2). The peak current evoked by a pH 6.9 stimulus was measured every minute and plotted. Six 30-second applications of ATP (50μM) were applied between pH tests and the peak pH evoked current increased slowly as a result of each application of ATP.

After more than 1 hour the pH evoked current was only slightly smaller than the current measured immediately after the final ATP application. Currents evoked before ATP, immediately after ATP, and at the end of the experiment are plotted above the time course (figure 42A) demonstrating the magnitude and long lasting nature of modulation of ASIC3 by ATP. The long lasting nature of modulation implies that with P2X5 and ASIC3 present, the cell retained a memory of the transient appearance of ATP that long outlasted the degradation or washout of ATP. This long lasting action is likely to be physiologically important due to the presence of ecto-nucleotidases which rapidly hydrolyze extracellular ATP to ADP, AMP, and adenosine. Additionally, the large magnitude of modulation by ATP would make

ASIC3 much more sensitive to physiologically relevant pH changes when ATP is or has been present. The virtually irreversible modulation of ASIC3 resembles a kinetic trap. In a kinetic trap a protein is kept an unfavorable conformation due to a large energy barrier that prevents progression to a more stable conformation. A trigger that lowers the energy barrier catalyzes the transition to the more stable end product resulting in an irreversible reaction. A kinetic trap model is one potential explanation of how ASIC3 could be maintained in one conformation and then progress to another upon the appearance of ATP.

In addition to the physiological consequences of this long lasting modulation, the irreversible nature in CHO cells allowed the characterization of changes in the kinetic properties of ASIC3 by P2X5 dependent modulation. This study would be much more difficult in sensory neurons where the modulation desensitized gradually after several minutes. The irreversible nature of modulation and the control of ASIC and P2X subtype expression in cell lines led us to study ASIC3 modulation in cell lines rather than in sensory neurons.

Modulation by P2X5 altered proton sensitivity and increased peak currents. There are several potential mechanisms that would result in increased pH evoked current amplitude including increased proton sensitivity, increased conductance, and a larger number of channels on the membrane. Proton activation curves were measured in response to pH tests (2sec) in cells expressing ASIC3 and P2X5 before and after application of ATP (50μM, 30sec). Previous work demonstrated that

protons and calcium compete for a calcium binding site on ASIC3 and protons catalyze the release of calcium leading to opening of the channel. Thus there is an intimate interaction in which protons alter calcium affinity and calcium alters proton affinity. Therefore, the activation properties of ASIC3 were measured in the presence of varying calcium concentrations (10nM, 1mM, and 10mM). In the presence of 10nM free calcium, ASIC3 is expected to be virtually free of bound calcium at all pH values (Immke and McCleskey 2003). The peak current evoked under each pH and calcium condition was measured and normalized relative to the peak current evoked by pH 6.0 (1mM Calcium) before application of ATP and plotted (figure 4-3A). There is a small increase in the maximally evoked current and a leftward shift of the apparent proton affinity of ASIC3. Several conclusions can be drawn from this experiment. First, the mechanism of modulation was not purely an increase in the number of channels or an increase in conductance since the degree of modulation of maximally evoked currents was substantially less than the modulation seen at the foot of the activation curve (figure 4-3B). Increasing the number of channels or their conductance would have modulated currents to a similar extent regardless of the pH used to evoke the currents. There was a clear increase in apparent proton affinity of ASIC3 after modulation by ATP that resulted in a leftward shift of the proton activation curve.

To quantify the relative changes in half maximal pH of activation and the maximum evoked current, data in figure 4-3A were fit Using the Hill equation shown below and best fits were plotted in figure 4-3A.

Modified Hill Equation:

$$I_{pH} = Imax * \frac{pH^n}{pH_{50}^n + pH^n}$$

I_{pH} is the relative current amplitude evoked by a given pH. Imax is the maximum pH evoked current amplitude, pH_{50} is the half-maximal proton concentration in negative log units, pH is the proton concentration in negative log units and n is the Hill slope. The table in figure 3C displays the fit parameters under the three different calcium conditions before and after modulation by ATP.

There was some modulation of ASIC3 currents even when the channel should be fully opened and calcium completely unbound, pH 6.0 and low calcium (10nM) (figure 4-3A). This was highlighted by the increase in Imax in the table in figure 4-3C. On first glance, modulation appeared to mimic the effect of decreasing extracellular calcium, but modulation occurred when calcium should have been completely unbound suggesting that modulation was doing something other than decreasing calcium affinity for the channel. There are two possible explanations for this observation: 1) apparent calcium affinity was not affected while apparent proton affinity was altered suggesting a dissociation of proton binding and calcium unbinding. 2) P2X5 repressed ASIC3 activity by increasing calcium affinity to the point that even when free calcium and pH were low (10nM Ca^{2+}, pH6.0), a significant portion of ASICs remained calcium bound. Each of these possibilities was tested.

P2X5 depressed the proton sensitivity of ASIC3, ATP relieved the depression.

Two simple models of ATP dependent modulation were considered. 1) ASIC3 was initially unaffected by P2X5 and ATP application induced an effect upon ASIC3 after which it was modulated (potentiation). 2) P2X5 constitutively affected ASIC3 and ATP caused a reversal of the effect (relief of repression). Compared to ASIC3 expressed alone, ASIC3 co-expressed with P2X5 was less sensitive to protons. Proton activation curves were created for ASIC3 co-expressed with P2X5 before and after modulation by ATP and compared to ASIC3 expressed alone and the data were fit using the Hill equation (figure 4-4B). To compare ASIC3 responses between different conditions, all responses were normalized to the current evoked by pH 6.0 under that condition, even though there was an ATP dependent increase in pH 6.0 evoked currents when ASIC3 and P2X5were co-expressed. ASIC3 co-expressed with P2X5 had decreased proton sensitivity compared to ASIC3 and application of ATP shifted proton sensitivity to a value that was not significantly different from wild type. This suggested that the relief of repression model was most realistic (pH_{50}= 6.63, 6.81, 6.78 for ASIC3/P2X5 pre ATP, ASIC3/P2X5 post ATP, ASIC3 alone respectively). This result implied that P2X5 was constitutively interacting with ASIC3 and application of ATP resulted in either the disruption of the interaction or a change in the nature of the interaction allowing ASIC3 to behave as if P2X5 were absent. Comparing the relative current amplitude at pH 6.9 and 6.0 (figure 4-4A) relief of repression can be seen qualitatively. Each pair of traces are currents evoked by pH 6.9 (smaller) and pH 6.0 (larger) in cells expressing ASIC3 alone, ASIC3 + P2X5 before modulation, and ASIC3 + P2X5 after modulation. ASIC3 + P2X5 after modulation by ATP most closely resembled ASIC3 expressed alone. The relief of repression

model is consistent with the model of a kinetic trap where ASIC3 was held away from a most stable conformation and ATP catalyzes the conversion of ASIC3 between the unfavorable and more favorable state.

Current ratios reveal P2X subtype specificity in ASIC3 interactions

The result that the proton sensitivity of ASIC3 appeared depressed by P2X5 and was relieved by ATP was unexpected and required closer investigation. There was a clear difference between the relative amplitudes of currents evoked by pH6.9 and pH6.0 upon modulation by ATP (figure 4-4). To compare a larger number of data points from multiple transfections and solutions only the current near the peak (pH6.0) and foot (pH6.9) of the activation curve were measured to provide a snapshot of how far up the proton response curve pH 6.9 was. To minimize any effects of daily variations in pH values, divalent ion concentrations, or solution exchange speed, the current ratios in at least five cells expressing ASIC3 alone each day were measured and averaged. All other current ratios from cells expressing ASIC3 with various P2X receptors were then normalized relative to the daily average of ASIC3 alone. Cells were then pooled according to which combination of channels they expressed. The results (figure 4-5, table 4-2) agree with the activation curve data for ASIC3 alone and co-expressed with P2X5 receptors: P2X5 depressed the proton sensitivity of ASIC3 and ATP relieved it. Unexpectedly, P2X2, 3, and 4 had different effects. P2X4 co-expression made ASIC3 more sensitive to pH6.9 before ATP and modulation by ATP even further increased the proton sensitivity of ASIC3, increasing the current ratio. P2X2 affected ASIC3 initially by depressing proton sensitivity and potentiated

sensitivity after ATP application. Surprisingly P2X3 (which was shown in chapter 3 to have no modulatory effect on ASIC3 in response to ATP) depressed the proton sensing ability of ASIC3 strongly. Thus, P2X3 could potentially constitutively inhibit the acid sensing of ASIC3 and co-expression of other P2X receptors could produce an array of ASIC3 phenotypes in vivo. Alternatively, P2X3 may modulate ASIC3 in response to ATP under more physiological temperatures when the rapid, complete and long-lasting desensitization of P2X3 may have different kinetic features.

P2X2 and P2X4 interact with ASIC3 differently.

It was previously shown that ASIC3 is also modulated by P2X2 and P2X4. Data comparing the relative current amplitudes evoked by pH6.9 and pH6.0 demonstrated that each P2X subtype interacted in a unique manner with ASIC3. Full proton activation curves for ASIC3 expressed alone or in tandem with P2X2 or P2X4 were measured to confirm the results seen from the current ratio experiments (Figure 4-6, summary table 4-1). Data were collected as described previously. To minimize the effects of slightly different measurements due to pH electrode or ion concentration fluctuations or changes in the speed of solution exchange, activation curves for ASIC3 co-expressed with each P2X receptor was recorded together with ASIC3 alone on the same day using the same solutions and are plotted together. Data from ASIC3 alone from different experiments were not found to be significantly different from one another and were pooled into one data set for analysis in Table 1, but they are kept separate in each activation curve graph. Results for ASIC3 + P2X2 and ASIC3 + P2X4 are shown in figure 4-6 A and B respectively.

In agreement with the pH current ratio data (I6.9/I6.0), P2X2 slightly depressed the proton sensitivity of ASIC3 before ATP application and ATP caused an increase in the half maximal pH of activation (pH50= 6.69 before ATP and 6.84 after ATP for ASIC3 + P2X2) making ASIC3 + P2X2 after ATP more sensitive to protons than ASIC3 alone (pH50=6.78). Again, ASIC3 + P2X4 was similar to ASIC3 alone and ATP increased in ASIC3 proton sensitivity beyond that of ASIC3 alone (pH50= 6.80 before ATP and 6.94 after ATP for ASIC3 + P2X4). Results from the best fit of the Hill equation to all activation curve data suggested that each P2X receptor had a unique interaction with ASIC3 that was subtype specific (table 4-1). With the exception of P2X3, ATP caused a similar shift in the proton sensitivity of ASIC3 shifting the half-maximal pH of activation by about 0.15pH unit. This small change in half-maximal proton concentration has large functional effects since proton activation of ASIC3 has a Hill slope of around 4.

Modulation of ASIC3 by P2X4 occurs at low calcium concentrations and low pH.

P2X5 was shown to modulate ASIC3 most strongly at sub-saturating pH values, but there was a reproducible increase in the pH evoked current even at low pH and minimal calcium (pH 6.0, 10nM calcium figure 3). Two possible explanations for this are that 1) P2X5 increased the calcium affinity of ASIC3 to such a degree that calcium never unbound or 2) modulation was affecting proton activation at least somewhat independent of calcium unbinding. P2X5 repressed the proton sensitivity

of ASIC3 and ATP relieved the repression which would be consistent with changing calcium affinity as a mechanism for modulation. P2X4 on the other hand, did not strongly affect ASIC3 sensitivity before modulation (or slightly potentiated it) but ATP modulation potentiated the proton sensitivity well beyond that of ASIC3 alone. Therefore, modulation by P2X4 pH 6.0 in the absence of calcium was examined. Under these conditions ASIC3 should be maximally open and fully unblocked by calcium. If calcium affinity changes play a primary role in the modulation of ASIC3 proton sensitivity, an ATP dependent increase in current amplitude at pH 6.0 in the absence of calcium would not be expected. Currents evoked in cells expressing ASIC3 and P2X4 in response to pH 7.0 (1mM calcium), pH 6.0 (1mM calcium), and pH 6.0 (10mM EDTA) were measured and modulation by ATP was assayed (figure 4-7). After modulation the currents evoked by pH 7.0 (1mM calcium) greatly increased in amplitude. Although the currents evoked by pH 6.0 under both calcium conditions increased far less than those at pH 7.0, there was a significant increase in the current amplitude at pH 6.0 (1mM calcium) and pH 6.0 (10mM EDTA). These results support the hypothesis that P2X receptors did not simply alter the calcium binding site and suggest that changes in calcium affinity were not the sole mechanism for increased proton sensitivity. There was also a dramatic slowing in the time course of desensitization at pH 6.0 in the absence of calcium after ATP. The slowing of the time constant of desensitization seen in figure 4-7A suggested another possible mechanism of modulation. Perhaps slowing desensitization allowed more channels to be open at any one time and thus produced larger currents. ASIC3 desensitization was

investigated to look for changes in the desensitization time constant due to modulation under more physiological pH and calcium conditions.

The desensitization time constant was modulated by ATP.

The time constant of desensitization of ASIC3 was affected in a manner that mirrors changes in apparent proton affinity and current ratio data. ASIC3 desensitized nearly completely in the continued presence of protons (figure 4-8). Currents evoked by pH 6.8 (2sec) were measured in cells expressing ASIC3 alone or in tandem with P2X2, 4, or 5 before and after ATP application. The pH solution was changed to pH 6.8 in order to achieve a more rapid and concerted opening of the channels and nearly complete desensitization (relative to pH 7.0 or 6.9). This proton concentration also minimized artifacts due to series resistance errors that might occur due to large current amplitude. In fact, however, time constant data from lower pH (pH 6.0) gave essentially identical results despite the small increase in current amplitude seen at this pH. The desensitizing phase of the current was well fit with a single exponential yielding a time constant (τ) of about 250 milliseconds (figure 4-8A, table 4-2).

ASIC3 when expressed alone decayed with a time constant of 242 +/- 6ms. When P2X5 was co-expressed with ASIC3 τ decreased to 198 +/- 9ms. Upon application and washout of ATP, τ increased to 260 +/- 20msec, not significantly different from ASIC3 alone. The τ of desensitization for ASIC3 in the presence of P2X4 changed from 254 +/- 8ms before application of ATP to 390 +/- 7 ms after. P2X2 again influenced ASIC3 both before and after ATP modulation (τ= 222+/- 7msec before

and 320 +/- 39ms after ATP). Normalized current traces evoked by pH 6.8 with ASIC3 alone (black), ASIC3 + P2X4 before ATP (light gray) and ASIC3 + P2X4 after ATP (dark gray) demonstrate the magnitude of changes in the rate of desensitization cause by ATP modulation (figure 4-8B). Interestingly, the dynamics of desensitization times mirrored the changes in current ratio values and apparent proton affinity: P2X5 decreased proton sensitivity and sped desensitization and ATP relieves the changes, while P2X4 in response to ATP increased proton sensitivity relative to ASIC3 alone and slowed the rate of desensitization. This may suggest a link between desensitization time and the efficiency of activation but further studies will be necessary to determine whether a connection exists.

Modulation by P2X5 does not alter calcium affinity.

Previous results suggested that changes in calcium binding alone could not explain all aspects of ASIC3 modulation since there was still some modulation when calcium should have been completely unbound. It has been demonstrated that calcium and protons compete for a calcium binding site and ASIC3 can be opened by decreasing pH (increasing proton concentration) or decreasing calcium concentration. Calcium activation of ASIC3 was directly measured. Decreasing calcium concentration from 1mM to micromolar or nanomolar concentrations dose-dependently opened ASIC3 in the absence of pH changes allowing a direct measure of apparent calcium affinity. Application of ATP (50μM, 30 sec) increased the amplitude of currents evoked by decreased calcium. Calcium activation curves revealed that ATP dependent modulation of ASIC3 by P2X5 increased current amplitude at all calcium

concentrations (figure 4-9A). In contrast to apparent proton affinity, no change in apparent affinity for calcium was seen. Normalization of activation curves before and after ATP application highlight this finding (Figure 4-9B).

Since proton activation experiments demonstrated that an increased number of channels is likely not the explanation for modulation, it seems that conductance or efficacy was affected when ASIC3 is opened by decreasing calcium. This may also shed light on the interaction between calcium and protons in ASIC gating, suggesting that calcium unbinding and proton binding are not functionally identical. Another possibility that is not mutually exclusive is that no change in calcium affinity of ASIC3 was observed because the changes are very slight (about .15 log unit) and the Hill slope of calcium activation was relatively shallow ($n \approx 1$ calcium activation, $n \approx 4$ proton activation) which prevented measurement of a small change in affinity. While this may be true, the large increase in current amplitude at the peak of the calcium activation curve suggests a clearly different effect on calcium dependent gating that was not present in proton gating conditions (figure 4-10). Even though calcium may be unbound and the channel may be open, an unprotonated channel is clearly different from a protonated one. Modulation by ATP may titrate acidic residues that are important for conductance and when calcium is removed, the channel is able to conduct more efficiently. Alternatively, modulation may allow more efficient transduction of calcium unbinding into channel gating.

Steady state inactivation was unaffected.

In addition to the strong pH dependence of ASIC3 for gating, the degree of steady state inactivation has been shown to be steeply dependent on pH. At pH below about 7.4 in the presence of calcium (1mM), ASIC3 begins to desensitize decreasing the pool of channels available to be activated. The degree of steady state inactivation was examined looking for changes due to ATP dependent modulation. The pH of the bath solution was incrementally changed from pH 8.0 down to 7.0 and the amplitude of a current evoked by pH 6.8 (2 sec) was measured after 20 seconds in each bath solution (Figure 4-11). This was done before and after ATP application that resulted in maximal modulation of ASIC3, usually about 2 minutes, in cells co-expressing ASIC3 and P2X5. Each condition was normalized to the current evoked by a pH change from pH 8.0 to 6.8 (Figure 4-11B). Despite the steep proton dependence of steady state inactivation (Hill slope= 8) and the modulation of the pH 6.8 evoked current (Figure 4-11B), there was no change in the half-maximal pH of inactivation (pH50= 7.21 before ATP, 7.23 after ATP, pH 50 of best fit of Hill equation).

Sustained currents were modulated by ATP.

ASIC3 can produce a sustained current under physiologically relevant conditions due to a window current when steady state inactivation is incomplete while there is partial activation. Since steady state inactivation was not affected by ATP dependent modulation while proton sensitivity was increased, a sustained current that is modulated by ATP in a manner similar to the peak current was predicted. While P2X5 passed very little current on its own, prolonged application of ATP (50μM) resulted in an increase in amplitude of the sustained current of ASIC3 evoked by pH

7.0 (2mM Ca^{2+}, 1mM Mg^{2+}) that took over a minute to reach its peak (figure 4-12A) in cells expressing ASIC3 and P2X5. The slow time course of modulation by P2X5 was seen directly with this experimental paradigm. The increase in current was not due to current passed directly through P2X5 since it persisted after the washout of ATP (Figure 4-2B), and was not due to ATP altering the pH of the pH 7.0 solution, since it was a slowly occurring change and persisted after a switch back to the pH 7.0 solution not containing ATP. Also note the increase in the current noise that accompanied the increase in sustained current amplitude. The two effects, amplitude and noise, may synergize to promote repetitive firing of sensory neurons necessary to trigger a prolonged sensation like angina.

The slow time course of modulation was P2X receptor dependent.

Chimeric constructs containing domains of P2X5 and P2X3 were constructed in an effort to identify regions of P2X that potentially interacted with ASIC3. Unexpectedly, pH current ratio data suggested that P2X3 interacted with ASIC3 but was unable to modulate the interaction. Any results using chimeric constructs to look for modulation of ASIC3 would not reflect the ability of P2X domains to interact with ASIC3 and this line of investigation was not pursued. One chimera constructed from the N-terminus, first transmembrane domain and extracellular loop of P2X5 and the second transmembrane domain and C-terminus of P2X3 (figure 4-13C) passed large slowly desensitizing currents and robustly modulated ASIC3 with unique features. A two second application of ATP (50μM) resulted in robust modulation of the transient and sustained ASIC3 currents (figure 4-13A, B). This contrasted markedly with

modulation of the sustained current of ASIC3 by P2X5 (figure 4-12) which took minutes to reach a peak. This further supported the suggestion that the slow nature of P2X dependent modulation was a result of properties intrinsic to the P2X receptor and not an extremely slow signaling process.

Towards a mechanism of modulation

Truncation of the C-terminal tail of P2X2 was reported to disrupt the interaction between P2X2 and GABA channels (Boue-Grabot, Emerit et al. 2004). P2X4, however, has a relatively short C-terminal tail similar in length to the P2X2 truncation making it unlikely that this region was involved in modulation of ASIC3. Truncations of P2X2 (P2X2 375Δ) and the correlate P2X5 truncation (P2X5 381Δ) were constructed and both constructs were able to modulate the proton sensitivity of ASIC3 in response to ATP (figure 4-14). Thus, the C-terminal tail distal to a necessary trafficking motif was unnecessary for modulation.

Arachidonic acid (AA), an amphipathic fatty acid, has been reported to interact with ASICs and modulate proton sensitivity similar to modulation by P2X (Allen and Attwell 2002; Smith, Cadiou et al. 2007). This was found to be the result of a direct action of AA on channel function independent of signaling activity of AA or its metabolites. This result was confirmed in cells expressing ASIC3 and P2X4. AA (10μM) slowly increased the amplitude of pH evoked currents over 100 seconds (figure 4-15A). Subsequent application of ATP (50μM, 20 sec) in the continued presence of AA had no effect on the amplitude of pH evoked currents but did slow

desensitization (figure 4-15B). AA did not inhibit P2X4 and likely potentiated the currents (not shown) since the current evoked by ATP with a -30mV holding potential was greater than 10nA- much larger than normal P2X4 evoked currents (2-4nA, -70mV). Thus, AA appeared to occlude modulatory effects of ATP on current amplitude but it did not appear to prevent modulation since the time constant of desensitization was still prolonged after ATP application.

The action of AA on other ion channels has been reported previously and was attributed to effects on membrane shape and thickness. Lysophosphatidyl choline (LPC) another amphipathic lipid- but with a net neutral charge and large hydrophilic head group- was reported to have opposite effects on membrane shape and channel function (Casado and Ascher 1998). LPC action on ASIC3 activity was investigated in an effort to determine if membrane dynamics may play a role in modulation of ASIC3 by P2X. Contrary to what was expected, LPC (2.5μM) also increased the amplitude of pH evoked ASIC3 currents (figure 4-15C) in cells expressing ASIC3 and P2X4. LPC both increased current amplitude and slowed desensitization. Washout of LPC partially reversed both effects. Subsequent application of ATP (50μM, 20 sec) mimicked but did not exceed the effects of LPC. Typically, P2X4 increased pH evoked current amplitude by 150-200%, which was substantially larger than the increase after LPC. These data indicate that amphipathic membrane localize molecules could interact with ASIC3, increasing proton sensitivity perhaps similarly to modulation by P2X4 but more data are necessary to determine if this is truly occlusion of ATP dependent modulation.

Outside-out membrane patches were excised in attempt to determine if modulation could occur in the absence of intracellular effectors. In cells expressing ASIC3 and P2X5 ATP dependent modulation was not observed in patches but the activation characteristics of ASIC3 appeared altered (not shown). Since P2X5 is electrically quiet, it was impossible to know if P2X5 was present in the patch in sufficient quantities to trigger modulation. Activation curves for the excised patches were measured and compared to whole cell ASIC3 currents (figure 4-16A). Patch excision mimicked modulation of ASIC3 shifting the pH_{50} of ASIC3/P2X5 patches to 6.98 compared to 6.78-ASIC3 alone whole cell, and 6.62-ASIC3/P2X5 whole cell.

Since patch excision dramatically increased proton sensitivity, the effect of ATP and AA on ASIC3 currents in ASIC3/P2X4 patches was examined (figure 4-16B). There was a small increase in the current amplitude of pH 7.0 evoked currents in response to ATP and virtually no change in response to AA, with both effects largely occluded by patch excision. Arachidonic acid appeared to largely occlude modulation of ASIC3 by P2X4 and patch excision occluded modulation by both AA and P2X4/ATP. This may suggest that all three manipulations, ATP, AA, and patch excision, have similar effects on the proton sensitivity of ASIC3. There may be an intimate association between ASIC3, P2X, the membrane and perhaps the cytoskeleton which all affect the efficiency of proton sensing. Further investigations may reveal the effects of the environment on ASIC sensitivity and the relationship between the various interacting factors.

Correlation between permeability changes and modulation

P2X2, 4, 5, and 7 have been reported to undergo slow permeability transitions becoming increasingly permeable to the large organic cation N-methyl-D-glucamine (NMG) (Khakh, Bao et al. 1999; Virginio, MacKenzie et al. 1999; Virginio, MacKenzie et al. 1999). Since both permeability changes of P2X2 and modulation of ASIC3 by P2X2 occur on a slow time scale, ATP was applied in an external solution with all monovalent cations replaced with NMG. When ATP was applied in the presence of NMG at -50mV in cells expressing ASIC3 and P2X2 several different current waveforms were seen (figure 4-17). In a cell in which no modulation occurred (top), ATP (50μM, 20 sec) evoked a small NMG permeable current with no changes in the current amplitude over the course of application of ATP. Immediately after ATP application the bath solution was returned to standard extracellular solution and a large transient inward current indicated that P2X2 was expressed. When some modulation of ASIC3 current was observed (figure 4-17, middle traces), ATP evoked a larger current that rapidly activated, decreased in amplitude and then slowly increased again before desensitizing. In the lower trace there was large modulation of the ASIC3 currents and a large change in current waveform over the course of the 20 second ATP application. A similar fluctuation in P2X2 current amplitude can be seen in the P2X2 truncation mutant with standard external solution (figure 4-14) and was typical of P2X2 currents that modulated ASIC3 but the large amplitude and somewhat jagged current waveform seemed untrustworthy. The currents evoked in NMG, by contrast were of smaller amplitude and had smoother fluctuations in current

amplitude reducing the likelihood that these changes were artifacts due to large ion flux or seal breakdown. With this limited number of examples there appeared to be a correlation between modulation and P2X2 current waveform which may be pursued further in the future.

Discussion:

Summary

It was demonstrated that modulation of ASIC3 by P2X receptors is a property shared by many P2X receptors. Modulation by ATP made ASIC3 both more sensitive to protons and slightly potentiated the peak response to pH. Interestingly, there was no increase in the apparent calcium affinity, rather the current amplitude increased equally at all calcium concentrations demonstrating a clear difference between pH and calcium activation and suggesting that modulation affected a uniquely proton dependent process. While the proton sensitivity of activation was increased, steady state inactivation was unaffected which resulted in an increase in the amplitude of a physiologically important sustained current.

Each P2X subtype was shown to interact with ASIC3 differently. P2X5 repressed the proton sensitivity of ASIC3 and ATP relieved the repression. P2X4 conversely had little effect on ASIC3 proton sensitivity before modulation by ATP but potentiated the sensitivity afterwards. P2X2 was a hybrid of these two effects, repressing before ATP modulation and potentiating afterwards. P2X3 which did not modulate ASIC3 repressed the proton sensitivity of ASIC3 constitutively. This allows for a potential

spectrum of ASIC3 sensitivities that could be tuned by the collection of P2X receptors that serve as interacting partners.

Importance of sustained currents

The sustained current produced by ASIC3 in response to physiologically relevant pH changes is of key importance in sensing of persistent stimuli with a desensitizing channel. Previous work has demonstrated that the sustained current is the result of an overlap between proton dependent activation and steady state inactivation (Yagi, Wenk et al. 2006). In this chapter it was demonstrated that the degree of steady state inactivation did not change upon modulation by ATP while both activation and rate of desensitization did change. If the change in the rate of desensitization was the result of slower desensitization rather than less concerted channel opening or a relatively quicker rate of closing compared to the rate of desensitization, channels will spend more time open before desensitizing. More frequent and longer openings may synergize to increase the sustained current to a greater extent than the peak currents further amplifying the effects of modulation on current amplitude. Since steady state inactivation and activation both have very steep proton dependence (Hill slopes of aprox. 8 and 4 respectively), the window current occurs only over a small pH range. Over this pH range the small differences in ASIC3 proton affinity seen with different P2X subunits may play a very important role in the sustained currents passed by ASIC3.

Series resistance

One problem when observing changes in current amplitude is the potential for the contribution of artifacts due to changing series resistance. Care was taken when recording to eliminate any artifacts due to changing series resistance. Series resistance was kept to a minimum, usually below 6MΩ and compensated by about 80%. Current amplitude was kept at a minimum and at pH 6.8 the current amplitude was generally less than 2nA. The two general effects of modulation that were described- increasing current amplitude and prolonging the desensitization time constant- would be affected by series resistance in opposing fashion. To explain increased current amplitude by series resistance errors would require a dramatic decrease in series resistance, which was not the case. On the other hand, series resistance would have to increase dramatically to slow the time constant of desensitization. Both can clearly not happen at once. Furthermore, the changes in current amplitude and time constant of desensitization are consistent from cell to cell despite variability in current amplitude ranging from 50-100pA to 3-4nA. Since series resistance errors affect larger currents more than smaller currents a correlation between current amplitude and tau or percent increase in current would be expected which was not observed.

Steady state inactivation and desensitization

At first glance, the changes in the time constant of desensitization may seem incompatible with the fact that there were no measurable changes in the degree of steady state inactivation. These two measures are likely examining different aspects of channel function. The desensitization time constant is dominated by the rate and

synchrony of channel opening, the stability of the open state and relative rates of desensitization and closing/calcium rebinding. Steady state inactivation involves many steps as the channel cycles from closed to open to desensitized and back to open or closed states. It represents an equilibrium condition in which the number of available channels is determined by the rate limiting step in this cycle. Nearly complete activation and desensitization of ASIC3 occurs within two seconds, activation (millisecond time scale) and desensitization (hundreds of milliseconds) are probably not rate limiting. The rate limiting step is likely a step involved in recovery from desensitization which occurs on the order of seconds in a calcium and proton dependent manner (higher calcium and lower proton concentrations speed recovery) (Immke and McCleskey 2003). Modulation likely affects activation and desensitization but doesn't affect the proton dependence of recovery from desensitization to a measurable extent. Since steady state inactivation depends steeply on pH, with a Hill slope greater than 8, a change in steady state inactivation would have been measured if it were present.

Physical interaction supported

In the previous chapter evidence was presented suggesting that a physical interaction between ASIC3 and P2X5 was responsible for modulation of ASIC3. This theory was further supported by the finding that each P2X subtype interacted uniquely with ASIC3 altering the proton sensitivity in a subtype dependent manner. This finding is most easily explained by a unique physical association with each P2X subtype interacting with ASIC3 in specific manner. Prolonged exposure to ATP may alter the

interaction by promoting long lived conformational changes in the P2X receptor. To explain the finding that each P2X subtype affects ASIC3 differently with signal transduction mechanisms would require multiple transduction pathways or a complicated feedback system with constitutive activity that can be tuned up or down in response to different triggers. Since ATP dependent modulation has been demonstrated in sensory neurons and HEK-293, COS, and CHO cell lines it would likely have to be a fairly common signaling pathway which does not involve kinases, phosphatases and G-proteins. While possible, this is less likely than a direct interaction which, by its nature, would be subtype specific.

Channel efficacy may be increased by modulation

The specific effect of P2X modulation on ASIC gating remains elusive. To definitively determine changes in ASIC3 gating, a single channel study of modulation is necessary. Unfortunately, the process of excising outside out patches changes the proton sensitivity of ASIC3 mimicking modulation by P2X4. This appeared to occlude further P2X dependent modulation, making study of an ASIC3/P2X interaction in excised patches impossible at this time. Since amphipathic lipids were able to mimic ATP dependent modulation it is possible that some amphipathic or perhaps non polar lipid compounds could have the opposite effect. If such a compound were found, it could potentially reverse the effects of patch excision and allow for study of evoked single channel events and their changes due to modulation by P2X.

The increase in peak currents seen at low pH in the absence of calcium could be explained by an increase in the efficacy of gating— increases in efficacy can have the effect of both increasing the Imax and increasing the apparent affinity of an ion channel for ligand (Colquhoun 1998; Hall 2000). This would potentially require separate proton binding/ calcium unbinding and gating steps which would raise questions about the validity of the gating model in which calcium blocks the channel and protons relieve the block without a gating step. In excised patches a previous study found that in outside-out patches containing 3 ASIC3 channels, all 3 channels opened in 17 of 20 pH trials and two of three channels opened on the other 3 trials in 1mM calcium at pH 6.0. Over the course of this experiment there were 57 of a possible 60 channel openings, a very high open probability of 95% (Immke and McCleskey 2003). This high open probability could explain why excising patches occluded P2X dependent modulation of ASIC3 if the mechanism of modulation is through increasing efficacy of gating although efficacy can still increase as the open probably approaches 100%. Perhaps efficacy and maximum open probability is significantly less in an intact cell and as a result, increasing gating efficiciency by P2X modulation is possible.

Interaction between protons and calcium

A slight increase in the peak proton evoked currents and increased proton sensitivity could be due to an increase in the efficiency of gating secondary to proton binding and calcium unbinding. A proposed model of ASIC gating that suggested that calcium and protons compete for a calcium binding site. Protons simply catalyze the

release of calcium from the binding site and the channel opens without a conformational change. This model also correctly predicted that calcium would block the channel and thus lowering calcium would increase single channel conductance. A calcium blocking site that when mutated relieved calcium dependent block of ASIC1 expressed in oocytes but did not affect activation was recently described suggesting separate gating and block sites for calcium binding (Paukert, Babini et al. 2004). This is also consistent with the recent crystal structure of chicken ASIC1 which identified potential proton gating sites that are quite removed from the permeation pathway and likely to not serve as a calcium blocking site (Jasti, Furukawa et al. 2007). Modulation of ASIC3 by P2X had clearly different effects on calcium dependent gating and proton dependent gating. Together, these results suggest that while there may be a competition between calcium and protons for a binding site responsible for gating, there is clearly a more complex relationship between protons and calcium with perhaps multiple binding sites for both protons and calcium and perhaps gating steps that are proton dependent and calcium independent that should be addressed by future studies.

A few insights can be gained from the calcium activation studies. There was clear modulation of the current activated by decreasing calcium at pH 8.0. These currents did not desensitize and are fully unbound from calcium. This implies that modulation increased either the single channel conductance or the channel open probability promoting a greater fraction of open channels at any one time independent of the rate of desensitization. Increased conductance could not explain the effect seen with

proton activation, however since conductance increases affect current amplitude regardless of open probability. On-cell single channel measurements of currents at pH 8.0 and low calcium may shed light on this but it is possible that ASIC3 rapidly opens and shuts at this particular pH which, if rapid enough, could make changes in open probability indistinguishable from conductance changes electrically.

Since apparent calcium affinity was not affected by modulation, interactions with P2X did not appear to affect the calcium gating site. Likewise, modification of a potential calcium blocking site was likely not the primary change due to modulation since there was still modulation in minimal calcium/ low pH conditions when calcium should have been completely dissociated from ASIC3.

This supports the idea that there was an increase in the efficacy of gating resulting in a larger percentage of the channels being opened at once perhaps through an allosteric mechanism. There are several kinetic mechanisms which could fall under the broad category of "increased efficacy" that could explain the results described here. One mechanism could be an increased efficiency of the initial transduction of proton binding into channel gating. If 100% of ASIC3 channels do not open with low pH tests, perhaps there was not always transduction of proton binding and calcium release to the gate to trigger gating. This would necessarily require separate calcium unbinding and gating steps. A second possibility is modulation resulted in an increase in the coincidence of calcium unbinding among channels. If the channels before modulation open somewhat asynchronously and then quickly desensitize it makes it

less likely that all channels would be open at any one time. If increased synchrony of channel opening was the sole change in ASIC3 kinetics, modulation would be expected to decrease the time constant of desensitization rather than increase it. More asynchronous opening should lead to more asynchronous and thus slower desensitization rates. This is the opposite of what was observed; modulation slowed desensitization, although there is no evidence to directly link increased proton sensitivity with slowed desensitization. A third potential mechanism is that modulation stabilized the open state of the channel, slowing desensitization and therefore increasing the number of channels that are open at any one time. This effect on stabilizing the open state could explain both the increase in peak currents and the slowing of the rate of desensitization and would not necessarily require an independent binding and gating steps. A detailed single channel kinetic study is necessary to determine which aspects of gating: proton binding, opening, closing and desensitization; were effected by ATP dependent modulation which is not possible at this time.

A fourth explanation for seeing larger currents at low pH values could be attributed to solution exchange artifacts. Since the cell is attached to a coverslip, there is not a laminar flow around the cell. Proton concentration will change more slowly on the bottom of the cell than on the top. When rapid activation and desensitization occur in a solution exchange limited system the shape of the activation curve could be affected, artificially occluding the peak currents and making the channel seem less sensitive to protons and preventing saturation. This is likely not the reason that an

increase in currents at the peak of the activation curve was observed since a linear component of the activation curve after saturation would be expected since, for example a pH 5.0 solution will drop the pH under the cell to pH 6.0 more quickly than pH 6.0 solution resulting in a larger current at pH 5.0 even if pH 6.0 were truly saturating. However, essentially equal current amplitude at pH 5.0 and 6.0 was observed and modulation increased both of these currents proportionally. Lifting of the cells off the coverslip would prevent this potential artifact, but that was not practical for these experiments.

Interaction between ASIC3 and amphipathic lipids

The unique trimeric structure of ASICs and P2X receptors with large extracellular domains and two transmembrane domains per subunit are different from other channels in their minimalism. Only six transmembrane domains contribute to formation of the channel which contrasts markedly with the 24 transmembrane domains seen in voltage gated channels. Based on the crystal structure of ASIC1 and the overall structural homology between ASIC and P2X it is apparent that ASICs and P2X receptors interact intimately with their environment. Lipids, phospholipids, fatty acids, and membrane bound molecules and proteins may have a large effect on the functional properties of these channels as they may potentially interact directly with transmembrane regions responsible for permeability, gating and desensitization. Membrane order has been suggested to affect ENaC activity (Awayda, Shao et al. 2004).It is possible that there are many ASIC and P2X modulators that will be discovered.

Arachidonic acid and lysophosphatidyl choline both mimicked and potentially occluded modulation of ASIC3 by P2X4 increasing current amplitude to an extent that subsequent modulation by P2X4 had no further effect. Two potential proton binding sites were discovered in the crystal structure of ASIC1 (Jasti, Furukawa et al. 2007). These sites are removed from the transmembrane domains their environment could conceivably be influenced by the extracellular domain of P2X. It is possible that modulation by P2X, AA, and LPC promote efficient transduction of proton binding into gating. Alternatively, P2X modulation of ASIC could result from changes in P2X structure that alter interactions between the transmembrane regions and the lipid bilayer. This could subsequently alter the local composition of the membrane affecting the efficiency of gating of nearby ASICs resulting in greater proton sensitivity. Future electropysiological and structural studies could address these issues.

Modulation was not an artifact of solution exchange.

It is possible that the speed of solution exchange created an artifact resulting in apparently larger currents due to more rapid solution exchange after ATP application perhaps due to the cell being less adhered to the coverslip and therefore more accessible to rapid solution exchanges. However, robust modulation of sustained currents was observed when solution exchange speed played no role in determining current amplitude.

Figure 4-1: Extracellular ATP causes an increase in the ASIC3 mediated current evoked by a pH 6.9 stimulus.

Two second applications of a pH 6.9 stimulus evoke ASIC3 mediated currents in CHO cells expressing either ASIC3 (A) or ASIC3 and P2X5 (B). After a 30 second application and washout of 50μM ATP the amplitude of the pH evoked current is increased when P2X5 is present (B). There is no change in current amplitude in the absence of P2X5 (A).

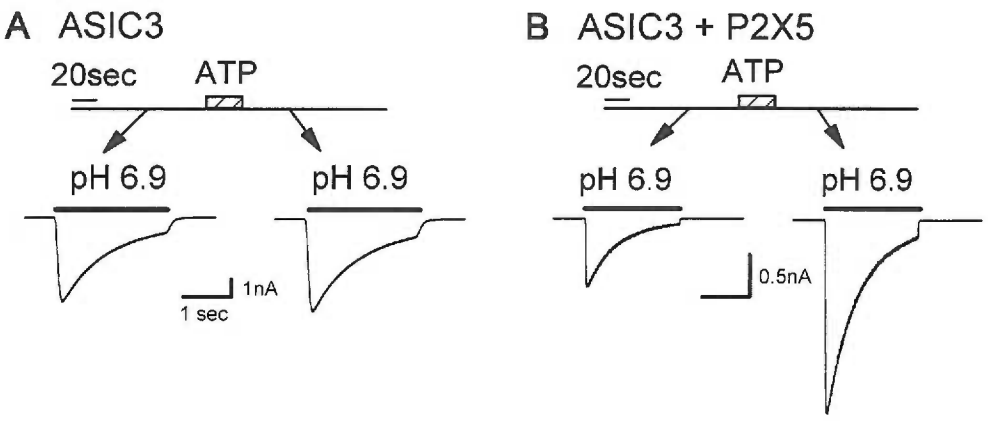
A ASIC3
20sec
ATP
pH 6.9
pH 6.9
1nA
1 sec
B ASIC3 + P2X5
20sec
ATP
pH 6.9
pH 6.9
0.5nA

Figure 4-2: Modulation is slow to initiate and does not reverse over time scale of experiment.

A. Currents evoked by 2 second applications of pH 6.9 in cells co-expressing ASIC3 and P2X5 before (1), immediately after ATP application (2), and at the end of experiment (3) from the timecourse shown in B. Application of ATP slowly increases the current amplitude. The increase never returns to baseline values. Scale: 0.5 sec, 200pA. B. Timecourse of modulation. Peak current amplitude evoked by pH 6.9 was measured and plotted every minute. Two black bars represent 2 sets of 3 X 30 second applications of 50μM ATP. One 30 second application was delivered between each pH test. Current amplitude slowly increases with each 30 second application of ATP. Numbers show timepoints of each trace shown in A.

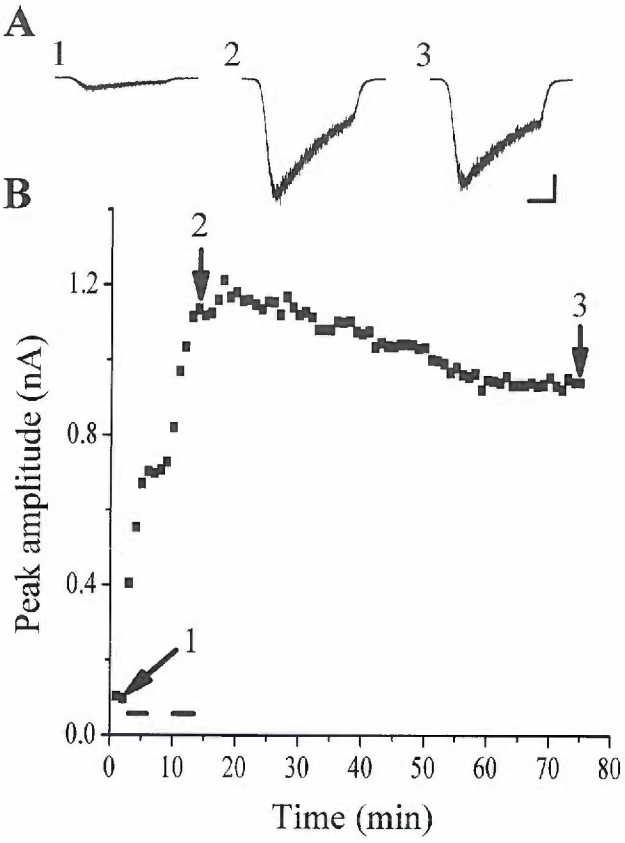
A
1
2
3
B
2
3
1
1.2
0.8
0.4
0.0
Peak amplitude (nA)
0
10
20
30
40
50
60
70
80
Time (min)

Figure 4-3: Modulation of ASIC3 by P2X5 makes ASIC3 more sensitive to protons. A. Activation of ASIC3 by protons in 10nM (gray), 1mM (black), or 10mM (open) calcium is shown before (squares) and after (circles) a 2 minute application of 50uM ATP. Test pulses of various pH values were delivered before and after ATP application and the peak current evoked by each pH was measured, averaged and plotted. All data points were normalized to the current evoked by pH 6.0/ 1mM calcium before ATP application. Data were fit with the Hill equation and the best fit of each dataset are plotted. At all calcium concentrations the maximally evoked current is modulated only slightly, whereas the currents near the foot of the activation curve are modulated more dramatically. Interestingly, even at pH 6.0 and 10nM calcium, when ASIC3 is maximally activated, the current is still somewhat modulated. All points were normalized to the current evoked by pH 6.0 at 1mM calcium noted with *. Gray and open diamonds indicate degree of modulation at pH 6.0 1mM calcium when activation curves for 10nM calcium or 10mM calcium respectively were measured. B. Bar graph plotting the percent increase in maximal current as function of pH from data in A with 1mM calcium showing that modulation by ATP affects sub-maximal pH evoked currents to a greater extent than at the peak of the activation curve. C. Table below summarizes the results of fitting data in A with the Hill equation comparing the half-maximal pH of activation, maximum relative current and Hill slope. Modulation by ATP slightly increases the maximal current and shifts the half-maximal pH revealing increased sensitivity to protons.

A

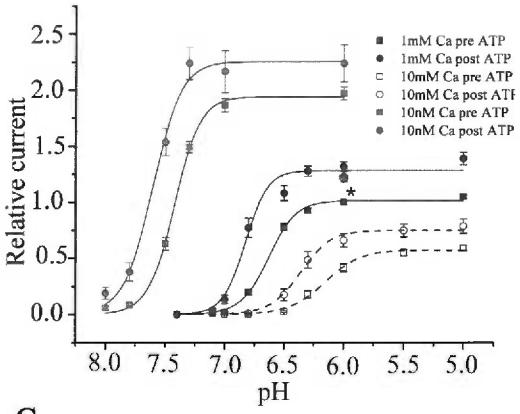

B

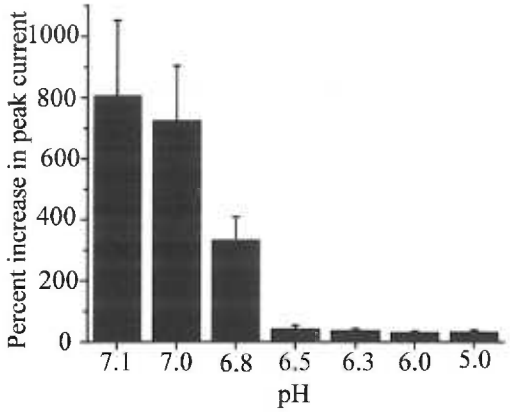

C

$[Ca^{2+}]$	I_{max} (normalized)		pH_{50}		Hill Slope		R^2	
	Pre	Post	Pre	Post	Pre	Post	Pre	Post
10nM	1.94	2.26	7.42	7.61	4.01	3.59	0.999	0.991
1mM	1.02	1.29	6.63	6.82	3.72	4.47	0.998	0.983
10mM	0.57	0.752	6.16	6.36	2.90	3.37	0.996	0.995

Figure 4-4: P2X5 depresses proton sensitivity of ASIC3, ATP relieves depression. A. Voltage clamp recordings of pH evoked currents from cells expressing ASIC3, ASIC3 + P2X5, and ASIC3 + P2X5 after modulation by ATP. Each pair of traces shows representative currents evoked by pH 6.9 (smaller) and pH 6.0 (larger). ASIC3 + P2X5 after ATP modulation most closely resembles ASIC3 alone. Scale bar: 0.5sec, 0.5nA. B. Activation curves of ASIC3 (black squares), ASIC3 + P2X5 (open circles), and ASIC3 + P2X5 after application and washout of 50μM ATP (gray triangles) expressed in CHO cells. ATP was applied until currents evoked by pH 6.9 no longer increased in amplitude, usually about 2 minutes. All activation curves are normalized to the peak current amplitude evoked at pH 6.0 and fit using the Hill Equation. Co-expression of P2X5 with ASIC3 alters proton sensitivity making ASIC3 less sensitive to protons. Application of ATP increases ASIC3 proton sensitivity returning to a level resembling that of ASIC3 when expressed in the absence of P2X5. n= 3-6 for each data point.

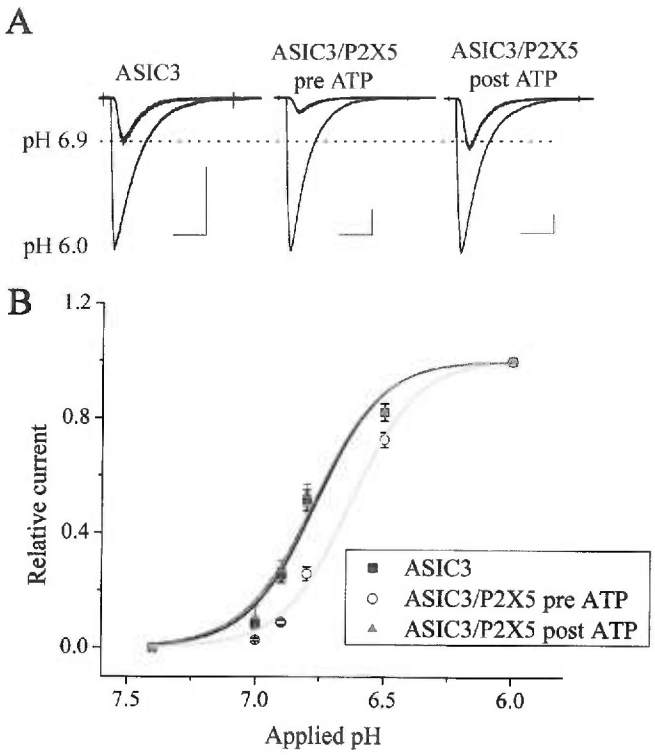
A
ASIC3
ASIC3/P2X5
pre ATP
ASIC3/P2X5
post ATP
pH 6.9
pH 6.0
B
1.2
0.8
0.4
0.0
Relative current
7.5
7.0
6.5
6.0
Applied pH
ASIC3
ASIC3/P2X5 pre ATP
ASIC3/P2X5 post ATP

Figure 4-5: Ratio of peak currents evoked by pH 6.9 and pH 6.0 reveal differences between P2X subtypes.

The ratio of peak currents evoked by pH 6.9 (submaximal) and pH 6.0 (nearly maximal) were measured for ASIC3 expressed alone or in tandem with P2X2, 3, 4, or 5 before and after application of ATP. 50μM ATP was applied until pH evoked currents were no longer modulated. A larger I6.9/I6.0 ratio indicates that pH 6.9 evoked a response farther up the dose response curve and thus increased proton sensitivity. Conversely, a smaller ratio is indicative of decreased proton sensitivity. All conditions are normalized to I6.9/ I6.0 for ASIC3 alone. Each day at least 5 cells expressing ASIC3 alone were recorded to get an average I6.9/I6.0 ratio and all recordings on that day were reported relative to that normalized ratio. This was done to eliminate any variability between experiments due to slight differences in pH, divalent ion concentration, or solution exchange speed. Current ratios are plotted on log scale for visual purposes so that a 10 fold increase or decrease in current ratio is visually similar. Individual cells are shown in black squares and average of each population is in open squares with a line connecting average current ratio before and after modulation by ATP under various transfection conditions. Unexpectedly, P2X3 decreased the proton sensitivity of ASIC3 even though we have previously shown that P2X3 does not modulate ASIC3 in response to ATP. n=7-44.

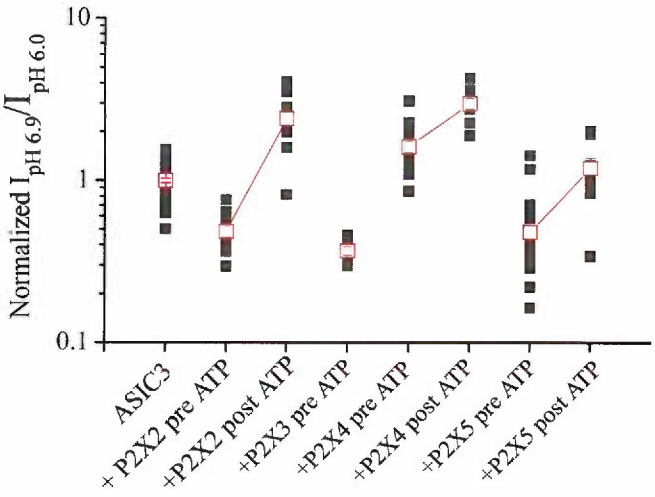
10
1
0.1
Normalized $I_{pH\ 6.9}/I_{pH\ 6.0}$
ASIC3
+ P2X2 pre ATP
+P2X2 post ATP
+P2X3 pre ATP
+P2X4 pre ATP
+P2X4 post ATP
+P2X5 pre ATP
+P2X5 post ATP

Figure 4-6: Proton activation curves of ASIC3 with P2X2 and P2X4 are consistent with current ratio data.

Proton activation curves were measured by plotting peak current amplitudes evoked by various pH tests relative to the current evoked by pH 6.0. This was done with cells expressing ASIC3 alone (black squares) or ASIC3 with P2X2 (A) or P2X4 (B) both before (open circles) and after (gray triangles) application of 50μM ATP. ATP was applied until the current at pH 6.9 was maximally modulated. Data collected for ASIC3 alone were collected in tandem with data for ASIC3+ P2X2 or ASIC3+ P2X4 and are separate data sets in A and B. n=3-6 for each data point. Data were fit using the Hill equation and the best fit of each data set is plotted.

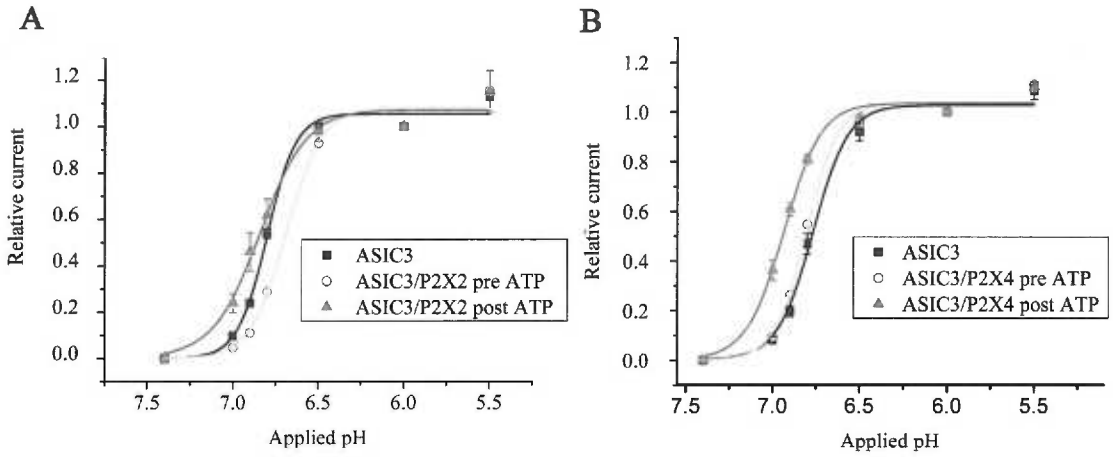
A
Relative current
1.2
1.0
0.8
0.6
0.4
0.2
0.0
7.5
7.0
6.5
6.0
5.5
Applied pH
ASIC3
ASIC3/P2X2 pre ATP
ASIC3/P2X2 post ATP
B
Relative current
1.2
1.0
0.8
0.6
0.4
0.2
0.0
7.5
7.0
6.5
6.0
5.5
Applied pH
ASIC3
ASIC3/P2X4 pre ATP
ASIC3/P2X4 post ATP

Table 4-1: Summary of fits of proton activation data

Data of proton activation of ASIC3, and ASIC3 co-expressing P2X2, 4, or 5 from figures 4-4 and 4-6 are summarized. Data were normalized to pH 6.0 and fit with the Hill Equation. All ASIC3 data sets that are plotted individually in figure 4-4 and 4-6 A and B were pooled into one data set and fit since there was no difference in pH50 between the three data sets. The half maximal pH of activation (pH50) shifts to more alkaline pH upon application of ATP when ASIC3 is co-expressed with P2X2, 4, or 5 but the exact pH50 before and after ATP application varies with the P2X subtype.

	ATP	pH_{50}	Hill Slope	I_{max}	R^2
ASIC3	Pre	6.78	4.09	1.03	0.991
ASIC3/P2X2	Pre	6.69	4.22	1.08	0.992
	Post	6.84	3.15	1.07	0.988
ASIC3/P2X4	Pre	6.80	4.71	1.04	0.993
	Post	6.94	4.02	1.04	0.993
ASIC3/P2X5	Pre	6.63	3.31	1.00	0.996
	Post	6.81	3.96	0.947	0.986

Figure 4-7: P2X4 dependent modulation of ASIC3 occurs even at low pH and zero calcium.

A. Currents evoked at pH 7.0 and 6.0 with 1mM calcium and 6.0 with no calcium and 10mM EDTA were modulated by ATP in cells co-expressing ASIC3 and P2X4. Each pair of representative traces shows the evoked currents before (arrow) and after a 20 second application of 50μM ATP at the indicated pH and calcium condition. The pH evoked current increased in all conditions even though pH 6.0/ no calcium should maximally activate ASIC3. All traces are from the same cell. Scale bar: 0.5sec, 200pA. B. Summary of data from experiments described above. Peak currents evoked under each condition (pH7.0/ 1mM Ca++, pH6.0/1mM Ca++, pH 6.0 no Ca++) were measured before and after ATP application. Bar graph represents average percent increase in peak current +/- sem n=7. C. Peak current amplitude evoked by pH 6.0/ no calcium before and after modulation by ATP. Individual cells represented by black squares with lines connecting individual cells under the two conditions. Averages +/- sem are shown with open circles. There is a small but significant increase in current amplitude due to ATP dependent modulation (paired t-Test; p=0.012).

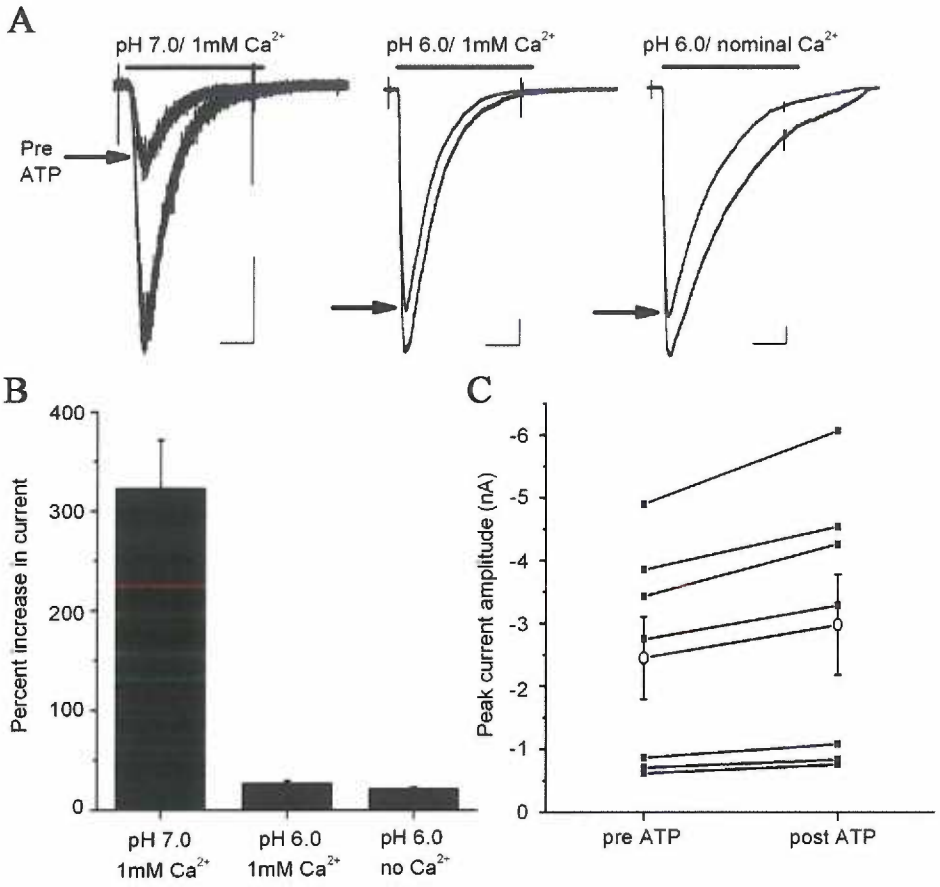
A
pH 7.0/ 1mM Ca2+
pH 6.0/ 1mM Ca2+
pH 6.0/ nominal Ca2+
Pre
ATP
B
Percent increase in current
400
300
200
100
0
pH 7.0
1mM Ca2+
pH 6.0
1mM Ca2+
pH 6.0
no Ca2+
C
Peak current amplitude (nA)
-6
-5
-4
-3
-2
-1
0
pre ATP
post ATP

Figure 4-8: Desensitization is modulated in a manner similar to proton sensitivity. A. ASIC3 desensitizes in the continued presence of protons. Desensitization rate was measured by fitting the decaying phase of the pH 6.8 evoked current to a single exponential fit $I=I0 + Ae-t/\tau$, where τ is the time constant of desensitization in milliseconds plotted as mean +/- sem. Changes in the rate of desensitization mirror changes in apparent proton affinity. Open bars indicate time constant before ATP application and closed bars are after ATP application. * values are significantly different between before and after ATP populations $p< 0.01$ unpaired t-Test. # indicates time constant significantly different from ASIC3 alone $p< 0.01$ from unpaired t-Test; n=4-19. The time constant of desensitization changes in a manner similar to changes in the proton affinity of ASIC3 when various P2X subunits are co-expressed. B. Normalized representative traces evoked at pH 6.8 for ASIC3 (black) , ASIC3 + P2X4 before ATP (light gray), and ASIC3 +P2X4 after ATP modulation (dark gray) demonstrate the changes in the rate of desensitization in response to a 2 second pH test. Time scale; 1sec.

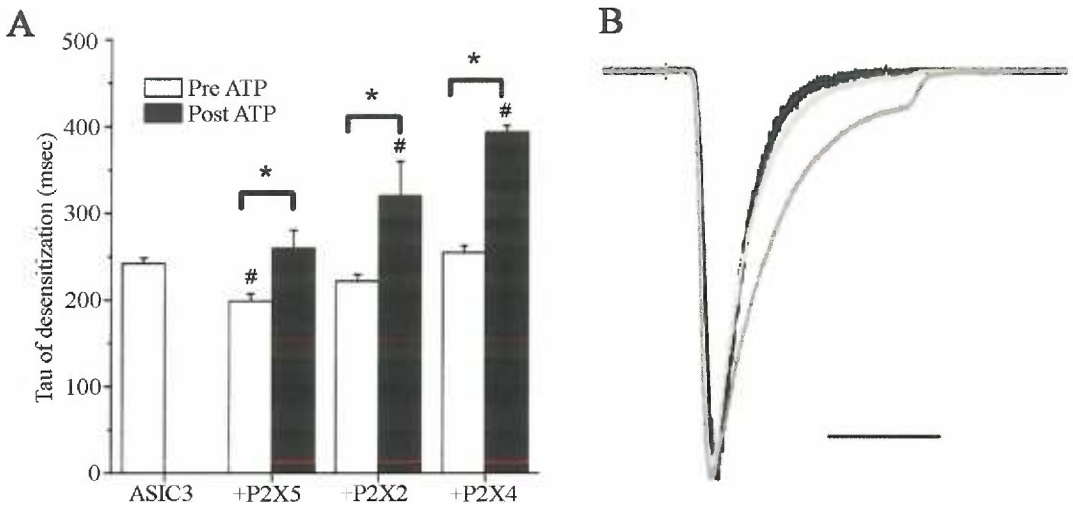
A
B
Pre ATP
Post ATP
Tau of desensitization (msec)
500
400
300
200
100
0
ASIC3
+P2X5
+P2X2
+P2X4
*
#

Table 4-2: Summary of I6.9/I6.0 and desensitization data show similar trends.

Summary of the average population data of the normalized ratio of currents evoked by pH6.9 and pH 6.0 (I6.9/I6.0) from figure 4-5 and time constant of desensitization data from figure 4-8 in cells expressing ASIC3 alone or in tandem with P2X2, 4, or 5 is shown. Current ratio data were normalized to the average current ratio of ASIC3 expressed alone. * indicates populations significantly different between pre and post ATP, # represents data which are significantly different from those of ASIC3 expressed alone $p<0.01$ unpaired T-test.

	ATP	I6.9/I6.0 +/- sem	Tau desensitization (msec) +/- sem
ASIC3	Pre	1+/-0.03	242+/-6
ASIC3/P2X2	Pre	0.49+/-0.04#	222+/-7
	Post	2.40+/-0.37*#	321+/-39*#
ASIC3/P2X4	Pre	1.61+/-0.13#	255+/-7
	Post	2.97+/-0.23*#	394+/-7*#
ASIC3/P2X5	Pre	0.47+/-0.08#	199+/-9#
	Post	1.18+/-0.20*	260+/-20*

Figure 4-9: Calcium sensitivity for ASIC3 co-expressed with P2X5 does not change. A. Currents were evoked by maintaining the bath pH at 8.0 and decreasing calcium concentration from 1 mM to the stated values before (black) and after (red) application of 50μM ATP to modulate ASIC3 in cells expressing ASIC3 and P2X5. Modulation increases current amplitudes at all calcium concentrations. Peak currents were measured and plotted relative to the peak current evoked by 10nM Calcium before ATP application. B. When the two curves are normalized to peak current evoked by 10nM calcium, there is no change in the apparent affinity of ASIC3 for calcium. The large error bars present in A are the result of a wide range in the extent of modulation with a small sample size n=3, which disappear when traces are normalized to the peak evoked current in B. Data were fit with the Hill equation and the best fit of the data are plotted.

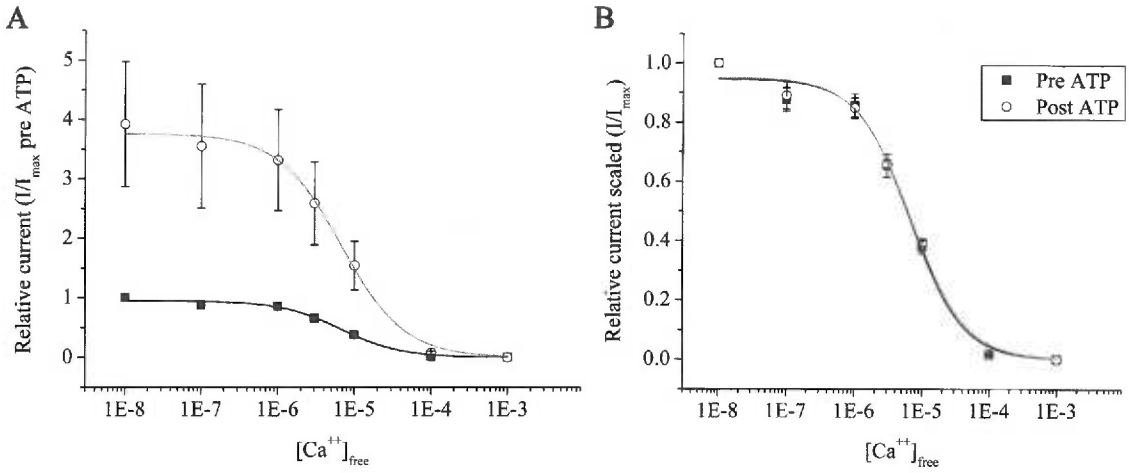
A
Relative current (I/I_{max} pre ATP)
5
4
3
2
1
0
1E-8
1E-7
1E-6
1E-5
1E-4
1E-3
$[Ca^{++}]_{free}$
B
Relative current scaled (I/I_{max})
1.0
0.8
0.6
0.4
0.2
0.0
Pre ATP
Post ATP
1E-8
1E-7
1E-6
1E-5
1E-4
1E-3
$[Ca^{++}]_{free}$

Figure 4-10: ATP modulates Calcium activated currents equally, regardless of degree of openness.

ASIC3 is activated either by an increase in proton concentration or a decrease in calcium concentration. A. Acid evoked currents in a representative cell expressing ASIC3 and P2X5 before (arrows) and after application of 50μM ATP at pH 7.0, 6.8, and 6.0. ATP modulates currents at the foot of the activation curve to a greater extent than currents at the peak. Bar indicates 2 second application of stated pH. B. Currents evoked by decreasing calcium concentration. 10μM calcium evokes sub-maximal currents in ASIC3 expressing cells whereas 10nM calcium evokes maximum currents from ASIC3 when pH is held constant at pH 8.0. Application of ATP modulates currents evoked by decreasing calcium to an equal degree regardless of whether the decrease in calcium is saturating or sub-maximal. Time of application is 2 seconds. Scale bars: 200pA, 0.5 sec. A and B are different cells.

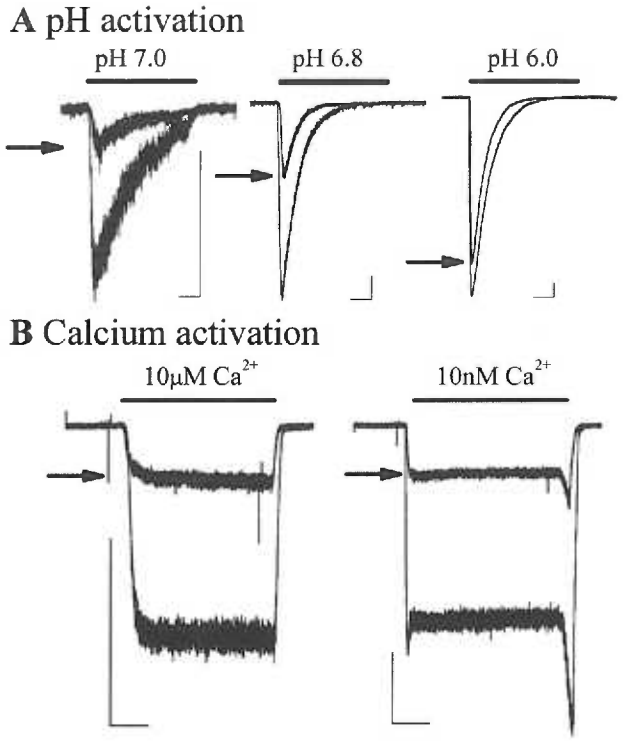
A pH activation
pH 7.0
pH 6.8
pH 6.0
B Calcium activation
10μM Ca2+
10nM Ca2+

Figure 4-11: Steady-state inactivation is not altered by modulation of ASIC3.

A. Steady state inactivation was measured by applying a pH 6.8 stimulus while the pH of the bath solution was changed to progressively lower pH values ranging from pH 8.0 to pH 7.0 in cells expressing ASIC3 and P2X5. Upper traces are before ATP application (50μM about 2 minutes) and lower traces are after modulation. The pH of the bath solution is indicated above the current traces. Scale: 2nA, 1 sec. B. The pair of currents evoked by 2 second pH 6.8 applications from pH 8.0 bath solution before and after ATP application are plotted demonstrating that modulation of ASIC3 currents occurs. Traces are from same cell as in A. Scale: 2nA, 0.5 sec. C. Peak currents from the pH 6.8 stimulus were measured and plotted relative to the current evoked when the bath pH was pH 8.0. Solid squares are before modulation and open circles are after. Data points were fit with the Hill equation and the best fit is plotted before (black) and after (gray) modulation. There is no change in the half-maximal pH of steady state incativation. n=3.

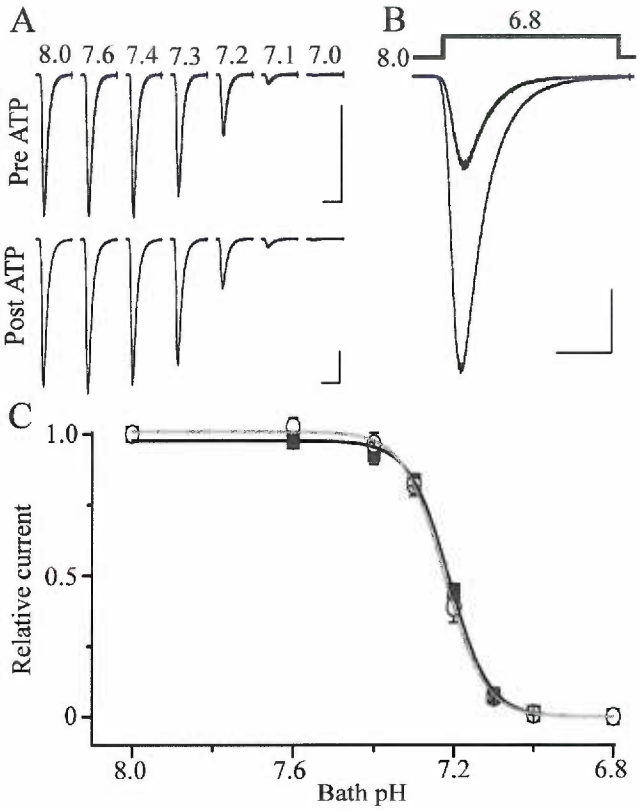
A
8.0 7.6 7.4 7.3 7.2 7.1 7.0
Pre ATP
Post ATP
B
6.8
8.0
C
1.0
0.5
0
Relative current
8.0
7.6
7.2
6.8
Bath pH

Figure 4-12: Sustained currents through ASIC3 are modulated by ATP application. A. Sustained currents are passed by ASIC3 at pH 7.0 in the presence 2mM calcium and 1mM magnesium. In cells expressing ASIC3 and P2X5 the sustained current slowly increases in amplitude over several minutes when 50μM ATP is co-applied with pH 7.0. Removal of ATP and pH demonstrate that the current in not due to leak. B. Increase in sustained current persists after washout of ATP. Sustained currents evoked by pH 7.0 before (smaller) and after (larger) application and washout of ATP demonstrate that the sustained current increase was not carried by P2X5 and was not due to any change in the pH or divalent ion concentration in the pH 7.0 test solution due to the presence of ATP.

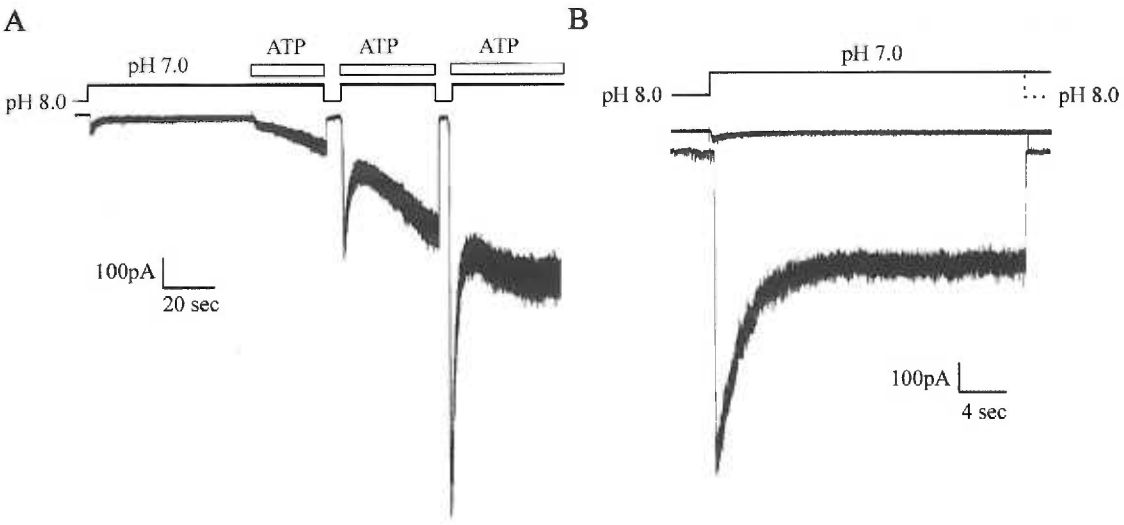
A
pH 7.0
ATP
ATP
ATP
pH 8.0
100pA
20 sec
B
pH 7.0
pH 8.0
pH 8.0
100pA
4 sec

Figure 4-13: Rate of modulation by ATP is dependent on kinetic features of P2X receptors.

A. A chimeric P2X receptor was constructed from P2X5 and P2X3 as indicated in C. A two second application of 50μM ATP elicits a relatively large inward current that displays moderate desensitization. A pH 6.8 stimulus after the ATP application is larger than that evoked before application demonstrating significant modulation by P2X from two seconds of ATP application. This contrasts with the slow time course of modulation seen in the previous figure which takes tens of seconds to modulate. B. Sustained currents passed by ASIC3 in pH 7.0 are modulated by a two second application of ATP/pH 7.0 in cells expressing ASIC3 and the chimeric P2X5/3. Some modulation continues for several seconds after removal of ATP. C. Diagram of chimeric P2X5/3 construct consisting of P2X5 up to the predicted second transmembrane domain and the second transmembrane domain and c-terminal tail of P2X3. Scale bars in A: 1nA, 1 sec; B: 100pA, 10sec.

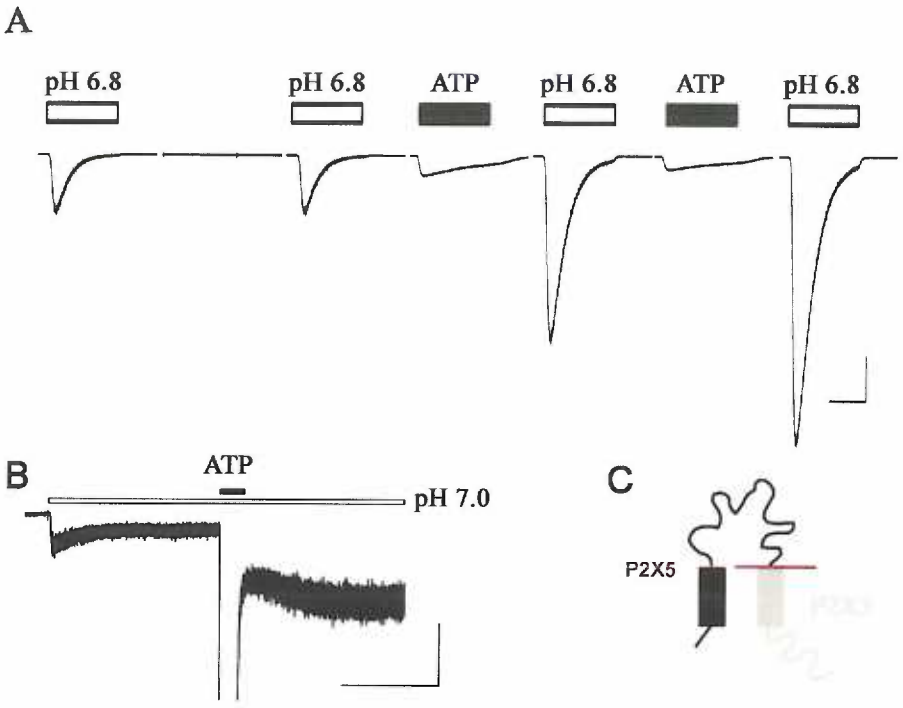
A
pH 6.8
pH 6.8
ATP
pH 6.8
ATP
pH 6.8
B
ATP
pH 7.0
C
P2X5

Figure 4-14: C-terminal truncations of P2X2 and P2X5 do not affect modulation of ASIC3.

A Traces display currents evoked by pH 6.9 before (first) and after (last) ATP (50μM, 20 sec; middle trace) in cells expressing ASIC3 and P2X2 375Δ. Scale: pH traces 0.5nA, 0.5 sec; ATP trace 2nA, 5sec. B Currents were evoked by pH 6.9 every 20 seconds in cell expressing ASIC3 and P2X5 381Δ. ATP (50μM) was added to the bath but not pH test solution after the third pH test. Scale: 1nA, 2sec.

A P2X2-375Δ/ ASIC3

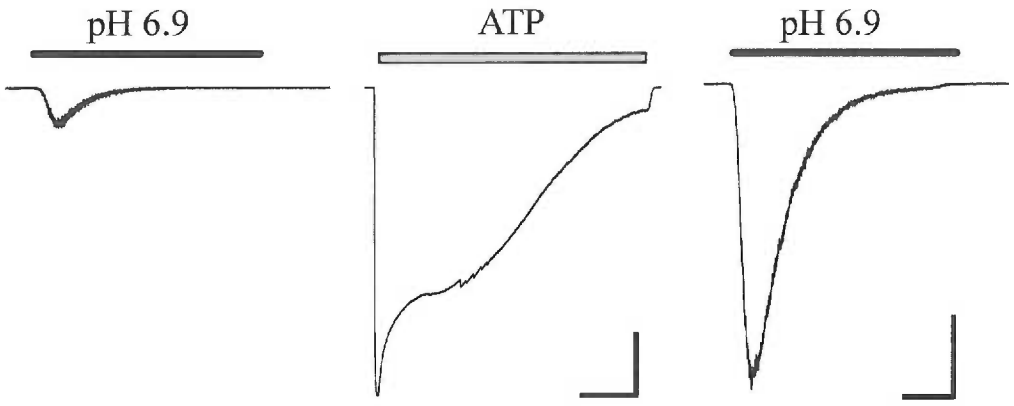

B P2X5-381Δ/ ASIC3

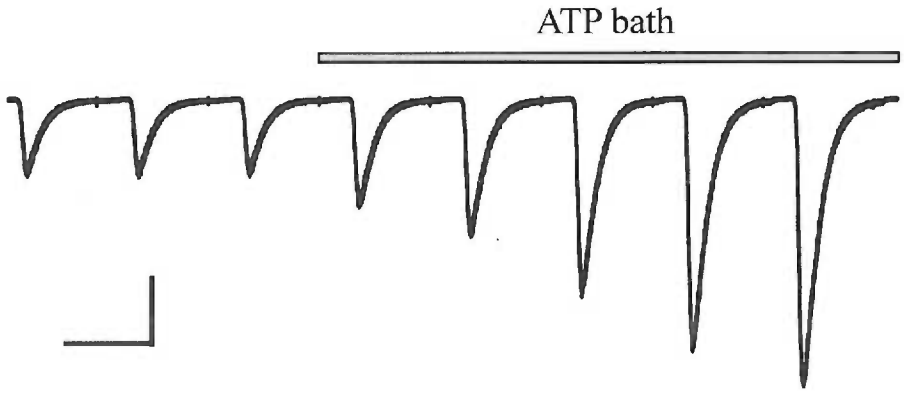

Figure 4-15: ASIC3 currents are slowly potentiated by arachidonic acid (AA)

A Currents evoked every 20 seconds by pH 7.0 are gradually potentiated by arachidonic acid (AA, 10μM) over 100 seconds. Time of AA application, in seconds, is shown on left of traces in A. AA was only present in the bath solution, pH test solution was unchanged. B Potentiation by AA occluded further potentiation by a 20 second activation of P2X4 by ATP (50μM). Modulation by P2X4 did slow the rate of desensitization. AA was present in bath and ATP solution. Acid evoked currents were first fully potentiated by AA (shown in A) and then ATP was added in the continued presence of AA. AA does not inhibit P2X4 current (P2X4 current amplitude was >10nA -30mV not shown) and likely potentiates it. C Lysophosphatidylcholilne (LPC, 2.5μM) mimicked the effect of ATP on pH evoked currents. Currents evoked by pH 7.0 were potentiated when LPC was added to the bath solution. Current amplitude increased and the desensitization time constant slowed, similar to ATP dependent modulation by P2X. After partial washout of LPC, ATP (50μM) increased the amplitude of the pH 7.0 evoked current similar to the effect LPC. Normalized currents demonstrate the slowed desensitization caused by both ATP and LPC. Each trace in the set of normalized traces corresponds to the trace of similar gray-scale color in the previous 4 traces. Scales: 200pA, 0.5 sec.

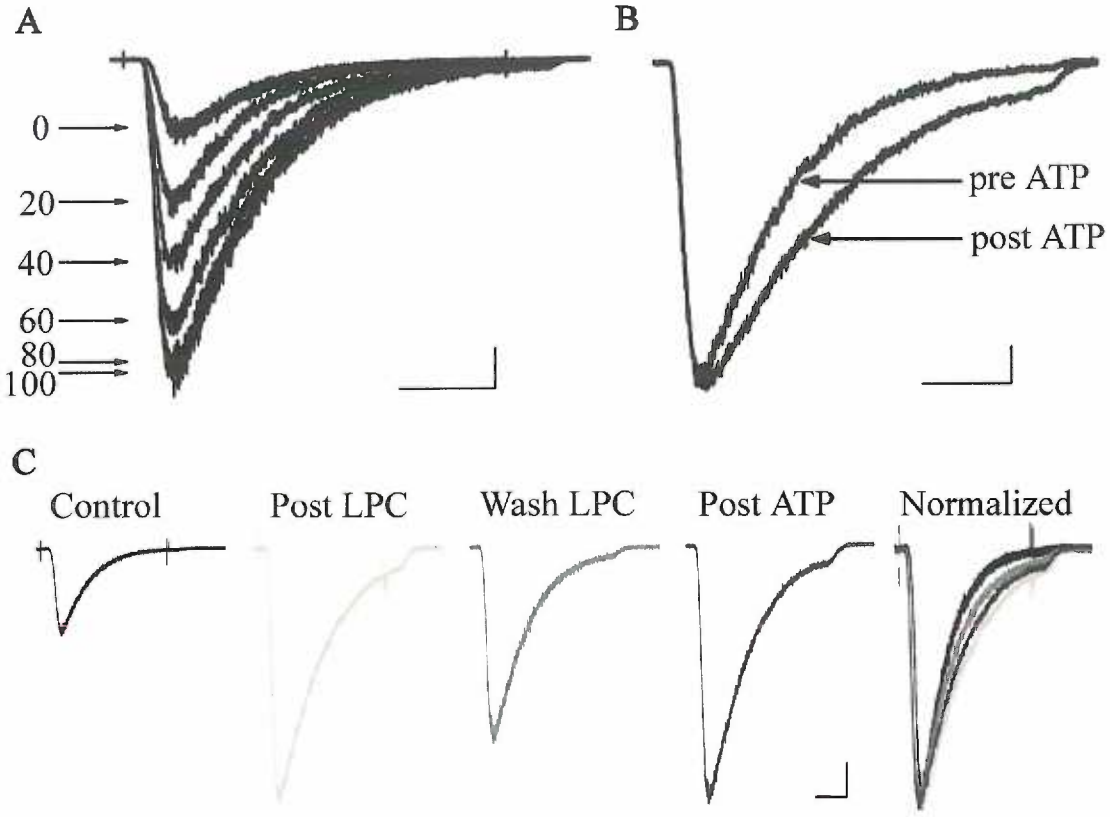
A
0
20
40
60
80
100
B
pre ATP
post ATP
C
Control
Post LPC
Wash LPC
Post ATP
Normalized

Figure 4-16: Proton activation of ASIC3 in outside-out patches is left-shifted relative to ASIC3 alone or ASIC3/P2X5.

A Proton activation curve of outside-out patches from cells expressing ASIC3 and P2X5 (open circles) compared with whole cell activation curve data from cells expressing ASIC3 alone (solid squares). Half-maximal activation occurs at pH 6.98 in excised patches, compared to 6.78 in whole cell recordings of ASIC3 expressing cells and 6.62 for cells expressing ASIC3/P2X5 (not shown). Peak evoked currents from a 2-second pH test at the stated pH values were measured and normalized to current evoked by pH 6.0 and plotted. Results were fitted with the Hill equation to determine half-maximal pH. B Currents evoked by pH 7.0 from outside out patches of CHO cells expressing ASIC3 and P2X4 were measured before and after application of AA (10μM) or ATP (50μM). Patch excision largely occluded the modulatory effects of both AA and ATP on ASIC3 currents.

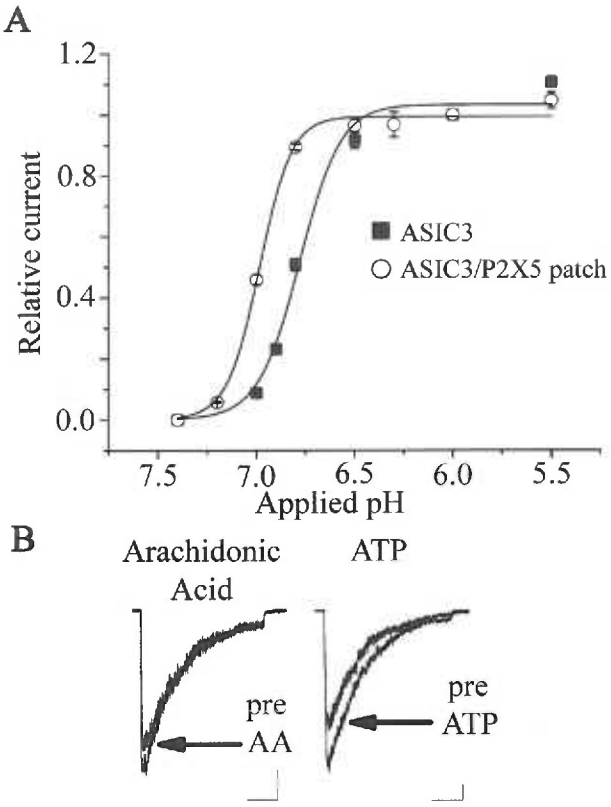
A
1.2
0.8
0.4
0.0
Relative current
ASIC3
ASIC3/P2X5 patch
7.5
7.0
6.5
6.0
5.5
Applied pH
B
Arachidonic Acid
ATP
pre AA
pre ATP

Figure 4-17: Changes in P2X2 permeability to NMG correlate with modulation of ASIC3.

Each triplet of traces are pH evoked currents before and after ATP application flanking currents evoked by a 20second ATP application in an external solution in which all monovalent cations were replaced with N-methyl-D-glucamine (NMG) Each row represents a unique cell. ATP (50μM) was added to cells expressing ASIC3 and P2X2 in an external solution containing NMG as the only monovalent cation at a holding potential of -50mV. Time dependent changes in P2X2 current (seen in rows 2 and 3) correlated with modulation of ASIC3 current, while the ATP evoked current in the first row did not display current changes or modulate ASIC3. Note the increase in current at the end of each ATP application resulting in return to a standard sodium and potassium-containing external solution which demonstrates that a large number of channels were open during the ATP application in row 1. Scale: 200pA, 5 sec (ATP traces), 0.5 sec (pH traces).

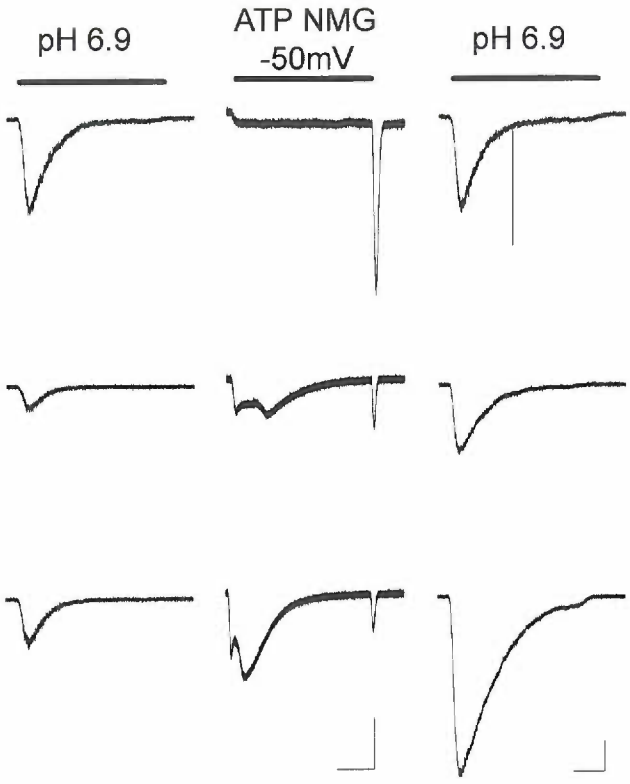
pH 6.9
ATP NMG
-50mV
pH 6.9

Chapter 5: Discussion

Discussion and relevance:

In the previous chapters a novel interaction between acid-sensing ion channels and the ATP gated P2X channels was described. This work provides a solution to the paradox that while ASICs are highly expressed on putative ischemia sensitive sensory neurons and acid is necessary for sensing ischemia, acid alone is insufficient to activate these neurons and trigger ischemic pain. It has previously been demonstrated that ASIC3 is more sensitive to lactic acidosis than other forms of acidosis (Immke and McCleskey 2001). Now, it appears that coincident detection of acid, ATP, and lactate may act synergistically to make ASIC3 more sensitive to ischemic acidosis than other forms of acidosis. As mentioned earlier it has long been recognized that a factor released from working muscle was responsible for triggering ischemic pain and many potential triggers for this mysterious "Factor P" have been suggested. The difficulty in identifying a trigger has likely been due to the contribution of multiple signals via multiple receptors. The discovery of a functional interaction between two channels sensing several potential metabolites may offer some resolution.

Functional interactions and synergism between ion channels may turn out to be a consistent theme in cellular physiology as a mechanism to tune activity to specific contexts and conditions. Both ASIC and P2X receptors are known to be involved in interactions with other ion channels making it likely that other physiologically important interactions will be discovered.

It is hypothesized that some classes of nociceptors serve sensory transduction roles and become nociceptive when hyper excited. Since ASICs are highly expressed on cardiac sensory neurons and ischemic heart pain is only rarely felt, a more physiological role must exist for ASICs beyond pain transduction. There is increasing evidence for a role of both ASIC and P2X in pressor responses that maintain cardiovascular homeostasis in response to exercise of skeletal muscle and it is logical that cardiac metaboreceptors would serve a physiological role in maintaining cardiovascular homeostasis as well.

Exercise physiology, acid, ASICs and ATP

Several groups are currently investigating a role of acid and ATP in muscle physiology and ASICs and P2X have been implicated as potential mediators of the exercise pressor reflex (Li, Maile et al. 2004; Hayes, Kindig et al. 2007; Hayes, McCord et al. 2007). One colleague, Alan Light has been working on an extension of the findings described in this thesis. In those studies calcium imaging was performed on sensory neurons that had innervated skeletal muscle in response to various combinations of metabolites focusing on acid, lactate and ATP based on our work. He found a synergistic effect of the three metabolites, with all three metabolites being much more effective at eliciting calcium influx than the sum of the three metabolites individually. The cocktail of metabolites resulted in both more cells showing calcium responses and larger amplitude calcium responses. Pharmacology implicated a role for both ASICs and P2X receptors in this process. Importantly, the metabolite concentrations used were based on an exhaustive literature search of measurements of

metabolic changes in response to moderate non-painful exercise and more severe painful ischemic exercise. Their results suggested two populations of metaboreceptors both consisting of ASICs and P2X receptors with slightly different pharmacology suggesting that a mixture of different ASIC and P2X subtypes may form complexes to sense metabolites over a broad concentration range with a potential contribution by the vanilloid receptor TRPV1 (Alan Light, personal communication). The concentrations of metabolites used in the study are summarized in Table 6-1. Modulation of ASIC was observed in response to ATP concentrations at and above 1μM and at pH 7.0 large modulation of the sustained current was seen, conditions that are realized during modest ischemic episodes.

A recent study with ASIC3 knock-out mice found increased exercise induced muscle fatigue in knockout mice compare to wild-type (Burnes, Kolker et al. 2008). Interestingly, this difference was sex specific affecting only male mice, however in ASIC3+/+ but not ASIC3-/- female mice testosterone and ovarectomy decreased muscle fatigue. This suggested that ASIC3 may indeed play a metabosensory role triggering vascular or respiratory responses to exercise that increase exercise tolerance and reduce fatigue in a manner that is regulated by testosterone.

ATP sources

Every cell contains millimolar concentrations of ATP so extracellular ATP could come from many sources. In the case of muscle ischemia it is hypothesized that ATP is released directly from muscle and acts on sensory endings innervating the muscle.

Sensory afferents and efferents make up only a tiny fraction of the volume of bulk muscle tissue and relatively high concentrations of ATP are measured in effluent from working skeletal and cardiac muscle making myocytes the likely source of ATP. There has been much debate about the exact release mechanism of ATP release. It has been hypothesized that ATP is released through small tears in the muscle membrane, through transporters, vesicularly, and through an ATP permeable anion channel. Recently, currents carried by ATP that were responsive to ischemia were measured in cultured myocytes supporting the possibility that channels may mediate ATP efflux (Lader, Xiao et al. 2000; Dutta, Sabirov et al. 2004). ATP has a large electrical and chemical gradient which would promote efflux through a sufficiently permeable channel.

Intrinsic properties of P2X

One unsuspected finding in chapter 4 was that, judging from current ratio experiments, P2X3 repressed the proton sensitivity of ASIC3. This suggested that P2X3, which is the major current carrier in sensory neurons, is capable of interacting with ASIC3. It also suggested that interaction with ASIC3 is a common feature of P2X receptors and a subset of these receptors have an ability to change their interaction in response to ATP activation. Interestingly, P2X2, 4, and 5 are all slowly desensitizing while P2X1 and 3 are quickly desensitizing. Perhaps the rapid desensitization of P2X3 prevents modulation in response to long applications of ATP. In vivo, P2X3 may behave differently. Physiological temperatures speed recovery of P2X3 from desensitization and may promote modulation of ASIC3, which could be

investigated in the future (Sean Cook, Greg Dussor, unpublished results). One problem with this hypothesis is the finding that P2X2/3 heteromers do not modulate ASIC3 even though they are slowly desensitizing like P2X2. It is thought that P2X2/3 heteromers are largely comprised of 2-P2X3 and 1-P2X2 subunits. Therefore the inability of P2X2/3 to modulate ASIC3 may reflect an intrinsic inability of the P2X3 subtype to carry out modulation, which is presumably some sort of slow conformational change in response to prolonged applications of ATP. Alternatively, P2X2/3 may be like P2X2 in its strong dependence on current amplitude for modulation. It is possible modulation by P2X2/3 was never observed because sufficient expression density of P2X2/3 was never achieved. Nevertheless, P2X2/3 is not like P2X2, 4 and 5 which readily modulate ASIC3 despite their similar slow rate of desensitization.

As mentioned previously, changes in P2X receptor selectivity in response to prolonged exposure to ATP have been described. The phenomenon, termed pore dilation, has generally been observed by measuring the current carried by large cations that are initially impermeable through P2X channels and gradually become more permeable. The dynamics of permeability changes are distinctly different from the kinetics of activation or desensitization of P2X receptors and may be dependent on expression density. FRET measurements have demonstrated that slow conformational changes in P2X2 occur that temporally correlate with the changes in selectivity and dye uptake (Fisher, Girdler et al. 2004). The observed changes in selectivity suggest that there are potentially several open states of P2X receptors

which has been suggested in single channel studies of P2X2 (Ding and Sachs 1999), although selectivity changes have never been observed at the single channel level. Observed changes in P2X permeability persisted long after removal of ATP and subsequent application of ATP resulted in the channel rapidly returning to the dilated state. This resembles the kinetic trap model of modulation of ASIC3 by P2X5. Perhaps interactions between P2X receptors and ASIC are constitutive and their modulation is the result of a kinetic trap inherent in P2X receptors in response to prolonged ATP applications.

Interestingly, the P2X subunits that have demonstrated an ability to undergo pore dilation all modulate ASIC3 with the exception of P2X7, which was not tested for its ability to modulate ASIC3 since it is not expressed in sensory neurons. Modulation of ASIC3 and pore dilation both require prolonged applications of ATP to occur and in a small number of cells changes in P2X2 permeability to NMG correlated with the degree of modulation of ASIC3 suggesting a possible link between the two phenomena, but the connection may be purely coincidental and future work should address this. Unfortunately, pore dilation is most well-studied with P2X2 and most mutations that eliminate permeability changes generally do not express as efficiently as wild type receptors. Since P2X2 is strongly dependent upon expression density for modulation of ASIC3- pore dilation has been reported to be density dependent as well, interpretation of any results using such mutants is potentially misleading.

Other channel-channel interactions

As stated previously, P2X2 has been shown to interact with several other ion channels including the nicotinic acetylcholine receptor. This interaction resulted in a mutual inhibition in which the current from both channels is less than the expected current from the sum of the channels activated individually (Khakh, Zhou et al. 2000). In contrast to the channel-channel interaction presented here this finding does not seem to have an obvious physiological significance since either ATP or acetylcholine has an effect similar to both ATP and acetylcholine.

A recent report has described an interaction between ASIC1 and the large conductance calcium and voltage activated potassium channel BK (Petroff, Price et al. 2008). ASIC1 inhibited BK activation and low pH relieved the inhibition. This interaction likely involved a sequence in the extracellular domain of ASIC1 that resembles a family of scorpion toxins that inhibit potassium channels. A reciprocal interaction whereby BK changed the current kinetics of ASIC2 slowing the rate of desensitization was also reported.

The fact that previously described channel-channel interactions involving both ASIC and P2X are bidirectional suggests that there is the potential for a reciprocal interaction between ASIC and P2X. Pursuing this idea would involve probing P2X receptors for changes in kinetics due to ASIC3 expression. One compounding factor making this difficult is that assaying P2X activity by ATP application alters the interaction between ASIC and P2X potentially masking effects of ASIC. Perhaps

examining channels with short applications of ATP or examining the initial desensitization properties of P2X receptors in the presence and absence of ASIC3 would shed light on this subject and extend the initial findings, further supporting a model of a direct physical coupling between ASIC3 and P2X. Partial agonists may activate P2X receptors without promoting modulation of ASIC. The partial agonist BzATP opens P2X2 at high concentrations without promoting changes in NMG permeability (Baljit Khakh, personal communication), so if the two processes— modulation and permeability changes— are related BzATP may not promote modulation. This has not been investigated but it would provide a method to characterize any reciprocal effect of ASIC on P2X activity without altering the interaction.

P2X modulation of epithelial sodium channels?

Several recent reports have linked ATP release to sodium transport in epithelial tissues. Evidence suggested an involvement of both P2X and P2Y in modulating ENaC activity to regulate sodium uptake(Wildman, Marks et al. 2005; Wildman, Marks et al. 2008). Though the results are somewhat cloudy it appears that P2X4 or P2X4/6 can modulate ENaCs. In one report, modulation either increased or decreased the amplitude of amiloride sensitive currents depending on the extracellular sodium concentration in a manner that involved P2X. ASICs and ENaCs are members of the same family of ion channels, but ENaCs are not classical ligand gated channels. Rather, they are constitutively active and their activity is modulated by altering open probability and surface expression. It is intriguing to hypothesize that this ENaC

modulation by P2X4 is similar to ASIC modulation described in this dissertation and perhaps P2X alters the open probability of ASIC3 independent of proton binding.

Future Directions:

Research presented in this dissertation has shed some light onto a possible mechanism of ischemia sensing and a mechanism of communication between channels. Many questions are still left unanswered and new questions have arisen with some being discussed in the previous pages. This section will address some future questions and approaches that will build upon this work ranging from molecular to systems level.

What is the structural mechanism of the interaction between ASIC and P2X?

It has been demonstrated that a physical interaction between ASIC and P2X likely exists but no interaction domains have been found. Experiments examining structure-function relationships between P2X and ASIC would shed light on the exact mechanism of interaction and ASIC gating. Unfortunately, large portions of the both ASIC and P2X are either membrane spanning or extracellular. Mutations or deletions in these domains would likely prove difficult and would not provide interpretable results since overall channel integrity would likely be affected. One method to assay for regions of P2X involved in modulation of ASIC3 would be an approach using chimeras. This would involve creating a full length P2X construct using domains from various P2X receptors. An attempt was made using chimeras of P2X3 and P2X5 but the results were not clear. Some chimeras did not modulate ASIC3 but it was impossible to know if it was a problem of overall P2X function or kinetics or a

disruption in the interaction with ASIC3. A better approach with a higher likelihood of success would be to construct chimeras from two P2X receptors that are known to modulate ASIC3; P2X5 and P2X4.

As demonstrated previously, P2X4 and P2X5 interact with ASIC3 but in different ways- P2X4 increases proton sensitivity of ASIC3 while P2X5 depresses it. ATP increases the proton sensitivity of ASIC3 when either P2X is expressed. Chimeric constructs would be expected to interact with ASIC3 also and an assay of ATP dependent modulation would suggest a functional interaction between the P2X chimera and ASIC3. By using current ratio measurements (I6.9/I6.0) as an assay, it would be possible to characterize chimeras of P2X4 and P2X5 as being P2X4-like or P2X5-like in their interactions with ASIC3. Different phenotypes of ASIC3 interactions could then be attributed to specific regions of P2X primary structure. This approach could potentially highlight a region of P2X responsible for interacting with ASIC. That region would then be used to screen regions of ASIC3 to find the P2X interaction site. Knowing the regions involved in the interaction would

Do other ASIC/P2X interactions occur in native tissues?

ASICs are widely expressed in the central and peripheral nervous system (Waldmann, Champigny et al. 1996; Waldmann, Champigny et al. 1997), their physiological role remains elusive and synaptic ASIC currents have never been recorded. Better pharmacology has recently become available with the discovery of the sea anemone toxin APETx2 which is a selective blocker of ASIC3, and the ASIC1a specific

tarantula toxin psalmotoxin (PcTx1) and ASICs are the active focus of several pharmaceutical companies so specific small molecule ASIC inhibitors are more likely in the years to come. Better pharmacology coupled with knockout mice will be of great help in searching for physiological roles for ASICs particularly in the central nervous system where synaptic roles for ASICs have not been demonstrated.

ASIC1 was shown to be modulated by P2X4 and P2X5 when co-expressed in cell lines. Both ASIC1 and P2X4 have broad overlapping distributions in the CNS (Waldmann, Champigny et al. 1997; Bo, Kim et al. 2003). Both are present in particularly active and well studied brain regions such as the hippocampus and cerebellum and midbrain dopamine neurons. Searching for ATP dependent modulation of proton gated currents or firing rate should be possible in brain slices from these areas and give an idea of whether P2X/ ASIC interactions are widespread. Finding evidence for an interaction between P2X4 and ASIC1 in native tissues may be an important first step towards addressing the physiological role of

Elucidating a functional role for ASIC1 requires a method to evoke ASIC currents with physiological stimuli which is lacking in the field of ASIC physiology. Attempts to record synaptic ASIC currents have not been successful. It is possible that ASICs function presynaptically (Cho and Askwith 2008) or are activated in response to prolonged synaptic activity, perhaps in systems that exhibit tonic activity and high firing rates a role for AISCs could be identified. Finally, integrating these two potential findings- a role for ASICs and an interaction between ASIC1 and P2X4-

into looking for effects of P2X4 on native ASIC1 activity evoked physiologically would be a very important long term contribution to the ASIC and P2X fields and physiology in general.

Coincident detection of acid and ATP by cardiac sensory neurons:

Work presented here demonstrated that ASIC3-like currents were modulated by ATP in sensory neurons. This was shown with unlabeled DRG sensory neurons and labeled skeletal muscle afferents but has not been demonstrated in cardiac sensory neurons. The heart is innervated by two distinct populations of sensory neurons. Those with their cell bodies in the dorsal root ganglia form the sensory arm of the sympathetic innervation that increases heart rate and blood pressure and is responsible for angina (Malliani, Schwartz et al. 1969; Uchida and Murao 1975; Walker, Thames et al. 1978; Longhurst, Tjen et al. 2001). Cardiac DRG express high levels of ASIC3. The second population of sensory neurons that innervates cardiac muscle follows the vagus nerve and has cell bodies in the nodose ganglion. Activation of nodose neurons evokes parasympathetic responses slowing heart rate and reducing blood pressure (Walker, Thames et al. 1978; Longhurst, Tjen et al. 2001). These neurons have been shown to express relatively little ASIC-like current but a robust P2X2-like current (Benson, Eckert et al. 1999). P2X2 is unique among the P2X subtypes because acidic pH potentiates the response of P2X2 to ATP making it more sensitive to acid and ATP (Stoop, Surprenant et al. 1997).

These two different populations of sensory neurons display somewhat divergent cardiac innervation (Uchida and Murao 1975), evoke opposite reflexes and may have two distinct mechanisms for sensing the coincident appearance of acid and ATP. This has never been demonstrated, however. Studying the acid and ATP responses of these two neuronal populations is an important extension of previous findings that is very technically achievable. These findings may be clinically relevant as well since sympathetic activation is generally cardio-destructive (Sinoway and Li 2005) while parasympathetic activation is considered cardio-protective and may correlate with different clinical outcomes of myocardial infarctions of different regions of the myocardium.

	Rest	Non-noxious		Painful		
pH	7.4	7.3	7.2	7.0	6.8	6.6
Lactate	1mM	5mM	10mM	15mM	20mM	50mM
ATP	300nM	400nM	500nM	1μM	2μM	5μM

Table 5-1: Estimates of metabolite concentrations:

Table summarizes estimates of metabolite concentrations at rest, during moderate exercise and during painful ischemic episodes. These values were estimated by Alan Light based on a previously published reports judging metabolite concentrations in humans, rats and mice. ASIC3 produces sustained currents in the presence of pH around 7.0 (from 7.2 to 6.8). ATP concentrations at or above 1μm are able to potentiate ASIC3 currents. Table adapted from Al Light.

Chapter 6: Summary and conclusions

Work presented in this dissertation demonstrated that prolonged appearance of extracellular ATP increased the proton sensitivity of Acid-sensing ion channels (ASIC) in DRG sensory neurons and with recombinantly expressed channels— an effect that lasted from minutes to more than an hour after removal of ATP. Surprisingly, the receptor for the ATP was another ion channel, a P2X channel. While recombinant P2X2, P2X4, and P2X5 could all modulate ASIC3, only P2X5 shared all the kinetic and pharmacological properties of the native DRG P2X receptor, implicating P2X5 as the likely endogenous P2X receptor responsible for modulation of ASIC3-like currents in sensory neurons. P2X5 had been studied only rarely since it passes very little current. Immunohistochemistry revealed co-expression of P2X5 and ASIC3 protein in DRG sensory neurons with the two channels showing significant cellular co-localization.

Despite the slow temporal characteristics, there was no evidence for a role of common second messengers in mediating modulation. Rather, a direct physical and functional coupling of ASIC and P2X was demonstrating consistent with a direct channel-channel interaction. A few examples of channel-channel interactions have been demonstrated previously but the interaction between ASIC and P2X is unique in several regards: 1) modulation persisted long after removal of ATP demonstrating a memory for the transient appearance of ATP, and 2) the interaction increased the

proton sensitivity of ASIC3 whereas other previously described interactions resulted in mutual inhibition of currents.

Each P2X receptor was found to interact with ASIC3 uniquely but in general modulation of ASIC3 by P2X increased the apparent affinity of ASIC3 for protons making ASIC3 more sensitive to proton after the appearance of ATP. Modulation by ATP slowed the desensitization kinetics of ASIC3 in a P2X subtype dependent manner that mirrored changes in proton sensitivity. In contrast, no changes were seen in the apparent calcium affinity or in the steady state desensitization properties of ASIC3. Increased proton sensitivity without a change in steady state desensitization resulted in an increase in the amplitude of a sustained window current mediated by ASIC3. The amplitude of the window current increased after the appearance of ATP in the pH range that occurs during ischemia, which is likely of critical physiological importance allowing the desensitizing ASIC3 channel to function as a persistent sensor of ischemia.

References

Abbracchio, M. P., G. Burnstock, et al. (2006). "International Union of Pharmacology LVIII: update on the P2Y G protein-coupled nucleotide receptors: from molecular mechanisms and pathophysiology to therapy." Pharmacol Rev 58(3): 281-341.

Alam, M. and F. H. Smirk (1937). "Observations in man upon a blood pressure raising reflex arising from the voluntary muscles." J Physiol 89(4): 372-383.

Allen, N. J. and D. Attwell (2002). "Modulation of ASIC channels in rat cerebellar Purkinje neurons by ischaemia-related signals." J Physiol (Lond) 543(2): 521-529.

Allen, N. J. and D. Attwell (2002). "Modulation of ASIC channels in rat cerebellar Purkinje neurons by ischaemia-related signals." J Physiol 543(Pt 2): 521-9.

Andrey, F., T. Tsintsadze, et al. (2005). "Acid sensing ionic channels: Modulation by redox reagents." Biochimica et Biophysica Acta (BBA) - Molecular Cell Research 1745(1): 1.

Anzai, N., E. Deval, et al. (2002). "The multivalent PDZ domain-containing protein CIPP is a partner of acid- sensing ion channel 3 in sensory neurons." J Biol Chem 277(19): 16655-61.

Awayda, M. S., W. Shao, et al. (2004). "ENaC-membrane interactions: regulation of channel activity by membrane order." J Gen Physiol 123(6): 709-27.

Axelrod, D. (1981). "Cell-substrate contacts illuminated by total internal reflection fluorescence." J. Cell Biol. 89(1): 141-145.

Bangsbo, J., L. Johansen, et al. (1993). "Lactate and H+ effluxes from human skeletal muscles during intense, dynamic exercise." J Physiol 462: 115-33.

Bardoni, R., P. A. Goldstein, et al. (1997). "ATP P2X receptors mediate fast synaptic transmission in the dorsal horn of the rat spinal cord." J Neurosci 17(14): 5297-304.

Benson, C. J., S. P. Eckert, et al. (1999). "Acid-Evoked Currents in Cardiac Sensory Neurons: A Possible Mediator of Myocardial Ischemic Sensation." Circ Res 84(8): 921-928.

Benson, C. J. and S. P. Sutherland (2001). "Toward an Understanding of the Molecules that Sense Myocardial Ischemia." Annals of the New York Academy of Sciences 940(1): 96-109.

Bo, X., L. H. Jiang, et al. (2003). "Pharmacological and biophysical properties of the human P2X5 receptor." Mol Pharmacol 63(6): 1407-16.

Bo, X., M. Kim, et al. (2003). "Tissue distribution of P2X 4 receptors studied with an ectodomain antibody." Cell and Tissue Research 313(2): 159.

Bo, X., Y. Zhang, et al. (1995). "A P2X purinoceptor cDNA conferring a novel pharmacological profile." FEBS Lett 375(1-2): 129-33.

Boehm, S. (1999). "ATP Stimulates Sympathetic Transmitter Release via Presynaptic P2X Purinoceptors." J. Neurosci. 19(2): 737-746.
Boue-Grabot, E., C. Barajas-Lopez, et al. (2003). "Intracellular cross talk and physical interaction between two classes of neurotransmitter-gated channels." J Neurosci 23(4): 1246-53.
Boue-Grabot, E., M. B. Emerit, et al. (2004). "Cross-talk and co-trafficking between rho1/GABA receptors and ATP-gated channels." J Biol Chem 279(8): 6967-75.
Boue-Grabot, E., E. Toulme, et al. (2004). "Subunit-specific coupling between gamma-aminobutyric acid type A and P2X2 receptor channels." J Biol Chem 279(50): 52517-25.
Burnes, L. A., S. J. Kolker, et al. (2008). "Enhanced muscle fatigue occurs in male but not female ASIC3-/- mice." Am J Physiol Regul Integr Comp Physiol 294(4): R1347-55.
Burnstock, G. (2007). "Purine and pyrimidine receptors." Cellular and Molecular Life Sciences (CMLS) 64(12): 1471.
Cadiou, H., M. Studer, et al. (2007). "Modulation of acid-sensing ion channel activity by nitric oxide." J Neurosci 27(48): 13251-60.
Casado, M. and P. Ascher (1998). "Opposite modulation of NMDA receptors by lysophospholipids and arachidonic acid: common features with mechanosensitivity." J Physiol 513(2): 317-330.
Catarsi, S., K. Babinski, et al. (2001). "Selective modulation of heteromeric ASIC proton-gated channels by neuropeptide FF." Neuropharmacology 41(5): 592-600.
Cho, J.-H. and C. C. Askwith (2008). "Presynaptic Release Probability Is Increased in Hippocampal Neurons From ASIC1 Knockout Mice." J Neurophysiol 99(2): 426-441.
Cho, J. H. and C. C. Askwith (2007). "Potentiation of acid-sensing ion channels by sulfhydryl compounds." Am J Physiol Cell Physiol 292(6): C2161-74.
Chu, X.-P., N. Close, et al. (2006). "ASIC1a-Specific Modulation of Acid-Sensing Ion Channels in Mouse Cortical Neurons by Redox Reagents." J. Neurosci. 26(20): 5329-5339.
Chu, X.-P., J. A. Wemmie, et al. (2004). "Subunit-Dependent High-Affinity Zinc Inhibition of Acid-Sensing Ion Channels." J. Neurosci. 24(40): 8678-8689.
Chu, X. P., N. Close, et al. (2006). "ASIC1a-specific modulation of acid-sensing ion channels in mouse cortical neurons by redox reagents." J Neurosci 26(20): 5329-39.
Clemens, M. G. and T. Forrester (1981). "Appearance of adenosine triphosphate in the coronary sinus effluent from isolated working rat heart in response to hypoxia." J Physiol 312: 143-58.
Cobbe, S. M. and P. A. Poole-Wilson (1980). "The time of onset and severity of acidosis in myocardial ischaemia." J Mol Cell Cardiol 12(8): 745-60.
Collo, G., R. A. North, et al. (1996). "Cloning OF P2X5 and P2X6 receptors and the distribution and properties of an extended family of ATP-gated ion channels." J Neurosci 16(8): 2495-507.

Colquhoun, D. (1998). "Binding, gating, affinity and efficacy: The interpretation of structure-activity relationships for agonists and of the effects of mutating receptors." Br J Pharmacol 125(5): 923-947.
Cook, S. P., L. Vulchanova, et al. (1997). "Distinct ATP receptors on pain-sensing and stretch-sensing neurons." Nature 387(6632): 505-8.
Coote, J. H., S. M. Hilton, et al. (1971). "The reflex nature of the pressor response to muscular exercise." J Physiol 215(3): 789-804.
Ding, S. and F. Sachs (1999). "Single Channel Properties of P2X2 Purinoceptors." J. Gen. Physiol. 113(5): 695-720.
Ding, S. and F. Sachs (2000). "Inactivation of P2X2 purinoceptors by divalent cations." J Physiol 522(2): 199-214.
Ding, S. and F. Sachs (2002). "Evidence for non-independent gating of P2X2 receptors expressed in Xenopus oocytes." BMC Neurosci 3: 17.
Dutta, A. K., R. Z. Sabirov, et al. (2004). "Role of ATP-conductive anion channel in ATP release from neonatal rat cardiomyocytes in ischaemic or hypoxic conditions." J Physiol 559(Pt 3): 799-812.
Egan, T., D. Samways, et al. (2006). "Biophysics of P2X receptors." Pflügers Archiv European Journal of Physiology 452(5): 501.
Eskandari, S., P. M. Snyder, et al. (1999). "Number of subunits comprising the epithelial sodium channel." J Biol Chem 274(38): 27281-6.
Evans, R. J. (1996). "Single channel properties of ATP-gated cation channels (P2X receptors) heterologously expressed in Chinese hamster ovary cells." Neuroscience Letters 212(3): 212.
Fisher, J. A., G. Girdler, et al. (2004). "Time-Resolved Measurement of State-Specific P2X2 Ion Channel Cytosolic Gating Motions." J. Neurosci. 24(46): 10475-10487.
Forrester, T. (1972). "An estimate of adenosine triphosphate release into the venous effluent from exercising human forearm muscle." J Physiol 224(3): 611-28.
Forrester, T. and C. A. Williams (1977). "Release of adenosine triphosphate from isolated adult heart cells in response to hypoxia." J Physiol 268(2): 371-90.
Gao, J., L. J. Wu, et al. (2004). "Properties of the proton-evoked currents and their modulation by Ca2+ and Zn2+ in the acutely dissociated hippocampus CA1 neurons." Brain Res 1017(1-2): 197-207.
Garcia-Guzman, M., F. Soto, et al. (1996). "Molecular cloning and functional expression of a novel rat heart P2X purinoceptor." FEBS Lett 388(2-3): 123-7.
Gever, J. R., D. A. Cockayne, et al. (2006). "Pharmacology of P2X channels." Pflugers Arch 452(5): 513-37.
Groschel-Stewart, U., M. Bardini, et al. (1999). "Localisation of P2X5 and P2X7 receptors by immunohistochemistry in rat stratified squamous epithelia." Cell Tissue Res 296(3): 599-605.
Guo, C., M. Masin, et al. (2007). "Evidence for functional P2X4/P2X7 heteromeric receptors." Mol Pharmacol 72(6): 1447-56.

Hall, D. A. (2000). "Modeling the functional effects of allosteric modulators at pharmacological receptors: an extension of the two-state model of receptor activation." Mol Pharmacol 58(6): 1412-23.
Hayes, S. G., A. E. Kindig, et al. (2007). "Blockade of acid sensing ion channels attenuates the exercise pressor reflex in cats." J Physiol 581(3): 1271-1282.
Hayes, S. G., J. L. McCord, et al. (2007). "Role played by P2X and P2Y receptors in evoking the Muscle Chemoreflex." J Appl Physiol: 00929.2007.
Hellsten, Y., D. Maclean, et al. (1998). "Adenosine concentrations in the interstitium of resting and contracting human skeletal muscle." Circulation 98(1): 6-8.
Hruska-Hageman, A. M., C. J. Benson, et al. (2004). "PSD-95 and Lin-7b interact with acid-sensing ion channel-3 and have opposite effects on H+-gated current." J Biol Chem 279(45): 46962-8.
Hruska-Hageman, A. M., J. A. Wemmie, et al. (2002). "Interaction of the synaptic protein PICK1 (protein interacting with C kinase 1) with the non-voltage gated sodium channels BNC1 (brain Na+ channel 1) and ASIC (acid-sensing ion channel)." Biochem J 361(Pt 3): 443-50.
Immke, D. C. and E. W. McCleskey (2001). "Lactate enhances the acid-sensing Na+ channel on ischemia-sensing neurons." Nat Neurosci 4(9): 869-70.
Immke, D. C. and E. W. McCleskey (2003). "Protons open Acid-sensing ion channels by catalyzing relief of ca(2+) blockade." Neuron 37(1): 75-84.
Issberner, U., P. W. Reeh, et al. (1996). "Pain due to tissue acidosis: a mechanism for inflammatory and ischemic myalgia?" Neuroscience Letters 208(3): 191-194.
Jasti, J., H. Furukawa, et al. (2007). "Structure of acid-sensing ion channel 1 at 1.9 A resolution and low pH." Nature 449(7160): 316-23.
Jiang, L.-H., F. Rassendren, et al. (2005). "N-methyl-D-glucamine and propidium dyes utilize different permeation pathways at rat P2X7 receptors." Am J Physiol Cell Physiol 289(5): C1295-1302.
Kaufman, M. P. (2003). "Has the phoenix risen?" J Physiol 548(Pt 3): 666.
Kaufman, M. P. and S. G. Hayes (2002). "The Exercise Pressor Reflex." Clinical Autonomic Research 12(6): 429.
Kawate, T. and E. Gouaux (2006). "Fluorescence-detection size-exclusion chromatography for precrystallization screening of integral membrane proteins." Structure 14(4): 673-81.
Khakh, B. S., X. R. Bao, et al. (1999). "Neuronal P2X transmitter-gated cation channels change their ion selectivity in seconds." Nat Neurosci 2(4): 322.
Khakh, B. S., J. A. Fisher, et al. (2005). "An angstrom scale interaction between plasma membrane ATP-gated P2X2 and alpha4beta2 nicotinic channels measured with fluorescence resonance energy transfer and total internal reflection fluorescence microscopy." J Neurosci 25(29): 6911-20.
Khakh, B. S. and R. A. North (2006). "P2X receptors as cell-surface ATP sensors in health and disease." Nature 442(7102): 527-32.

Khakh, B. S., X. Zhou, et al. (2000). "State-dependent cross-inhibition between transmitter-gated cation channels." Nature 406(6794): 405-10.
Kindig, A. E., S. G. Hayes, et al. (2006). "P2 antagonist PPADS attenuates responses of thin fiber afferents to static contraction and tendon stretch." Am J Physiol Heart Circ Physiol 290(3): H1214-9.
Kindig, A. E., S. G. Hayes, et al. (2007). "Blockade of purinergic 2 receptors attenuates the mechanoreceptor component of the exercise pressor reflex." Am J Physiol Heart Circ Physiol 293(5): H2995-3000.
Kobayashi, K., T. Fukuoka, et al. (2005). "Differential expression patterns of mRNAs for P2X receptor subunits in neurochemically characterized dorsal root ganglion neurons in the rat." J Comp Neurol 481(4): 377-90.
Krishtal, O. (2003). "The ASICs: signaling molecules? Modulators?" Trends Neurosci 26(9): 477-83.
Krishtal, O. A. and V. I. Pidoplichko (1980). "A receptor for protons in the nerve cell membrane." Neuroscience 5(12): 2325-7.
Krishtal, O. A. and V. I. Pidoplichko (1981). "Receptor for protons in the membrane of sensory neurons." Brain Research 214: 150-154.
Krishtal, O. A. and V. I. Pidoplichko (1981). "A "receptor" for protons in small neurons of trigeminal ganglia: possible role in nociception." Neuroscience Letters 24: 243-246.
Lader, A. S., Y. F. Xiao, et al. (2000). "cAMP activates an ATP-permeable pathway in neonatal rat cardiac myocytes." Am J Physiol Cell Physiol 279(1): C173-87.
Lewis, C., S. Neidhart, et al. (1995). "Coexpression of P2X2 and P2X3 receptor subunits can account for ATP-gated currents in sensory neurons." Nature 377(6548): 432.
Lewis, T. (1932). " Pain in muscular ischaemia: its relation to anginal pain." Arch Intern Med. 49: 713–727.
Lewis, T. and G. Pickering (1931). Heart 16: 33-51.
Li, J., N. C. King, et al. (2003). "ATP concentrations and muscle tension increase linearly with muscle contraction." J Appl Physiol 95(2): 577-83.
Li, J., M. D. Maile, et al. (2004). "Muscle pressor reflex: potential role of vanilloid type 1 receptor and acid-sensing ion channel." J Appl Physiol 97(5): 1709-1714.
Longhurst, J. C., A. L. S. C. Tjen, et al. (2001). "Cardiac sympathetic afferent activation provoked by myocardial ischemia and reperfusion. Mechanisms and reflexes." Ann N Y Acad Sci 940: 74-95.
Malliani, A., P. J. Schwartz, et al. (1969). "A sympathetic reflex elicited by experimental coronary occlusion." Am J Physiol 217(3): 703-709.
Meller, S. T. and G. F. Gebhart (1992). "A critical review of the afferent pathways and the potential chemical mediators involved in cardiac pain." Neuroscience 48(3): 501-24.
Meltzer, R. H., N. Kapoor, et al. (2007). "Heteromeric Assembly of Acid-sensitive Ion Channel and Epithelial Sodium Channel Subunits." J. Biol. Chem. 282(35): 25548-25559.

Miyawaki, A., O. Griesbeck, et al. (1999). "Dynamic and quantitative Ca2+ measurements using improved cameleons." PNAS 96(5): 2135-2140.
Mo, F. M. and H. J. Ballard (2001). "The effect of systemic hypoxia on interstitial and blood adenosine, AMP, ADP and ATP in dog skeletal muscle." J Physiol 536(Pt 2): 593-603.
Molliver, D. C., D. C. Immke, et al. (2005). "ASIC3, an acid-sensing ion channel, is expressed in metaboreceptive sensory neurons." Mol Pain 1: 35.
Momomura, S., J. S. Ingwall, et al. (1985). "The relationships of high energy phosphates, tissue pH, and regional blood flow to diastolic distensibility in the ischemic dog myocardium." Circ Res 57(6): 822-35.
Nakazawa, K. (1994). "ATP-activated current and its interaction with acetylcholine-activated current in rat sympathetic neurons." J. Neurosci. 14(2): 740-750.
Nicke, A., H. G. Baumert, et al. (1998). "P2X1 and P2X3 receptors form stable trimers: a novel structural motif of ligand-gated ion channels." Embo J 17(11): 3016-28.
Ormö, M., A. B. Cubitt, et al. (1996). "Crystal Structure of the Aequorea victoria Green Fluorescent Protein." Science 273(5280): 1392-1395.
Pan, H. L., J. C. Longhurst, et al. (1999). "Role of protons in activation of cardiac sympathetic C-fibre afferents during ischaemia in cats." J Physiol 518 (Pt 3): 857-66.
Paukert, M., E. Babini, et al. (2004). "Identification of the Ca2+ Blocking Site of Acid-sensing Ion Channel (ASIC) 1: Implications for Channel Gating." J. Gen. Physiol. 124(4): 383-394.
Petroff, E. Y., M. P. Price, et al. (2008). "Acid-sensing ion channels interact with and inhibit BK K+ channels." Proc Natl Acad Sci U S A 105(8): 3140-4.
Price, M. P., R. J. Thompson, et al. (2004). "Stomatin Modulates Gating of Acid-sensing Ion Channels." J. Biol. Chem. 279(51): 53886-53891.
Roberts, J., C. Vial, et al. (2006). "Molecular properties of P2X receptors." Pflügers Archiv European Journal of Physiology 452(5): 486.
Robson, S., J. Sévigny, et al. (2006). "The E-NTPDase family of ectonucleotidases: Structure function relationships and pathophysiological significance." Purinergic Signalling 2(2): 409.
Rozas, J. L., A. V. Paternain, et al. (2003). "Noncanonical signaling by ionotropic kainate receptors." Neuron 39(3): 543-53.
Ryten, M., P. M. Dunn, et al. (2002). "ATP regulates the differentiation of mammalian skeletal muscle by activation of a P2X5 receptor on satellite cells." J Cell Biol 158(2): 345-55.
Sherwood, T. W. and C. C. Askwith (2008). "Endogenous arginine-phenylalanine-amide-related peptides alter steady-state desensitization of ASIC1a." J Biol Chem 283(4): 1818-30.
Sieber, J. J., K. I. Willig, et al. (2007). "Anatomy and Dynamics of a Supramolecular Membrane Protein Cluster." Science 317(5841): 1072-1076.
Sinoway, L., S. Prophet, et al. (1989). "Muscle acidosis during static exercise is associated with calf vasoconstriction." J Appl Physiol 66(1): 429-36.

Sinoway, L. I. and J. Li (2005). "A perspective on the muscle reflex: implications for congestive heart failure." J Appl Physiol 99(1): 5-22.
Smith, E. S., H. Cadiou, et al. (2007). "Arachidonic acid potentiates acid-sensing ion channels in rat sensory neurons by a direct action." Neuroscience 145(2): 686-98.
Steyer, J. A. and W. Almers (2001). "A real-time view of life within 100 nm of the plasma membrane." Nat Rev Mol Cell Biol 2(4): 268.
Stoop, R., A. Surprenant, et al. (1997). "Different Sensitivities to pH of ATP-Induced Currents at Four Cloned P2X Receptors." J Neurophysiol 78(4): 1837-1840.
Sutherland, S. P., C. J. Benson, et al. (2001). "Acid-sensing ion channel 3 matches the acid-gated current in cardiac ischemia-sensing neurons." Proc Natl Acad Sci U S A 98(2): 711-6.
Sutherland, S. P., S. P. Cook, et al. (2000). "Chemical mediators of pain due to tissue damage and ischemia." Prog Brain Res 129: 21-38.
Takago, H., Y. Nakamura, et al. (2005). "G protein-dependent presynaptic inhibition mediated by AMPA receptors at the calyx of Held." Proceedings of the National Academy of Sciences 102(20): 7368-7373.
Torres, G. E., T. M. Egan, et al. (1999). "Hetero-oligomeric assembly of P2X receptor subunits. Specificities exist with regard to possible partners." J Biol Chem 274(10): 6653-9.
Uchida, Y. and S. Murao (1975). "Acid-induced excitation of afferent cardiac sympathetic nerve fibers." Am J Physiol 228(1): 27-33.
Virginio, C., A. MacKenzie, et al. (1999). "Kinetics of cell lysis, dye uptake and permeability changes in cells expressing the rat P2X7 receptor." J Physiol 519(2): 335-346.
Virginio, C., A. MacKenzie, et al. (1999). "Pore dilation of neuronal P2X receptor channels." Nat Neurosci 2(4): 315.
Vulchanova, L., M. S. Riedl, et al. (1997). "Immunohistochemical study of the P2X2 and P2X3 receptor subunits in rat and monkey sensory neurons and their central terminals." Neuropharmacology 36(9): 1229.
Waldmann, R., F. Bassilana, et al. (1997). "Molecular cloning of a non-inactivating proton-gated Na+ channel specific for sensory neurons." J Biol Chem 272(34): 20975-8.
Waldmann, R., G. Champigny, et al. (1997). "A proton-gated cation channel involved in acid-sensing." Nature 386(6621): 173-7.
Waldmann, R., G. Champigny, et al. (1999). "H(+)-gated cation channels." Ann N Y Acad Sci 868: 67-76.
Waldmann, R., G. Champigny, et al. (1996). "The mammalian degenerin MDEG, an amiloride-sensitive cation channel activated by mutations causing neurodegeneration in Caenorhabditis elegans." J Biol Chem 271(18): 10433-6.
Walker, J. L., M. D. Thames, et al. (1978). "Preferential distribution of inhbititory cardiac receptors in left ventricle of the dog." Am J Physiol Heart Circ Physiol 235(2): H188-192.

Wang, W., Y. Yu, et al. (2007). "Modulation of acid-sensing ion channels by Cu(2+) in cultured hypothalamic neurons of the rat." Neuroscience 145(2): 631-41.

Wang, W. Z., X. P. Chu, et al. (2006). "Modulation of acid-sensing ion channel currents, acid-induced increase of intracellular Ca2+, and acidosis-mediated neuronal injury by intracellular pH." J Biol Chem 281(39): 29369-78.

Wemmie, J. A., M. P. Price, et al. (2006). "Acid-sensing ion channels: advances, questions and therapeutic opportunities." Trends Neurosci 29(10): 578-86.

Wildman, S. S., J. Marks, et al. (2005). "Regulatory Interdependence of Cloned Epithelial Na+ Channels and P2X Receptors." J Am Soc Nephrol 16(9): 2586-2597.

Wildman, S. S. P., J. Marks, et al. (2008). "Sodium-Dependent Regulation of Renal Amiloride-Sensitive Currents by Apical P2 Receptors." J Am Soc Nephrol 19(4): 731-742.

Wu, L.-J., B. Duan, et al. (2004). "Characterization of Acid-sensing Ion Channels in Dorsal Horn Neurons of Rat Spinal Cord." J. Biol. Chem. 279(42): 43716-43724.

Xiong, Z. G., X. M. Zhu, et al. (2004). "Neuroprotection in ischemia: blocking calcium-permeable acid-sensing ion channels." Cell 118(6): 687-98.

Xu, T. L. and Z. G. Xiong (2007). "Dynamic regulation of acid-sensing ion channels by extracellular and intracellular modulators." Curr Med Chem 14(16): 1753-63.

Yagi, J., H. N. Wenk, et al. (2006). "Sustained Currents Through ASIC3 Ion Channels at the Modest pH Changes That Occur During Myocardial Ischemia." Circ Res 99: 501-509.